

Some pages of this thesis may have been removed for copyright restrictions.

If you have discovered material in AURA which is unlawful e.g. breaches copyright, (either yours or that of a third party) or any other law, including but not limited to those relating to patent, trademark, confidentiality, data protection, obscenity, defamation, libel, then please read our Takedown Policy and contact the service immediately

LITHIUM - ALUMINIUM CASTING ALLOYS AND
THEIR ASSOCIATED METAL - MOULD REACTIONS

by

ANDREW GELDER

Submitted for the Degree of

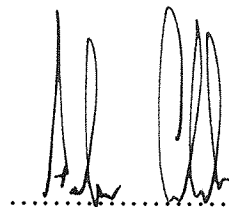
DOCTOR OF PHILOSOPHY

at the University of Aston in Birmingham

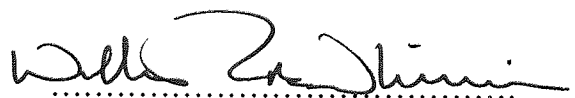
May 1992

The copy of this thesis has been supplied on condition that anyone who consults it is understood to recognise that its copyright rests with the author and that no quotation from the thesis and no information derived from it may be published without the author's consent.

The work described in this thesis was carried out between October 1988 and September 1991 at the University of Aston. It has been carried out independently and has not been submitted for any other degree.

A handwritten signature in black ink, consisting of stylized, overlapping loops and vertical strokes, positioned above a horizontal dotted line.

Andrew Gelder

A handwritten signature in black ink, featuring a large, sweeping 'W' followed by a cursive 'R' and 'McWhinnie', positioned above a horizontal dotted line.

Professor W.R. McWhinnie

The University of Aston in Birmingham
ALUMINIUM - LITHIUM CASTING ALLOYS AND
THEIR ASSOCIATED METAL - MOULD REACTIONS

Andrew Gelder

A thesis submitted for the degree of Doctor of Philosophy 1992

Aluminium - lithium alloys are specialist alloys used exclusively by the aerospace industry. They have properties that are favourable to the production of modern military aircraft. The addition of approximately 2.5 weight percent lithium to aluminium increases the strength characteristics of the new alloy by 10 percent. The same addition has the added advantage of decreasing the density of the resulting alloy by a similar percentage. The disadvantages associated with this alloy are primarily price and castability. The addition of 2.5 weight percent lithium to aluminium results in a price increase of 100% explaining the aerospace exclusivity. The processability of the alloys are restricted to ingot casting and wrought treatment but for complex components precision casting is required. Casting the alloys into sand and investment moulds creates a metal - mould reaction, the consequences of which are intolerable in the production of military hardware. The primary object of this project was to investigate and characterise the reactions occurring between the newly poured metal and surface of the mould and to propose a method of counteracting the metal - mould reaction.

The constituents of standard sand and investment moulds were pyrolysed with lithium metal in order to simplify the complex in-mould reaction and the products were studied by the solid state techniques of powder X-Ray diffraction and magic angle spinning nuclear magnetic resonance spectroscopy. The results of this study showed that the order of reaction was :

Organic reagents >> Silicate reagents > Non silicate reagents

Alphaset and Betaset were the two organic binders used to prepare the sand moulds throughout this project. Studies were carried out to characterise these resins in order to determine the factors involved in their reaction with lithium. Analysis revealed that during the curing process the phenolic hydroxide groups are not reacted out and that a redox reaction takes place between these hydroxides and the lithium in the molten alloy.

Casting experiments carried out to assess the protection afforded by various hydroxide protecting agents showed that modern effective, protecting chemicals such as bis-trimethyl silyl acetamide and hexamethyldisilazane did not inhibit the metal - mould reaction to a sufficiently high standard and that tri-methylchlorosilane was consistently the best performer. Tri-methyl chlorosilane has a simple functionalizing mechanism compared to other hydroxide protecting reagents and this factor is responsible for its superior inhibiting qualities.

Comparative studies of ^6Li and ^7Li N.M.R. spectra (M.A.S. and 'off angle') establish that, for solid state (and even solution) analytical purposes ^6Li is the preferred nucleus. ^6Li M.A.S.N.M.R. spectra were obtained for thermally treated laponite clay. At temperatures below 800°C both dehydrated and rehydrated samples were considered. The data are consistent with mobility of lithium ions from the trioctahedral clay sites at 600°C . The superior resolution achievable in ^6Li M.A.S.N.M.R. is demonstrated in the analysis of a microwave prepared lithium exchanged clay where ^6Li spectroscopy revealed two lithium sites in comparison to ^7Li M.A.S.N.M.R. which gave only a single lithium resonance.

KEYWORDS : Aluminium - Lithium alloys, Sand and Investment Casting, ^6Li M.A.S.N.M.R., Porosity Defect, Tri-Methyl Chloro Silane

To Stefanie

*for her incredible patience and
unending support throughout
the period of this research*

ACKNOWLEDGMENTS

I am indebted to Professor W.R. McWhinnie for his guidance, advice and support throughout the three years of this research. I would also like to thank him for being a friend as well as a supervisor. Additional thanks must also go to Professor F.M. Page for his useful contribution to my work, Mr Len Crane for providing Metallurgy expertise, Mr John Foden for his help on the metallography, Mr Roger Howes for the photography and Dr Mike Perry for carrying out all the n.m.r. experiments. A special thanks is reserved for Dr John Homer for his invaluable help on the lithium N.M.R. work.

I would also like to thank the Ministry of Defence for funding the research, Dr Peter Pitcher and Mr Brian Evans for their contribution to the work and Mr David Watkins for his work on the patent application.

I would like to thank my colleagues within the department for making the three years most enjoyable and also the members of my family who have offered their support and encouragement.

A very special thank-you must go to Stefanie for her unending patience, support and encouragement.

Chapter One
INTRODUCTION

1.1 Aluminium

1.1.1 History of Aluminium

In the world today aluminium is one of the most important metallic commodities. Its uses are very wide ranging and it is produced in many forms from very thin sheet foil through wires to cast, hardened structures for aircraft and buildings.

Although Hans Christian Oersted¹ is credited with the metal's discovery in 1825, its existence was hypothesised some twenty years earlier by Sir Humphrey Davy. Oersted produced the impure metal by heating together aluminium chloride and potassium amalgam but two years later in 1827 Friedrich Wöhler isolated a few grains of the metal as a grey powder by heating metallic potassium and aluminium chloride. It took until 1854 to create a process that was viable commercially. Henri Sainte Claire Deville exchanged Wöhler's potassium for the cheaper sodium and used the double salt of sodium aluminium chloride, a more stable compound than the known hygroscopic aluminium chloride. Over the next thirty years plants sprung up in America and Europe producing aluminium by the Deville method to a purity of 97 - 99 %. Without a doubt though, the most important year in the history of aluminium has to be 1886. Two men, Paul Louis Héroult in France and Charles Martin Hall in America, both aged 22, independently of each other filed patents reporting the production of aluminium through electrolysis of alumina dissolved in fused cryolite, a process that is still used today. This breakthrough was significant as cheap electricity was now available due to von Siemens development of the dynamo.

The Héroult-Hall process was such a significant breakthrough that it has hardly changed to this day. With careful selection of raw materials and operation of the plant, aluminium of 99.9% purity can be produced by this method although on average only 99.6% purity is achieved.

It was noted² that the aluminium produced by the Héroult-Hall process was very weak structurally and to improve the mechanical properties copper was added to the metal. Although this aided the mechanics, it had a detrimental effect on the corrosion resistance and many other binary and tertiary alloys were produced incorporating zinc, magnesium and silicon. In 1907 Wilm discovered that copper and magnesium alloys responded to thermal treatment at temperatures of 500°C followed by quenching and ageing. This gave a significant increase in hardness. Since this discovery other alloys have been discovered that respond to heat treatment and depending on composition, give enhanced corrosion resistance and notch toughness as well as mechanical hardness.

Currently most applications require an alloy and generally they contain varying amounts of Si, Mg, Mn, Zn, Fe, Cu, Cr and Ni.

In the years following Heroult's and Hall's discovery, the demand for aluminium increased, particularly at the times of the two World Wars. Unfortunately in the period following the wars, large slumps in sales occurred and given that the supply capability was already established, there was an incentive to find new markets for aluminium. After the Second World War work went into finding new outlets for existing alloys. Wrecked and obsolete aircraft were reclaimed for new housing, domestic utensils created an increased demand for sheet, and alloy products found outlets in electrical power distribution, structural engineering and road vehicles.

Since then there has been a proliferation of alloy compositions in the market for specific applications. To confuse matters, there were no specifications to standardise these alloys, and individual companies and countries produced their own. But there has been a concerted effort made in recent years and international standards have now been adopted. See section 1.1.5

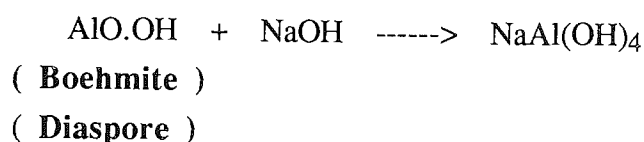
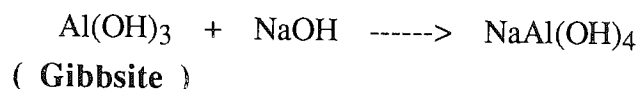
1.1.2 Production

Aluminium is the earth's third most abundant crustal element constituting 8% of the earth's crust³. Aluminium does not under any circumstances occur naturally in its elemental form but is found combined with oxygen and silicon in many silicate minerals. Silicates of aluminium are common constituents of igneous rock and in tropical conditions the effects of weathering and water attack leach the soluble iron, sodium, potassium and calcium components away leaving the insoluble silicates. The quartz tends to separate as sand leaving impure hydroxides of aluminium. Any rock containing large amounts of aluminium hydroxides is termed bauxite following Berthier's⁴ discovery of a ferroginous aluminous rock (27.6% Fe_2O_3 , 52% Al_2O_3 , 20.4% H_2O) near Les Baux in France. The name was coined later by Dufrenoy. Bauxite is now used to describe any mineral with a high aluminium hydroxide content.

There are many important hydrated forms of aluminium and from the aluminium industry's point of view it is important which form they get. It is much more economic to acquire aluminium as $\text{Al}(\text{OH})_3$ known as gibbsite, than as AlO.OH known as diaspore or its alternative form boehmite for reasons to be given later.

Bauxite⁵ is mined world-wide but the most important sites are in North and South America, Africa, Malaysia and Europe including France, Spain, Italy, Germany and Greece. It is generally mined by open cast working methods. It is then crushed, washed and dried ready for processing.

The process used for separating the alumina from the impurities is the Bayer process⁶. The alumina is dissolved in caustic soda and filtered to remove the impurities. The aluminium hydroxide is then reprecipitated and calcined to recover pure alumina.



It requires a greater concentration of caustic soda, greater pressure and greater temperature to extract the alumina from a boehmic or diasporic ore, with the result that investment for the process hardware is much greater .

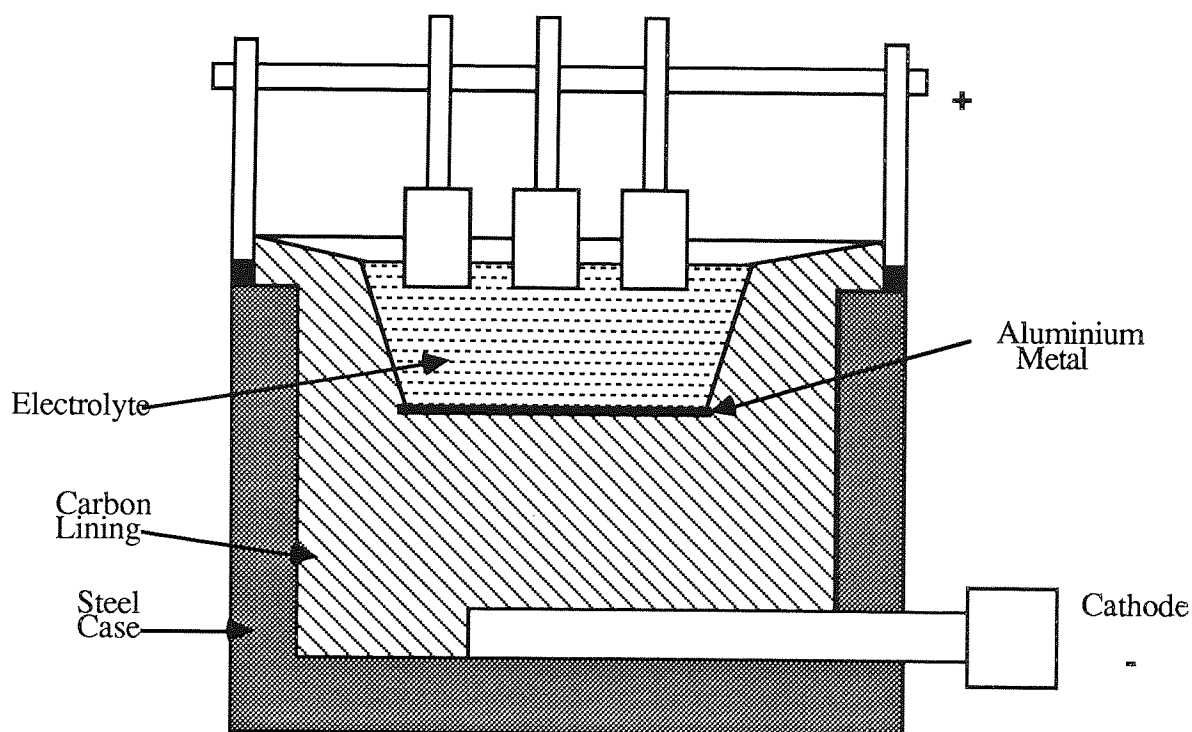
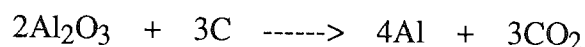


Fig 1.1 - A section through an aluminium electrolytic cell

The pure powdered alumina is transferred to a reducing cell where it is mixed with a solvent (in this case cryolite) to create an electrolyte. The Hérault-Hall process, as it is known, electrically reduces the alumina to form aluminium. The cryolite, a powerful solvent is rather difficult to contain but carbon being resistant to the molten salt and also being conductive is used as a lining for the cell. Carbon anodes are used at the top of the cell and are dipped into the electrolyte. The

density of the electrolyte is important because it has to be less dense than the aluminium so that the latter can sink and form the cathode by being in contact with the carbon lining. The liquid aluminium is tapped from the bottom of the cell and cast into ingots for further processing. The overall reaction is shown below:



Note here that carbon is used up in the process and this is from the anode. Hence the carbon used must be of very high purity so as to limit impurities in the electrolyte.

1.1.2a Electrolytic Refining⁷

The product from the Héroult-Hall process is at best 99.9% pure, but is generally of the order of 99.6% purity. This level is fine for some applications but for high purity a refining process has to be employed.

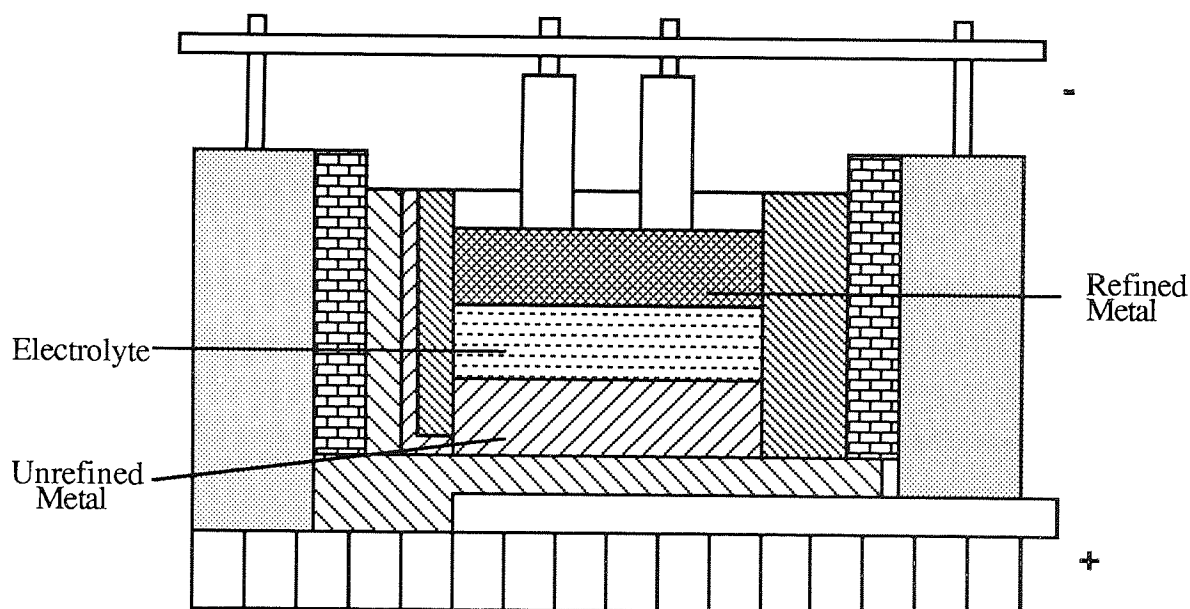


Fig 1.2 - A section through an electrolytic refining cell

The electrolytic refining process used today was first proposed by Hoopes in 1901 and improved by Betts in 1905. The important aspect of the cell used is the employment of a 3 liquid layer system. The lower and hence most dense layer is a binary aluminium-copper alloy containing typically 30-35% copper. This layer is in contact with the high purity carbon lining and forms the anode. The middle layer is the molten electrolyte containing such compounds as cryolite, $\text{AlF}_3 \cdot 3\text{NaF}$, AlF_3 , CaF_2 , BaF_2 and BaCl_2 . The density of this electrolyte has to be adjusted so

that it is less dense than the aluminium-copper alloy yet denser than the third layer - the high purity aluminium. This top layer forms the cathode with carbon rods dipped into it.

The aluminium from the alloy is taken into the electrolyte and redeposited in the cathode as the pure metal. Aluminium treated in this fashion can have a purity of 99.99%.

1.1.2b Zone Refining⁸

For research use further refining must be carried out to gain a purity of 99.998%. To reduce the last traces of impurities still present, use is made of the physics of the solid-liquid equilibrium. This process is known as zone refining and it relies on the fact that most impurities will preferentially concentrate either in the solid or the liquid as the aluminium freezes.

If the liquidus and solidus are lowered by the presence of an impurity then for any given temperature the impurity level of the solid will be less than that of the liquid. The ratio of the atomic fractions in the liquid and solid phases at a given temperature is given by

$$A_0 = (N_{\alpha\text{sol}} / N_{\alpha\text{liq}}) \text{ valid near the pure solvent end} \quad \dots\text{eq 1.1}$$

Purification of the metal will become easier as $A_0 \rightarrow 0$. This can be shown as follows.

If an equilibrium between solid and liquid can be set up by melting an area of metal, then a solid will form in which the atomic fraction $N'_{\alpha\text{sol}}$ is equal to $A_0 N_{\alpha\text{liq}}$ (A_0 being 0.25 for example). If that solid phase alone is taken and remelted to allow equilibrium to be set up between a new liquid and solid phase the atomic fraction $N'_{\alpha\text{sol}}$ will be $A_0 N'_{\alpha\text{liq}} = A_0^2 N_{\alpha\text{liq}}$. Since $A_0 < 1$ it is clearly possible by repeating the sequence of operations to eliminate the impurities progressively, the ultimate contents decreasing as $A_0 \rightarrow 0$.

In practice a small diameter bar of refined aluminium to be zone refined is heated at one end until it melts. For this process the bar is placed in a refractory container. Once the end of the bar is molten, the molten zone is moved slowly and uniformly along the length of the bar by moving the high frequency coil used for melting, care being taken to produce and maintain a clearly defined and small molten zone. As the far end of the bar is reached, the operation, always in the same direction is repeated and after a number of passes, six seven or eight, it is found that a significant proportion of the impurities with activation energies $A_0 > 1$ have moved with the molten zone towards the far end of the bar (and those with $A_0 < 1$ moved in the opposite direction). Once the process is finished the ends of the bar are discarded and super pure aluminium is left.

1.1.3 Production Amounts and Costs

Since Héroult and Hall made their epic discovery in 1886 production statistics have become readily available. Figure 1.3⁹ shows how the production of aluminium has increased since the late 19th century. The graph shows significant peaks at 1915-20 and in the early forties as the war efforts required more metal. But it was only after the second world war that the use of aluminium expanded rapidly and production roughly doubled between 1950 and 1960 and again between 1960 and 1970. In more recent times the rate of increase was maintained until the mid seventies when there was a fall in demand and an associated cut back in production, but demand increased again and, by 1980, world production reached 16×10^6 tonnes / annum but it then levelled off. Growth to 1990 was around 4% per annum and it is not expected to exceed this in the near future.

In the 1840's when Wöhler had isolated aluminium globules the metal was classed as precious and was exhibited next to the crown jewels at the Paris Exposition in 1855, and Emperor Louis Napoleon III used aluminium cutlery on state occasions. Table 1.1¹⁰ shows the price drop over a 130 year period from the discovery of aluminium to present day including the dramatic decreases due to the introduction of both the St Claire Deville and the Héroult-Hall processes.

Year	1852	1854	1855	1856	1857	1858	1886
Price \$/kg	1200	600	250	75	60	25	17

^ Introduction of St Claire Deville process

1888	1890	1895	1900	1950	1964	1974	1982
11.5	5	1.15	0.73	0.4	0.53	0.75	0.93

^Introduction of Héroult-Hall electrolysis

^Minimum

Table 1.1 - Comparison of prices of aluminium over the last 150 years

Year	1981	1982	1983	1984	1985	1986	1987	1988	1989
Price	57.274	44.966	65.342	56.526	47.850	52.179	71.004	117.33	88.508

Table 1.2 - London Metal Exchange Yearly Averages in U.S. cents / pound 99.5% ingot

On a more recent note¹¹ table 1.2 shows the price fluctuation over the last ten years which gives us a better idea of the cost of the metal today.

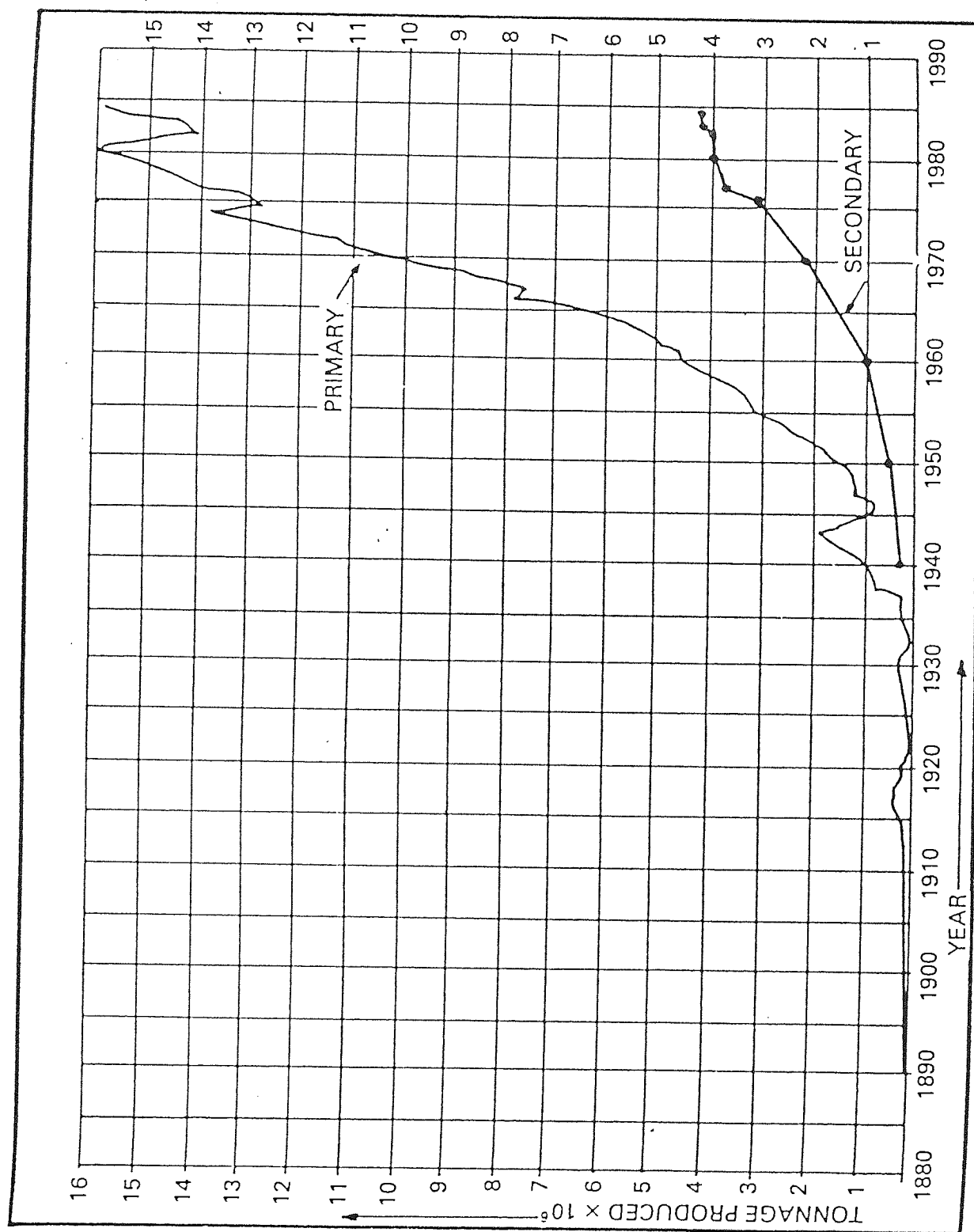


Fig 1.3 - Aluminium production amounts over the last century

1.1.4 Physical and Chemical Data

Aluminium, atomic number 13, is the second member of the third group in the periodic table of the elements. It has a relative atomic mass of 26.9815. It is a low density metal of a very high electromagnetic reflectivity, silver white in its pure form. It forms a thin transparent oxide coating in air which stabilizes it against further corrosion. This property is in fact the driving force behind many of its uses, together with the strength, low density and malleability.

Aluminium has one natural isotope of atomic mass 27. Several artificial isotopes are known. The neutral atom has a radius of 1.431 \AA and its electronic configuration in the ground state is $1s^2 2s^2 2p^6 3p^2 3p^1$. The crystalline form has a face centred cubic lattice with a unit cell dimension of 4.04959 \AA . The density of aluminium is 2.6989 g/cm^3 at 20°C and it melts at 660.24°C . Its normal boiling point is 2467°C . The heats of fusion and vaporisation are 2.55 and 70.7 kCal/mol respectively.

Electrical conductivity is normally expressed as a percentage of the International Annealed Copper Standard (I.A.C.S.). The electrical resistivity of 99.999% aluminium at 20°C is $2.6548 \times 10^{-8} \Omega\text{m}$ which equates to 65.45% I.A.C.S.. The thermal conductivity is $237 \text{ Wm}^{-1}\text{K}^{-1}$ at 300K and aluminium is weakly paramagnetic with a susceptibility of $7.7 \times 10^{-9} \text{ kg}^{-1}\text{m}^3$.

Aluminium is ordinarily trivalent (Al^{3+}) in its compounds but the mono (Al^+) and divalent (Al^{2+}) are known in high temperature compounds such as AlCl and AlS . Aluminium is of potentially high chemical reactivity as is seen in the very high energies of formation of its compounds with oxygen, carbon, sulphur and the halogens. The standard reduction potential is 1.67 volts for the couple $\text{Al} \rightarrow \text{Al}^{3+} + 3\text{e}^-$.

Aluminium is only superficially attacked by water or air at room temperature but it is rapidly oxidised at raised temperature (eg 200°C). Dilute or cold concentrated sulphuric acid or concentrated nitric acid have little effect on pure aluminium but their effect is more marked on contaminated aluminium. Hydrochloric acid solutions attack aluminium with hydrogen evolution. Strong alkalis attack aluminium violently also with the formation of hydrogen. Aluminium forms many compounds, the most useful of which is probably its oxide, alumina. Alumina is the starting material for many products, including of course, aluminium itself. They range from refractories through artificial rubies and sapphires to antiperspirants and catalysts. The aluminium alkyls and alkoxides, aluminium chloride and lithium aluminium hydride are also useful chemicals and are usually used in organic synthesis.

1.1.5 Alloy Types¹²

Wrought, and casting alloys and foundry ingots, must be classified in some way to give the purchaser an idea of what alloy they are buying. This classification is done by the internationally recognised four digit system. For wrought alloys the system is as shown in table 1.3

Alloying Element	Number
Al of 99% min purity	1xxx
Copper	2xxx
Manganese	3xxx
Silicon	4xxx
Magnesium	5xxx
Magnesium + Silicon	6xxx
Zinc	7xxx
Other elements	8xxx
Unused series	9xxx

Table 1.3 - Four digit designation for wrought alloys

The first digit indicates the alloy group. The 1xxx series is for minimum aluminium purities of 99.00% or greater, and the 2xxx through to 8xxx series group aluminium alloys by their major alloying elements. The last two digits in the number identify the aluminium alloy or indicate its purity, and the second digit indicates modification of the original alloy or impurity limits. For the 1xxx series the last two digits indicate the purity of the aluminium and the second digit indicates modification in the impurity limits

...eg. alloy 1045 shows it is a high purity aluminium alloy with 99.45% aluminium used and there are no controls needed on impurities.

For casting alloys the system is slightly different. This is shown in table 1.4. The first digit still indicates alloy group with the 1xx.x series representing alloys of 99.00% aluminium or greater, and the 2xx.x through to 9xx.x series classifies the alloys by their major alloying element. This time the second two digits identify the alloy or indicate the aluminium purity.

Alloying Element	Number
Al of 99% min purity	1xx.x
Copper	2xx.x
Silicon + Copper/Magnesium	3xx.x
Silicon	4xx.x
Magnesium	5xx.x
Unused Series	6xx.x
Zinc	7xx.x
Tin	8xx.x
Other Elements	9xx.x

Table 1.4 - Four digit designation for casting alloys

The last digit, separated by a decimal point, indicates the product form : xxx.0 indicates castings, xxx.1 indicates ingot which has certain chemical composition limits, and xxx.2 indicates ingot which has chemical composition limits which differ but fall within the limits for xxx.1 ingot.

For both wrought and casting alloys, experimental alloys are designated by the prefix X.

The temper designation system is used for all forms of wrought and cast aluminium alloys except ingot. It is based on the sequences of basic treatments used to produce various tempers. The temper designation follows the alloy designation, the two being separated by a hyphen. The basic temper designations are as follows.

- F - As Fabricated
- O - Annealed (wrought only)
- H - Strain Hardened (wrought only)
- W - Solution Heat Treated (Unstable Temper)
- T - Thermal Treated to Produce Stable Tempers other than F,O,H

There are subdivisions of the H and T tempers and they are described in reference 12

1.1.6 Uses of Aluminium Alloys¹³

The largest market for aluminium alloys is the building and construction industry. Residential siding, farm and industrial roofing and siding are all produced from 3003, 3004 and 3105 alloys. Guttering and downspout are also produced from these alloys. Doors and window frames are constructed from 6063 extrusions. Anodised and coloured aluminium panels are used in the curtain wall structures of many buildings and for shop fronts and other decorative applications. Good resistance to weathering, good strength and lightweight for handling are the basic properties required for these applications.

Another large area for aluminium alloys is transportation. In both commercial and military aircraft, heat treatable alloys, with high strength and toughness are used extensively in engines, frames, skin sheet and landing gear (see section 1.3). In the automotive industry aluminium is used extensively in wheels, interior and exterior trim through to air conditioners, intake manifolds and water pumps. Body panels, bumpers, radiators, oil coolers and engine blocks are also made of aluminium alloys to reduce weight and increase fuel efficiency. In commercial transport, alloys are used in lorry cabs and bus shells, bumpers and engine parts. Road signs, crash barriers and street lamps are all made from aluminium. In the marine world Al-Mg and Al-Mg-Si alloys are used for canoes, pleasure boat hulls, fishing boats, tanks for liquified natural gas, and deck houses for naval vessels. Aluminium alloys have also been used in the construction of satellites and moon rockets, to meet strict requirements for strength, toughness, lightness, weldability and reflectivity.

In the food industry aluminium is known in beverage cans, 3004 and 5185 are used for the can body and base respectively. It is also used in the manufacture of meat, pudding and fish cans and aerosols. Formed light gauge sheet and foil are used for frozen food trays, pie plates and similar applications.

In the home aluminium is used as foil (0.018mm thick), cooking utensils, appliances and hardware. It is also used for toys, sports equipment, lawn furniture, lawnmowers and portable tools.

Since aluminium has a volume conductivity 65% that of copper and a lower density, an aluminium conductor weighs only half as much as a copper conductor of equal current carrying capacity. Therefore aluminium is used extensively for overhead transmission lines. The alloys used for this purpose are conductor grades 1350 and 6201.

Aluminium has many uses in the chemical industry, e.g. for pipes and storage tanks using alloys 1100, 3003, 6061, 6063 and Al-Mg alloys. It is also used in the storage and packaging of chemicals ranging from large Al-Mg tanks for ammonium nitrate and liquified gas to collapsable tubes for dispensing pharmaceuticals and toiletries.

Various gears, bushings and small tools are made by powder technology. Aluminium powders are compacted then sintered for bonding with the advantage of eliminating machining operations. Aluminium powder has found other uses in paints, as well as in explosives and rocket fuels.

Alloy	Al	Si	Mg	Mn	Cu	Cr	Zn	Fe
1100					0.12			
1350	99.5							
3003					0.12			
3004				1.1				
3105			1.0	1.1				
5182			4.5	0.35				
6061		0.6	1.0		0.25	0.2		
6063		0.4	0.7					
6201		0.7	0.8					

Table 1.5 - Metal Specifications for some of the more frequently used Aluminium Alloys

1.2 Lithium

1.2.1 History of Lithium

The major minerals containing the alkali metal lithium were first discovered by a distinguished Brazilian scientist and statesman J6se Bonif6cio de Andrada e Silva¹⁴ (1763 - 1838) in the late 18th century. He described them in a letter published in January 1800 as petalite, an infusible, laminated material that dissolved slowly in nitric acid without effervescence, and the other he named spodumene. Vauquelin's analysis of spodumene in 1801 showed a loss of 9.5% but this was not explained until 1818 when J.A. Arfvedson¹⁵ discovered the metal lithium first in petalite and then in spodumene, and attributed the loss to this new element. After much analysis on both spodumene and lepidolite, attempts were made to isolate the metal, first by Arfvedson and Gmelin through electrolysis and then later by heating lithia (Li₂O) with iron and carbon, both routes proved fruitless at the time. Brande and Davy were the first to succeed albeit separately to isolate the

metal. Both used electrolysis with cells of much greater ampage than had first been used. Bunsen and Mathiesen managed to produce significant amounts (of the order of 1g) in 1855 to enable more analysis to be carried out.

For many years to come lithium remained of academic interest with no industrial applications until the early 1900's. The first real use came as an alloying element towards the end of the first World War when Metallgesellschaft A.G. used lithium in an aluminium zinc alloy known as Scleron. Shortly after the war lithium was used as a hardner in a lead alloy, B-metal¹⁶.

During World War Two interest in lithium grew due to U.S. Defence requirements¹⁷, such as:

- (i) LiCl for batteries
- (ii) LiH for H₂ generation in air-sea rescue
- (iii) Li metal for new alloys eg. Mg-Li
- (iv) Several Li compounds for organic synthesis

These projects have formed the basis of the lithium industry for the last fifty years. The industry now produces 80-90 lithium compounds¹⁸ with the major products being carbonate, hydroxide, chloride, hypochlorite, metal and butyllithium. The major uses of these compounds are in lithium batteries, the glass and ceramic industry, alloys, organic synthetic work and a small amount in a biological role.

1.2.2 Production

As stated earlier lithium is found in the minerals spodumene, lepidolite, petalite and other less well known minerals such as ambyglonite. The crustal abundance is of the order of 0.0065%. In comparison with the abundance of lithium throughout the solar system¹⁹ the crustal abundance can be classed as high. The three elements Li, Be and B are all mysteriously rare in the solar system and since it is assumed that the earth was made at the same time and from theoretically from the same materials as the solar system, their relatively high crustal abundance is problematical. It appears that cosmic rays are the cause. Cosmic rays originate from outside the solar system, probably from supernovae. They consist of nuclei travelling at very high velocity. Spallation reactions occur as the nuclei collide at very high energies and produce fragments of low mass number including in the range ⁶Li - ¹¹B. These rays hit the earth and hence over the millions of years the relative abundance of lithium has risen.

Lithium is a lithophilic element and hence the industrial source for lithium is primarily spodumene and the like. Unfortunately notwithstanding the relatively high quantity of lithium in

the earth's crust, actual deposits of sufficient concentration and quantity to warrant commercial mining are scarce. From data available²⁰ the occurrence is in the following order of commercial importance: North America, South Africa, South America, Europe, Australia and Asia. Even if a lithium rich seam is found, the lithium content is only 1.5% Li₂O in the case of spodumene and 1% Li in the case of lepidolite. So to make the extraction process worthwhile an enrichment procedure is undertaken²¹ which usually consists of handpicking, thermal treatment and flotation.

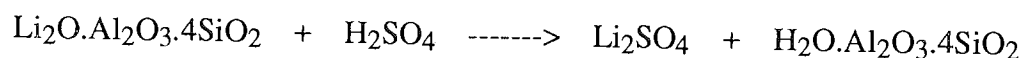
Thermal enrichment requires the α - spodumene (as is normally mined) to be heated to 1000 - 1100° C to transform it to the β - form which has a lower density. The resultant 24% increase in volume causes cracking and marked crushing of the mineral. The roasted product is then classified so as to separate the fine spodumene powder from the quartz grains.

Flotation is carried out using, oleic acid or sodium oleate, the lithium minerals are separated with the foamy product. This is known as direct flotation. The opposite can be done where the impurities are floated off leaving the minerals behind. This is reverse flotation.

Once the enrichment is complete, processing of the minerals can commence. The products of processing are lithium salts (LiCl, Li₂CO₃, Li₂SO₄). There are three methods of processing. (1) decomposition with sulphuric acid (2) with lime (3) with sulphate.

(i) Sulphuric Acid

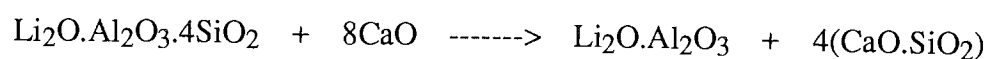
This processing method is based on the following reaction:

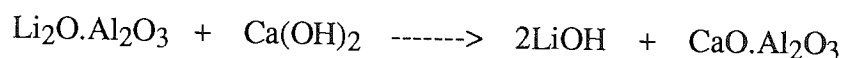


This is carried out by adding to excess 93% sulphuric acid to the minerals and reacting at 250°C for 10 minutes. The sinter is then cooled and leached with water to remove the Li₂SO₄. Chalk is also added to neutralise the excess acid. The solution is then filtered and the calcium and magnesium are removed by precipitation. Any aluminium and iron are removed by adding sulphuric acid up to pH 7 together with carbon black. The solution is again filtered, and Li₂CO₃ is precipitated by the addition of sodium carbonate, washed and dried for use.

(ii) Lime Method

The lime method is based on the following reactions:

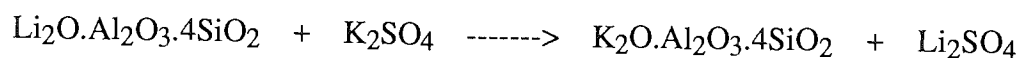




The spodumene is initially reacted with lime to form the lithium aluminate which then reacts with the excess lime to form the soluble hydroxide. Spodumene and lime are mixed in a furnace and roasted at 1150 - 1200°C. The sinter is then ground to 147μ and the LiOH is leached out and crystallized. The crystals are separated out by centrifuge and the product is dried for use

(iii) Sulphate Method

The sulphate method involves the substitution of the lithium in spodumene with potassium and is based on the following reaction:



The spodumene is mixed with an excess of potassium sulphate. This mixture is then sintered by heating for 2 hours at 1100 - 1150°C. The resulting sinter is then leached with cold water. The solution is separated by filtration and the solution containing the Li₂SO₄ plus the sulphates of sodium, potassium, aluminium and iron is treated with potassium carbonate to precipitate out the iron and aluminium. After filtration the solution is evaporated causing the precipitation of most of the potassium sulphate (together with the sodium sulphate) and these are removed by centrifuging. The remaining solution is then heated to 80 - 90°C and the lithium is precipitated out by the addition of a sodium carbonate solution. Lithium carbonate, separated by centrifugation, is dried ready for use.

1.2.2.1 Recovery from Brines

An alternative to recovery of lithium from mineral ores is the recovery from natural brines. A brine is a natural body of water e.g. a lake with a high content of alkali metal salts. Good sources for brine were rare until several salars in the Andes were discovered containing 200 -2000 ppm lithium²². The economical recovery, however, depends not only on lithium content but also on high elevation, high winds, low rainfall, low humidity and warm climate which are all conducive to solar evaporation of brines. Interfering ions play a part also especially magnesium and calcium. If the magnesium concentration is low then it can be precipitated out easily with lime. Most calcium ions are precipitated out as gypsum during evaporation, along with much sodium chloride. During these salting out processes and iterative evaporation, the lithium content rises to 3-4 weight percent. Any residual calcium and magnesium are removed with lime and soda ash before the lithium is precipitated out as the carbonate.

If, however, the magnesium concentration is too high then its removal would not be economic and the lithium must be selectively removed from the brine^{23,24,25}.

1.2.2.1 Recovery of Lithium Metal

The production of lithium metal is carried out by electrolysing LiCl. A typical electrolyte bath used for such a procedure is shown in figure 1.4.

Electrolysis is carried out on a LiCl + KCl mixture (1 : 1 by weight) which is close to the eutectic composition. The mixture contains about 60 mole % LiCl and melts at 352°C; the operating temperature of the electrolysis bath is approximately 450°C. The decomposition voltage of LiCl is approximately 3.9V but again operational voltages are higher at 5-8V. Current densities at the anode are 4-8 A/in². 1 kg of lithium requires approximately 50kWh to produce, with a current efficiency of 80%.

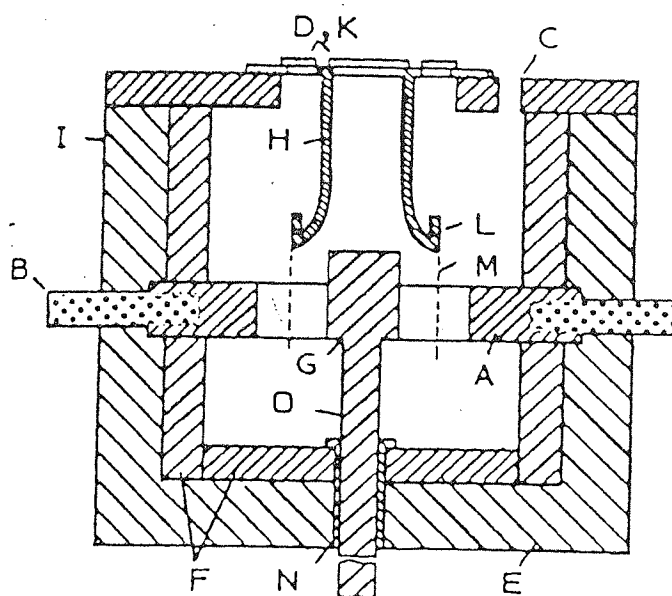
Fresh lithium chloride is periodically added to the melt to replace that already used and the lithium metal produced flows up to the surface of the electrolyte where it gathers in a collector in the cathodic space. The metal is scooped out by a ladle and cast into 1kg trapezoidal ingots where it is treated for protection against air. This usually entails brushing with a mineral oil but it can mean storage of the metal in an argon filled container or pressed in aluminium or copper shells.

1.2.3 Production Amounts and Costs

Except for the early 1900's when lithium metal was produced for specific applications, most lithium has been manufactured as carbonate or hydroxide. The production of lithium chemicals did not take off as an industry until the middle of this century and lithium metal has only just become a reasonably important commodity. The production of lithium metal is so small that the major metal statistic volumes have only recently quoted amounts or prices. In 1985 an estimate of production in the free world of lithium metal, was of the order of 450 Tonnes, which is small in comparison with other metals, and most of this production goes into batteries, alloys, organic synthesis, degassing agents, and torpedo fuel. Data for the last ten years can give a reasonable idea of the price fluctuation in recent times.

Year	1981	1984	1986	1987
Cost \$/lb	20.35	22.70	24.20	25.45

Table 1.6 - Lithium prices over the last decade(99.9% ingot 1000lb lots prices are in \$ per lb)



CELL FOR THE ELECTROLYSIS OF LITHIUM (DE GUSSA)

- A. GRAPHITE ANODE PLATES
- B. GRAPHITE ANODES
- C. EXIT FOR CHLORINE
- D. ENTRY PORT FOR LiCl
- E. INSULATION
- F. REFRACTORY PLATES
- G. HEAD OF STEEL CATHODE
- H. CAST IRON LITHIUM COLLECTOR
- I. STEEL CONTAINER
- K. STEEL COVER PLATES
- L. BORDER FOR FASTENING DIAPHRAGM
- M. DIAPHRAGM (WIRE NET)
- N. STEEL COLLAR
- O. STEEL SHAFT

Fig 1.4 - Schematic diagram of a lithium electrolytic cell

It should be noted here that on a price for price basis, the addition of 2.5% lithium to aluminium will approximately double the cost price of aluminium.

1.2.4. Physical and Chemical Properties

Lithium, atomic number 3, occurs as the second element of group 1. It is a silvery white metal and has a specific gravity of 0.534 and is the lightest of all solid elements. At normal temperatures the crystal structure of lithium is body centred cubic with a lattice constant of 3.50 Å at 20°C, but below -117°C the metal starts to transform to f.c.c.. Lithium occurs naturally as two isotopes ^7Li and ^6Li and relative atomic mass of 6.94 since the mass 7 isotope is more abundant by approximately 12:1. Three other nuclides have been artificially produced ^5Li , ^8Li and ^9Li but they are all unstable with half lives of less than 1 second.

Lithium is a highly reactive metal and given the correct conditions will react with all non-metals, inert gases excepted, most of the metalloids and many of the metals.

Atomic Number	3
Atomic Weight	6.94
Electron Configuration	$1s^2 2s^1$
Crystal Structure	b.c.c.
Lattice Constant	3.50 Å
Metallic Radius	1.225 Å
Density	0.534gcm^{-3}
Thermal Conductivity (273K)	0.17
Electrical Resistivity	8.6
Melting Point ^a	180.54°C
Boiling Point ^a	1342°C

a - Source Handbook of Chemistry and Physics, London Rubber Company, 1991

Table 1.7 - Chemical and Physical Data for Lithium

It reacts with all of the halogens to form the halides but somewhat less readily than the other alkali metals. Pure lithium is not readily reactive with dry oxygen at room temperature but forms dilithium oxide (Li_2O) at 100°C +. Similarly dry nitrogen does not react with lithium, if at all, but if any moisture is present Li_3N is formed even at room temperature. Lithium will react with carbon forming Li_2C_2 , an acetylide, but only at elevated temperatures. The reaction with hydrogen occurs readily at the melting point of lithium to form LiH , a compound that is

thermodynamically more stable than the corresponding compounds of other alkali metals. The reaction with water is vigorous, forming LiOH and evolving hydrogen gas, but again the reaction is not as rapid as that with sodium or potassium, partly due to the fact that the lithium doesn't melt during the reaction and partly due to the higher ionisation potential of lithium ($520.1 \text{ kJ mol}^{-1}$) compared with those of the other alkali metals (Na - $495.7 \text{ kJ mol}^{-1}$, K - $418.6 \text{ kJ mol}^{-1}$).

1.2.5 Uses of Lithium

(i) Chemical Intermediate

Lithium can be used as both a starting material or an intermediate for synthesis reactions. Compounds can be formed by direct combination i.e. LiH and Li_3N but if high purity is required reactions with an acid gas can be carried out. Very dry Li_2S can be formed by the reaction of lithium with H_2S^{26} . These reactions are expensive and hazardous though and are best avoided. The best known use of lithium is as the alkyl or aryl derivatives in organic synthesis.

(ii) Polymerisation Catalyst

Lithium has been used to polymerise butadiene, isoprene, styrene and acrylates, usually as a dispersion. It has also been used to produce copolymers.

(iii) High Strength Glass / Glass Ceramics

These are formed by immersing a sodium containing glass into a salt bath containing lithium compounds followed by heat treatment. The sodium ions are replaced by lithium ions at a temperature above that of the transformation point of the glass. During cooling a compressive layer is formed on the surface of the glass giving the glass high strength.

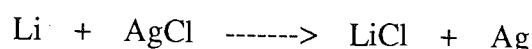
Glass ceramics are produced using mixtures containing lithium compounds. Heat treatment of the glass phase causes crystallisation of lithium containing phases such as spodumene and eucryptite. The ceramics are used to make cookware requiring high strength and a low coefficient of thermal expansion.

(iv) Electrochemical Cells

There is great interest in producing a practical voltaic cell containing lithium as the anode. Cells have been produced using a variety of elements and compounds as the cathode. The

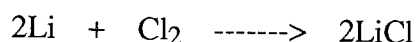
advantage of using lithium is that due to its low equivalent weight it has a high charge density. Several lithium cells have been put into use at varying temperatures.

Cells designed for low temperatures use organic liquids as electrolytes, usually with a dissolved salt to enhance the conductivity. Cathodes are normally metal halides, and the lithium / silver chloride cell is a good example.



Propylene carbonate with lithium chloride and aluminium chloride serves as the electrolyte. Sometimes the cathode is not a conductor so it has to be mixed with an electronic conductor such as graphite.

High temperature cells use a fused electrolyte and therefore must be operated at temperatures higher than the melting point of the electrolyte.



The cathode used in the cell utilising the above reaction is chlorine on porous graphite and the electrolyte is lithium chloride and potassium chloride.

(v) Lithium Alloys

A little has already been mentioned about the early alloys in section 1.2.1 and the more recent alloys will be dealt with in section 1.3.

1.3 Aluminium - Lithium Alloys

1.3.1 History of Aluminium - Lithium Alloys

When Duralumin, the world's first heat treatable aluminium alloy, was produced just prior to World War I it generated many efforts to find competitive alternatives. Needless to say, since lithium is one of just eight elements whose solid solubilities in aluminium exceed 1 atomic percent, and only three elements have higher solid solubilities, it was included in these investigations. Two patent applications were filed in 1919 for aluminium alloys containing lithium, and three years later the development of an alloy with a minor addition of lithium was announced²⁷. This alloy was called Scleron. There were doubts about the contribution of the lithium in the alloy, but nonetheless it was the first commercial lithium containing alloy. It was in general better than Duralumin,

particularly in yield strength in the naturally aged condition, but with inevitable improvements to the Duralumin system, Scleron and its counterparts soon fell from grace.

Lithium did not feature again in a commercial aluminium alloy until the late forties when AlCoA (the Aluminium Company of America) took out a patent on an Al-Cu-Li-X alloy²⁸. It was noted that this alloy showed an increase in strength particularly in conjunction with minor element additions, but as was the case 20 years prior, the introduction of alloy 7075, Al - 6.1Zn - 2.9Mg - 2.0Cu - 0.5Fe - 0.4Si - 0.35Cr - 0.3Mn, in 1943 overshadowed this development.

Interest was renewed when Hardy²⁹ clarified the role of the minor additions to the AlCoA alloy and Pechiney developed a process reducing the oxidation during melting. AlCoA continued research which culminated in the introduction X-2020³⁰. The composition was nominally Al - 4.5Cu - 1.1Li - 0.5Mn - 0.2Cd. This alloy was known to exhibit high strength and reduced density.

Trials conducted by AlCoA overcame the problems with melting and ingot casting, ie. protection of the melt from oxidation and control of cadmium vapours, sufficiently to cast ingots equivalent to the 7075 alloy. Once this had been carried out work on sheet production was finalised, and welding, rivet characteristics, and mechanical and corrosion behaviour were established.

Interest was now being shown by the aerospace industry and small amounts of 2020 were made available to several companies. This was an area which had almost been exclusive to standard 2xxx and 7xxx aerospace alloys. All engineering work was at that time focused in the U.S. while the metallurgy was being researched in Britain. Other work was also being carried out in Japan and the U.S.S.R..

The new X-2020 alloy looked to be extremely promising since it was free from exfoliation corrosion and stress corrosion cracking. It could also tolerate extended exposure to the high temperatures afforded by aircraft exceeding Mach 2.5.

Given all this positive information, the U.S.A.F. decided to give X-2020 a trial run on some of its aircraft and this afforded some quantification for the weight saving. The replaced parts were wing skins and/or wing panels and weight savings are shown in table 1.8³¹.

The Vigilante was the only aircraft that went into production carrying 2020. In all, 177 aircraft were built but the 2020 alloy was "notch sensitive" and care had to be taken to design out the possibility of fatigue crack.

Aircraft	Actual Weight Saving	Percentage Weight Saving
B - 58 Hustler	121kg	13%
F - 111 Fighter Bomber	59kg	15%
A - 5A Vigilante RA - 5C Vigilante	73kg	6%

Table 1.8 - Savings Derived from Using X-2020 in Some U.S. Aircraft

Problems in this area had been noticed by the developers of both the Hustler and the F - 111. Shattering after compressive buckling cancelled the Hustler program and poor fracture behavior forced a withdrawal from the F - 111. Other applications were considered but nothing came to fruition and effectively the 2020 program was doomed. AlCoA could not justify its production without applications. Work on the fatigue problem was continued but no improvements were made and production halted in 1969.

Research was stopped once again in the United States in order to concentrate on more pressing projects involving the 2xxx and 7xxx series, but in the Soviet Union results were beginning to appear and a new alloy was to be developed. It was designated 01420 and was an Al - Mg - Li - X type alloy. It contained 5% magnesium, 2% lithium and 0.5% manganese, and was patented in the late '60's. The properties of 01420 were not as good as the X2020 alloy from AlCoA and are really only comparable with the 2xxx series alloys. Nevertheless this alloy provoked great interest and in the late '70's Britain's interests were aroused.

The R.A.E. at Farnborough became interested in aluminium-lithium alloys and began to work with 01420³². They discovered that it was difficult to cast by direct chill methods, and in conjunction with the British Aluminium Company, it was discovered that the developed strength was not high enough although there was a good stiffness achieved. This prompted research into alloys and the systems investigated were Al-Mg-Li, Al-Li-Cu, Al-Li-Cu-Mg, Al-Li-Zn-Mg. Experience from the American 2020 alloy showed that the strength was no problem but the alloys were likely to be brittle. Work, therefore started on optimising the fracture toughness and this was achieved by modelling and calculating the maximum concentrations of alloy constituents that could be dissolved at solution treatment. Al-Li-Cu-Mg was chosen as the alloy for this work as it had already demonstrated the best balance between strength and fracture toughness. Hence the alloy F92 was developed and subsequently patented. This was then further developed and optimised and was registered as the alloy 8090.

Many design targets were set including a density decrease of 10% and a strength equivalent to the conventional alloys so that a direct substitution could be made without a large amount of redesigning from aerospace manufacturers. 8090, therefore, had to match the damage tolerant 2000 series, the medium strength general purpose alloys with a good resistance to stress corrosion cracking and the very high strength alloys. The truth was that the first two requirements could be matched by modification of the heat treatment sequence but 8090 could not match the very high strengths and therefore a modification was made resulting in 8091 coming on to the market.

These two alloys have been accepted by the aerospace industry and successful trials have been carried out on the British Aerospace EAP, the Dassault 'Rafale' and the McDonnell Douglas F15 'Eagle Fighter' and the alloys are being considered for use on helicopters³³.

The future will be based on the continued development of the 8090 and 8091 alloys with new tempers improving the quality all the time. These alloys are now beginning to form the basis of metal matrix composites (MMC).

1.3.2 Microstructure of Aluminium-Lithium Alloys

The addition of small amounts of minor metals to a base metal is known to change its properties and with skill and knowledge the basic properties can be enhanced or at least changed to suit the application that the metal will be used for. The addition of lithium in small amounts purveys special properties on aluminium such as enhanced strength and a major decrease in density. To understand such properties, it is necessary to analyse the microstructure of the alloy to establish the actions and interactions of the phases formed by alloying, and to ascertain which of these phases bestow the effectual properties.

A phase diagram must be constructed and, since some phases only occur between strict concentration and temperature limits, it is important to know the area in which the alloy being used is located. The phase diagram³⁴ for the binary system aluminium-lithium is provided in figure 1.5 and was constructed by A. J. McAlister from work carried out by a number of people over 45 years. For any alloy likely to be used in industry, the area of the diagram that is of great interest is that from 0 - 10 weight percent lithium (~30 atomic percent). Within this region the phases of interest are shown below.

- (i) α - This is based on pure aluminium with a maximum solubility of lithium of up to ~ 14 atomic percent
- (ii) An intermediate two phase equilibrium containing the lithium solution and δ an AlLi equilibrium intermetallic

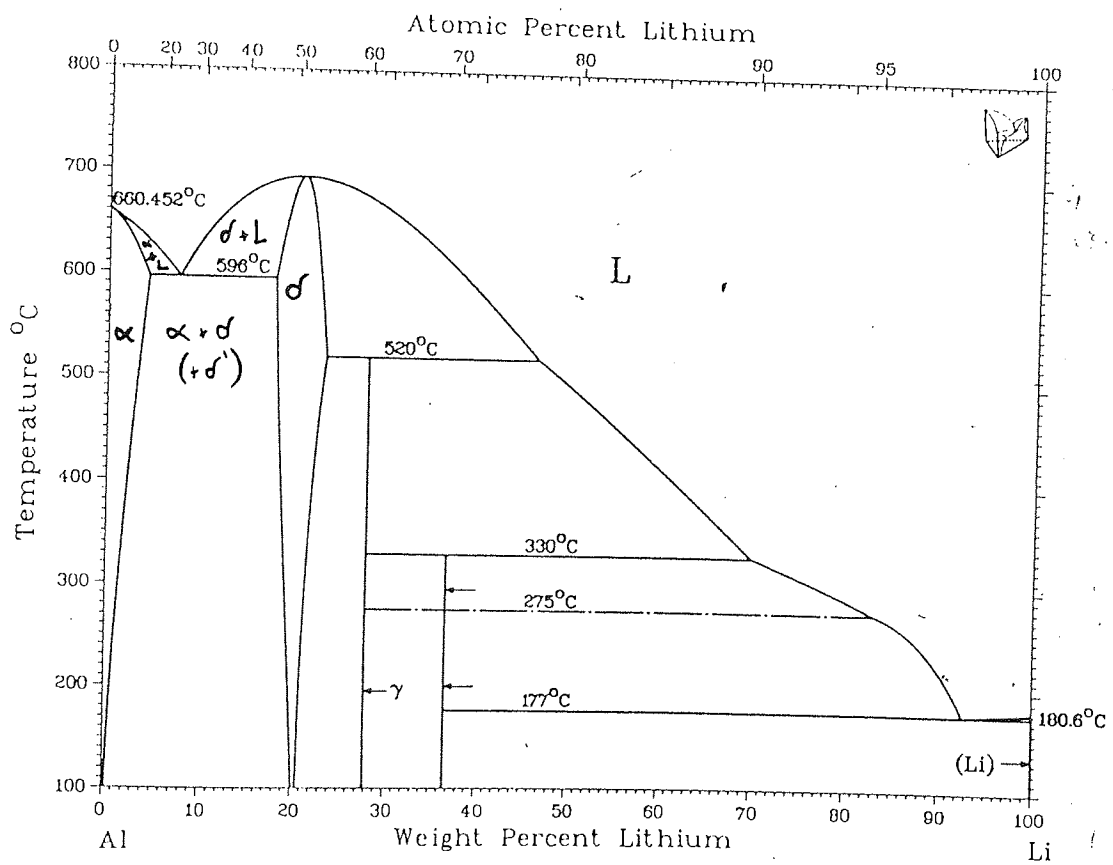
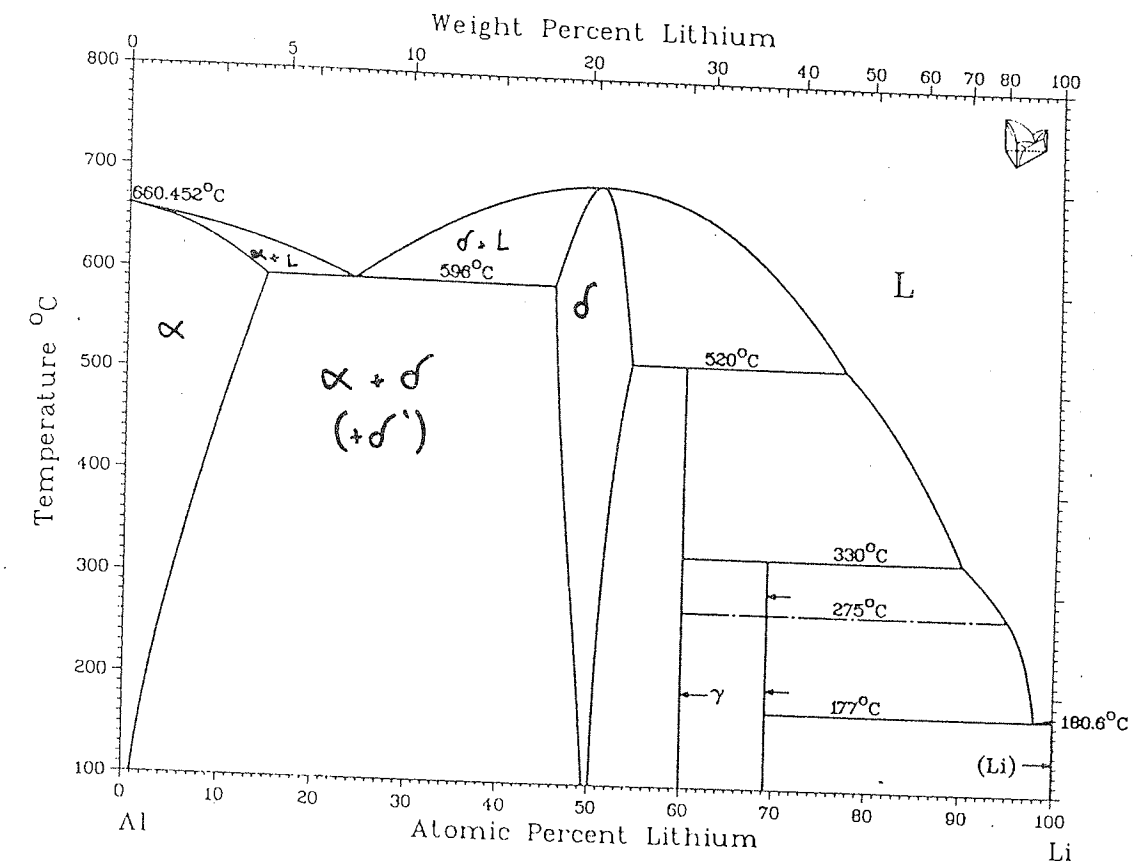


Fig 1.5 - Phase diagram for the aluminium - lithium binary alloy system

- (iii) δ' - A metastable ordered phase (not shown) of composition Al_3Li which precipitates within the $\alpha + \delta$ equilibrium.

Of these phases the most important is δ' as it is this that confers the basic precipitation hardening capability on the alloy.

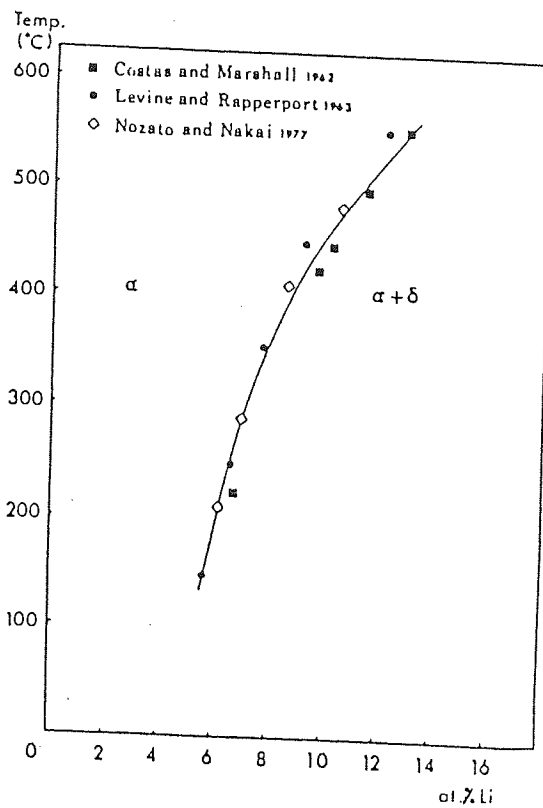
The study of the microstructure of Al-Li alloys has been carried out for many years but until ~ 1960 it was only the δ phase that was analysed. Silcock³⁵ first reported the occurrence of this superlattice δ' phase Al_3Li , as a precipitate within the $\alpha + \delta$ region. The δ' solvus line was defined by Noble and Thompson³⁶ in 1971 but it has since been redefined by Williams and Edington³⁷. Figure 1.6 shows 3 δ' solvus lines along with the δ solvus line defined in the '60's. The figure is related to the phase diagram in figure 1.4 by the δ solvus line, as this is the line separating α and $\alpha + \delta$. Therefore the two most important phases in the binary system are δ and δ' .

δ Phase

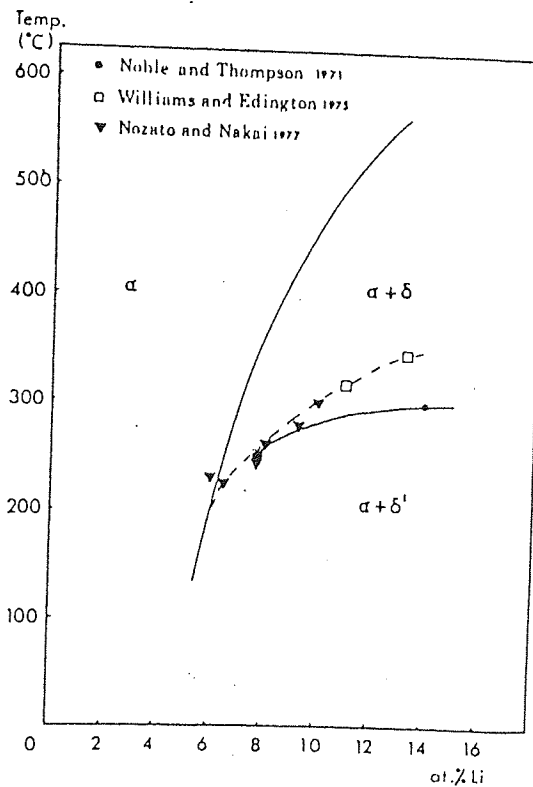
The Al-Li intermetallic phase has been discovered to be cubic with a lattice parameter of $6.37 \pm 0.01 \text{\AA}$ ^{35,38}. It was also confirmed that the structure is of NaTl type not CsCl as was first thought.

Observations of δ have been made by optical microscopy due to difficulty in thin foil preparation, but Williams and Edington³⁷ observed precipitates on grain boundaries within the matrix after relatively long ageing times. These precipitates are generally surrounded by dislocations and a δ' precipitate free zone. The large δ lattice precipitate would suggest that the α/δ boundary should be at least semi coherent giving rise to the dislocations and the more stable nature of δ would result in preferential dissolution of metastable δ' .

It has been suggested that these precipitates may be coarsened δ' but the coarsening behaviour is well documented^{36,37} and δ' particles have been observed growing to $\geq 0.03 \mu\text{m}$ whilst retaining their spherical shape. Clearly then these boundary precipitates cannot be δ' as there is no need for heterogeneous nucleation of that phase; therefore the only alternative is δ which forms heterogeneously at grain boundaries within the matrix. This will invariably result in the preferential dissolution of δ' and hence will explain the loss of age hardening with time³⁹.



(a)



(b)

Fig 1.6 - Solvus Lines for Al-Li Binary alloy a) d Solvus Line as Determined by the Most Recent Investigations. b) Three d' Solvus Lines Reported in the Literature

δ' - Formation

The process for precipitation of δ' is very uncertain but is invariably homogeneous throughout the matrix. There is doubt as to whether there is δ' formation during quenching from solution treatment temperature. Some report no δ' present³⁶, whereas others observe superlattice spots from which δ' can be imaged³⁷. Nozato and Nakai⁴⁰ proposed that the supersaturated solid solution α , undergoes a series of precipitation processes through GP1, GP2 and δ'' prior to δ' formation.

The possibility of a continuous ordering process similar to spinodal decomposition cannot be ruled out but resolving the difference between this and nucleation and growth would be difficult due to the elastic isotropy of the Al lattice. Small Angle X-Ray Scattering (S.A.X.S.) is probably the only technique capable of distinguishing unambiguously between the two, but given the rapid precipitation rate even this technique may even be inconclusive.

$\delta' \rightarrow \delta$ Transformation

It has been suggested that there is a possibility that δ can form directly from δ' but only one group has proposed a mechanism⁴¹. This involves several assumptions:

- (i) - δ' is not stoichiometric
- (ii) - δ' has sufficient vacancies to allow the absorption of lithium to create δ stoichiometry
- (iii) - δ' continues to absorb Li by substitution for Al
- (iv) - a two stage shift of the $(111)_{\text{fcc}}$ planes occurs to give a hexagonal or body centred monoclinic structure followed by a translation to $(010)_{\text{bcc}}$.

Unfortunately there is no conclusive evidence to support this mechanism. Alternatively, it has been proposed⁴² that δ nucleates independently of δ' and grows by the dissolution of surrounding metastable δ' .

1.3.3 Casting Problems Associated with Al-Li Alloys

It is often overlooked that when dealing with a commercial Al-Li alloy, before any extruding, rolling or other wrought process can be performed, the alloy itself must be made. This involves casting, and in this case, ingot casting. To get such alloys as X2020 and 8090 into commercial use a method of casting had to be developed and this involved overcoming several problems unique to Al-Li alloys.

The affinity of lithium for oxygen and water causes problems for foundrymen. In a scaled down controlled environment the casting can be carried out in an enclosed area filled with an inert gas such as helium or argon and this was described by Divecha and Karmarker⁴³. They were able to carry out small scale alloy manufacture in a dry box with helium atmosphere. The method they propose is fine for simple batch processing on a small scale in a foundry providing a dry, oxygen free helium/argon atmosphere can be maintained around the lithium. A problem that may be difficult and expensive for batch processing. An alternative would be continuous or semi-continuous casting. Most aluminium-lithium producing foundries employ semi-continuous casting⁴⁴ and mostly of the vertical type, although more horizontal types are being used. It is utilised in the production of thin strip that can then be processed further into a usable form. There are problems involved with this process also but they are not directly related to Al-Li alloys specifically and therefore will not be dealt with here.

A further problem that must be addressed that is directly related to Al-Li alloys is the choice of crucible material. Most crucibles use a mixture of insulating silicates and aluminosilicates⁴⁷ but these cannot be used for the lithium alloys due to reactivity as will be seen later in this volume. Divecha and Karmarker suggest the use of iron or tantalum crucibles but then withdrew the iron suggestion as there is considerable pick-up due to its solubility in aluminium. From an insulation point of view SiC crucibles or amorphous carbon would be better agents with lower reactivities than the silicate type.

Treatment of the melt prior to pouring also causes immense problems when applied to Al-Li alloys. When an alloy is melted reactions occur that create an imperfect product. The two major worries are the pick-up of gases from the surrounding atmosphere and the development of insoluble inclusions within the melt. These need to be removed before the metal can be poured.

The control of soluble gases mainly centres around hydrogen and oxygen. The removal of hydrogen is carried out using one of two methods. The first is to control the atmosphere - this can be done by increasing the oxygen content above the melt ensuring the hydrogen is burnt off. This also increases the oxygen content of the melt preventing hydrogen from dissolving. This method is highly unsatisfactory for Al-Li melts as the presence of oxygen in a damp atmosphere would increase oxidation of the lithium. Nevertheless hydrogen does get into the melt as (i) it was probably present in the solid aluminium ingot prior to melting and (ii) Al-Li alloys have a high hydrogen pick-up rate (100 times that of aluminium itself). The second way to eliminate hydrogen is to purge with an inert gas, argon or helium being the ideal choice. This subject is also tackled in section 1.5.

Inclusions such as insoluble oxides and solids from the atmosphere and crucible surface are removed by the addition of a cleaning agent. The cleaning agent for Al-Li alloys is a mixture of LiCl and KCl. The salts create dross and slag on the surface of the melt which can be removed manually before pouring.

The introduction of the metal to the ingot mould has been simplified by the introduction of semi-continuous direct chill casting since the metal can be introduced to the mould without further contact with the atmosphere. If batch casting is to be carried out the moulds used are not critical, as where direct chill is concerned there is little time for any adverse reaction and the moulds chosen are usually iron or brass in construction. One must be careful of the atmosphere again and the mould must be purged with helium or argon before pouring and attention must be paid to the area around the casting as even a short exposure to the air can cause sufficient oxidation to harm the ingot quality.

1.4 Defects⁴⁵

1.4.1. General Defects

Whenever a foundry carries out a casting run there is always the possibility of defects in the finished articles. This is particularly so if the casting is a new item and the procedure is not known in sufficient detail to predict any problems. Problems can occur when there is a fault in one or more of the following casting steps.

- (i) Design - The design of the casting is important and several of the problems outlined later in this section can be caused by poor design. In some cases they can be remedied by special foundry techniques but if the design is fundamentally bad then there is usually a higher incidence of scrap and inevitably higher production costs. The most common defects observed due to bad design are shrinkage cavities, shrinkage porosity, hot tears, cracks and blowholes. It should be noted also that a good design can also have a beneficial effect on misruns, cold laps, drops, swells and warped castings.
- (ii) Mould Preparation - Incorrect mould preparation such as low permeability of the mould due to high packing or low strength from insufficient ramming, too high a binder to sand ratio, poor application of mould dressing, inadequate venting and poor choice of materials all contribute to

several defects exhibited by castings. Examples are blow holes, contraction crack, hot tear, shrinkage porosity and veining.

- (iii) Melting - Poor melting procedure tends to compound rather than cause defects and are generally found in conjunction with other foundry mispractices when searching out reasons for problems. There are usually three main causes of defects which are: too high a temperature, too low a temperature and inclusions in the metal as it is poured. These inaccuracies contribute to such defects as blowholes, cold shut, gas holes, misrun, shrinkage cavities, shrinkage porosity and veining.

Once a defect occurs in a casting the cause must be determined quickly and a remedy sorted out, essentially to keep running costs down. Most of the defects mentioned above are common occurrences and the problems associated with them are well understood. In order to give the reader an idea of how and why defects occur and what is done to correct them several examples have been provided in this section.

Blowholes

Blowholes in casting may be large or small, they are usually rounded and smooth, holes within the body of metal. If they are large they are usually attributable to trapped air in the mould and several remedies are available. Designing a vent at the place the blowhole occurs is one method but increasing the permeability of the sand (if a sand mould is being used) is an alternative. Also avoidance of turbulent or rapid flow of the metal into the mould is a precautionary measure.

Generation of excessive gases from the mould is another source of this defect and this can be caused by too much binder. It can be remedied by using less binder or ensuring that the binder is properly mixed and that the mould is properly vented and permeable.

Too high a pouring temperature can create a reaction with the mixture in the mould, especially if the metal has not been deoxidised properly. The course of action to stop this is to make sure the metal is deoxidised and to reduce the pouring temperature.

Cold Shut

This defect can be seen on the surface of a casting as a pseudo-crack, but is actually a point where two streams of metal meet and do not join, due to formation of an oxide surface on the

metal streams. It is caused by either the metal being too cold as it is poured, an interrupted pour or by using an unsuitable alloy with a high freezing point.

The remedy for this defect is to increase the pouring temperature where possible and/or the number of ingates on the mould. The alloy composition must also be checked.

Contraction Crack

This problem occurs when there are restrictions within the mould. A crack forms by the metal pulling itself apart whilst cooling in the mould or shortly after its removal. It must not be mistaken for hot tear which occurs earlier in the cooling process. Suggested remedies for this problem are to use weaker sand for the mould (see section 1.5) and to make sure that bars in the moulding box do not restrict contraction.

Gas Holes

Gas holes are usually small spherical holes distributed throughout the body of the casting. They can be distinguished from blowholes by the fact that they are evenly distributed and not restricted to localised patches. The cause is due to gas in the metal and the obvious remedy is to make sure that the metal is degassed sufficiently and to make sure that all casting equipment is dry.

Hot Tear

Hot tear occurs when the cooling metal is put under tensile stress whilst cooling and as solidification takes place the metal is torn apart. It can usually be distinguished from contraction crack by its uneven edges and oxidised surface whilst the crack has neither of these. Hot tears are caused by hindered contraction within the mould and formation of hot spots. Prevention can be attained by making the cores and the mould more collapsible and by redesigning the mould to prevent the occurrence of steep thermal gradients within sections of the cooling mould.

Misrun

This defect is an incompletely filled mould cavity. It causes lugs, corners or thin edges to be not filled out or a smooth irregular shaped hole with rounded edges through the wall of a casting. It is caused by the metal solidifying in the mould before it has had chance to fill the cavity. The problem is an extreme example of cold shut and the remedy is the same, increase the pouring temperature and/or increase the number of ingates and check that the alloy used is not a high freezing point alloy.

Shrinkage Cavities

A shrinkage cavity is formed when the last pool of liquid metal in the mould transforms to the solid state. The cavity is formed when there is a lack of direction to the solidification ie. towards the ingates and risers. This problem usually affects heavy sections of castings. The defect can again be caused by too low a pouring temperature and incorrect gating and riser positioning. To cure, the metal temperature should be increased and ingates should be placed adjacent to heavy sections, each with an individual riser if possible.

Veining

This is shown by rough irregular fins found on the cored surface of a casting. They are caused when metal penetrates into cracks due to differential expansion of the core. It is accentuated by high pouring temperatures, hard baked cores and by the use of certain base sands. It is also usually only found on iron castings. To cure the problem a lower casting temperature will help but this is not always possible. An addition of iron oxide to the core is beneficial, and sometimes the use of zircon sand is recommended.

Warped Castings

This is where a deformation is experienced in a casting which develops between solidification and room temperature. This defect is inextricably linked with bad design. There can be uneven cooling in the casting due to a bad design putting stresses into the casting and there can also be uneven distribution of metal during pouring. Premature exposure of the casting or parts of it to the atmosphere can create differential stresses as can restrictions caused by projections within the casting such as phlanges etc.. Remedies are making suitable cambering allowances on the pattern and modifying ingates to give good metal distribution.

Dip Coat Buckling

The defect is manifested as a rough irregular projection on the surface of the casting and also shows veining around the edge. This defect is exclusive to investment casting and is caused when there is insufficient packing of the backing material behind the dip coat layer and the mould collapses under the weight of the metal. It can also be caused when there is a difference in the thermal expansion between the dip coating and backing material. To remedy it there should be checks made to ensure the thermal expansion rates of dip coat and backer are similar and that there is sufficient packing/bonding between the backing material and the dip coat. If necessary double dip the areas of weakness for added strength.

1.4.2. Aluminium-Lithium Defects

Most defects listed in section 1.4.1. can apply to aluminium-lithium alloys. A different problem for this type of alloy concerns the metal interacting with a mould surface as it is introduced to or whilst it cools within it. This problem, known as metal-mould reaction is not new and was encountered some years ago with aluminium-magnesium alloys. Magnesium has a diagonal relationship with lithium within the periodic table and hence various reactions are known to be similar for both metals. The problem exhibited by the magnesium alloy manifests itself as a ring of subsurface gas holes with black MgO inclusions. The defect is nearly always invisible on the surface of the casting and machining would be necessary to view it, but sometimes pinholing is witnessed giving evidence towards the serious subsurface defect.

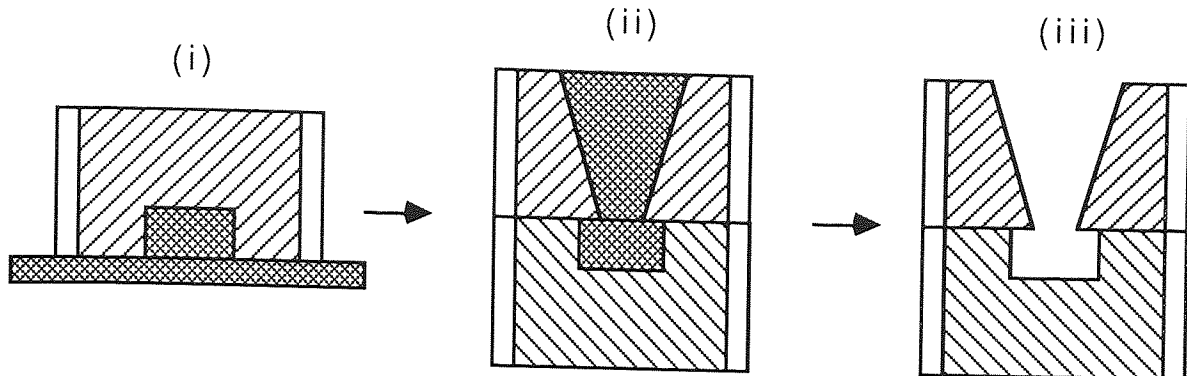
The cause of this defect in the magnesium alloy is given as⁴⁶ the result of the extreme reactivity of the alloy with the steam evolved at the mould face to form magnesium oxide and nascent hydrogen. The hydrogen is immediately absorbed into the metal forming gas holes, the magnesium oxide remaining as the black inclusions. Whilst this reasoning is no doubt true it is likely that in the case of the aluminium-lithium alloy the reaction must also involve the constituents of the mould, particularly in the case of investment casting where pre-casting preparations would almost certainly remove all traces of water. Given the chemical similarities of lithium and magnesium it is probable that magnesium alloys exhibit some reaction with the mould, even if it is to a lesser extent.

1.5 Chemistry of Casting^{48,49}

The art of casting aluminium-lithium alloys or any other metal is complex. There are 3 basic stages : (1) Mould Preparation (2) Melting of the alloy (3) Pouring, Cooling and Recovery of the finished casting.

The first stage in founding is the production of the mould. In its entirety the mould contains an impression of the casting and provisions for metal flow and feeding. A pattern is required for this and it is at the design of the pattern stage that the design of the whole mould is determined. The shape and size of the casting will determine the outlay of the pattern and how it is fed and gated. In turn the size and shape of the pattern determines the selection of the moulding box. In industry, economics takes high priority and the mould must be economic. The most space saving box must be chosen. The more patterns a box can hold, the less sand it requires and less moulding operations are needed.

There are three types of moulding technique but only one need be mentioned here. Loose pattern moulding is the simplest form of moulding and the parting line is formed during the sequence. The mould parts are rammed one on top of each other with a moisture resistant parting powder used for separation.



It is important here to mention what is actually in the mould material. Sand casting is a very broad base term but it is possible to break it down into two types, naturally bonded sands⁵⁰ and synthetic sands⁴⁹. Naturally bonded sands have deposits of clay associated with the refractory grain (sand particle). Addition of water forms a good bond but permeability and refractoriness are reduced.

Synthetic sands are the most widely used in foundries today. They are based on silica sands with minimal natural binders, and additions made to build up the strength and other properties (shatter index, permeability, moisture content). This obviously gives greater flexibility to the sand.

The refractory base has characteristics that are critical to casting and these are chemical composition, mechanical grading and grain shape. Composition affects refractoriness most and for maximum refractoriness feldspars, micas and alkali fluxes should be low in abundance. Ideally a high purity silica sand plus a minimum addition of binder is sought after. Grain size is of greater importance than composition. It can affect the moulding properties of the sand, most importantly, strength. The finer the sand, the stronger the mould (within strict limits). Probably more evident is its effect on permeability and surface fineness. Here the finer the sand, the better the finish to the casting. It can be seen that there is an inverse relationship between the strength of the mould and the surface finish of the casting over a range of grain sizes so it is important for the foundryman to choose the grade of his sand carefully for the type of casting he wants. Grain shape is pertinent to strength. This is due to packing reasons and it can easily be seen that round grains give better strength characteristics than angular grains.

The refractory grains do not form a strong mould on their own and a binder is required. Since these are not highly refractory, the required strength must be obtained with minimum addition.

Substances in use today are clays, resins and silicates. Clays are used to a lesser extent but have the advantage that the original bond can be regenerated by the addition of water. Other binders create irreversible bonds and the moulding materials must be discarded after a single casting run.

The addition of the resins and silicates is in a liquid form and the aim is to finely coat each grain. A curing agent is usually added i.e. methyl formate for resins, and esters for silicates. On compaction a lens like point of contact is formed. The more contact points, the stronger the bond. Normally the binder is left to cure and this can take anything from a few minutes to about an hour depending on the curing agent used. If an instant cure is required then the curing agent can be gaseous. The binder is added to the sand, the mould is rammed and then instantaneously cured by either amine gas for a resin or carbon dioxide for silicates.

A chosen binder must perform to certain standards. It must not breakdown on exposure to heat such as to cause the mould to collapse. There must be minimal evolution of gas and it must not react with the molten metal or leave a deposit on the surface of the casting.

Once a mould is complete it is ready to be presented to the molten metal, but before that can happen the metal must be melted and a lot of preparative work must be done before it can be poured. Initially a furnace must be chosen to carry out the melt and this is dependant on several factors such as metal quality, production requirements, alloy type and cost. It is not strictly a case of economics here, the finished casting does come first. There are different types of furnace that can be chosen, the hearth type, rotary type, crucible type and induction type. The furnace chosen must control the composition, i.e. losses of volatile metals and cleanliness. The crucible furnace is much better than the hearth furnace for this and would generally be chosen for good quality castings. This is due to the charge being isolated from the combustion process (heating process), and modern crucibles are highly impermeable to contaminants. For aluminium-lithium casting a crucible furnace would certainly be used due to lithium being extremely volatile and reactive to many contaminants (eg sulphur). Electric melting is not used as this type of melting is subject to the absorption of atmospheric gases due to the arc, which again will react with the lithium.

The furnace charge consists of pre-alloyed 'pig' or 'ingot', virgin metals and scrap from external sources or internal fettling operations. Externally supplied pig, ingot and alloy additions are supplied to certified analyses. Melting depends on the state of division as well as the composition of the charge. Large pieces have small surface areas and are therefore least susceptible to melt losses and contamination. Finely divided bulky material such as swarf or turnings are less satisfactory. They are readily absorbed in the melt, but introduce the factors of gas contamination.

Conditions can be varied in respect of the time-temperature sequence, the use of slags and fluxes, and the atmosphere in contact with the charge. The furnace atmosphere can contain water vapour, CO_2 , CO and SO_2 as products of fuel combustion plus normal atmospheric gases. The most common reaction experienced is between the melt constituents and oxygen present in the atmosphere and refractory linings. In the case of aluminium, stable oxides are formed at the surface and solubility of undesirable gases is negligible.

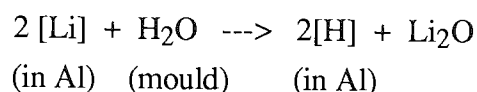
In heterogeneous reaction systems involving metal-slag or metal-gas contact, the overall reaction rate normally depends upon the rate of transport of the reacting elements to, and products from the interface. The degree of agitation and mixing is thus critical. The relationship between the various elements and oxygen is in most cases the predominant factor in melting. It affects compositional control in that losses of elements proceed at different rates. Therefore fast melting, with minimum disturbance is the aim, and this 'inert' practice is typical for aluminium alloys. Fluxes are also used as an aid to prevent gas absorption, particularly hydrogen, and these can be strongly oxidising but it is possible to use non-oxidising fluxes and control the furnace atmospheric conditions, which will minimise element losses. In the case of aluminium, strongly oxidising conditions are no protection against hydrogen absorption and degassing with a scavenger gas is required.

Gas absorption can be reduced by precautions in material selection and melting but there is always the presence of some gas in the melt. Residual gas can be eliminated by various degassing techniques, but the most effective is gas scavenging. Gas scavenging is used especially in the case of aluminium-lithium alloys where there is a particular susceptibility to hydrogen absorption. Three gases are used for the process in general aluminium alloys, argon, nitrogen and chlorine, but only argon is suitable for aluminium-lithium alloys due to the reactivity of the lithium with N_2 and Cl_2 . The technique is to bubble cylinder gas through the melt, and this provides a large gas-metal interface and general agitation.

One of the most important aspects of casting is the level of melting loss, particularly for aluminium-lithium alloys due to the high volatility of the lithium. The amount of lithium loss ranges from 0.2 - 10.7% depending on melt conditions. Control of the final composition is much easier these days since modern technology allows instant metal analysis of the melt using a cold chill. This is economically sound as the foundryman can be sure that the melt is correct on pouring. Pouring the molten metal is a crucial stage in casting, but there is little that can go wrong provided there is careful organisation and preparation.

Introduction of hot metal to the mould can result in gas blows from the sudden volatilisation of the mould constituents. This is a very direct form of gas porosity but a less direct form is via a

metal-mould reaction. Generally gas is precipitated into the surface region of the metal forming zones of porosity. These reactions are prevalent in light alloys such as magnesium and lithium alloys of aluminium. The critical reaction is between the element of highest oxygen affinity and free or combined water in the mould.



These reactions have caused many problems and much research has been carried out. This work has been summarised by Whitaker⁵¹ and Ruddle⁵². Reactions such as the one above can only proceed if there is direct contact between metal and gas. They will be impeded by oxide films and should the film be continuous then they will be checked. It follows then, that to suppress the metal-mould reaction the substitution of a surface film having the required continuity is necessary. This can be accomplished by the introduction of an alloying element with a still higher oxygen affinity than the offending element, but having an oxide with the required properties. An addition of 0.004% Be to an Al-10%Mg alloy⁵¹ satisfies the conditions and eliminates metal-mould reactions. Metal-mould reactions in light alloys are most commonly suppressed by the addition of inhibitors to the moulding sand, the aim being to replace the oxide film with an alternative compound film. Boric acid and ammonium bifluoride are suitable for this purpose⁵². Paint coatings can also be used as a vehicle for inhibitors. In magnesium-base castings, reaction is suppressed by the use of sands containing 1% sulphur combined with boric acid.

The susceptibility of a casting to gas porosity from metal-mould reaction will depend partly upon the initial gas content of the melt. Defects may be produced, even with normally acceptable levels of moisture in the moulding material, if the general hydrogen content is already close to the critical level; slight surface absorption may then be enough to produce local supersaturation on freezing.

Hopefully, an insight to the extensive chemical problems encountered throughout the casting process has been given here. No theoretical detail has been entered into as it is unnecessary for the reader to be well versed in such chemical complexities. This review should stimulate the mind to contemplate the many reactions occurring throughout the various stages and show that great care is required from both the moulder and the melter to produce a casting of quality.

1.6 Objectives

At present aluminium - lithium alloys are used for sections such as wing skins on military aircraft as they can be easily formed by wrought treatment. For more complex pieces,

manufacturers must rely on casting for their production. Strict quality requirements dictate that metallic parts must be defect free on analysis by X- rays and in order to achieve this standard, cast parts must be designed larger than necessary so that the defect affected metal can be machined off. This procedure creates a great deal of waste alloy and is carried out at great expense and noting that a 2.5 weight percent aluminium - lithium alloy costs approximately twice that of an ordinary aluminium alloy this manufacturing procedure is unacceptable, even to the Ministry of Defence.

In order to remove the defect from the casting the metal-mould reaction must be arrested. Characterisation of the reactions occurring between the incoming molten metal and the surface of the mould will allow an assessment to be made of the types of reactions causing the defect. Prioritising the metal-mould reactions will enable studies into possible corrective measures to be initiated. Any reagent used, either in the alloy or in conjunction with the mould, must not affect the surface quality of the casting, react with the incoming metal, cause problems with the casting process (i.e. reducing strip quality), or cause problems with the personnel in the area of casting, in the area near the foundry or the local environment. Any treatment should be easy to use and economic.

1.7 Other Work

Throughout the period of research it was necessary to employ solid state analysis techniques. Nuclear magnetic resonance spectroscopy was one such technique and several nuclei were observed. The analysis of solid components containing lithium is classically carried out by observing the ^7Li nucleus and the use of the alternative nucleus ^6Li has been less widely explored. ^6Li is less favourable than ^7Li in terms of N.M.R. spectroscopy due to its inferior receptivity and natural abundance, but ^6Li has one of the smallest quadrupole moments of all elements which can result in narrower spectral lines. ^6Li M.A.S.N.M.R. was employed to great effect during the research and the results obtained illustrate ^6Li ability to resolve resonances that remain masked in the equivalent ^7Li spectra.

Chapter Two

**PRELIMINARY CASTING
STUDIES**

2.1 Introduction

The casting of aluminium-lithium alloys into standard sand and investment moulds induces a metal mould reaction resulting in the porosity defect explained in section 1.4.2. Investigation of such a reaction requires the analysis of the casting process and this is complex in terms of its chemistry. Casting is carried out in an industrial environment where many variables exist such as melt composition, casting atmosphere, mould constituents and pouring temperatures, and from a scientific approach, no casting run can be the same as the last. In order to assess the effects of the various constituents of the mould upon the aluminium-lithium alloy the most fundamental and effective approach was to eliminate all possible variables and carry out controlled simple reactions.

2.2. Experiments with the Tube Furnace

Since the defect in question is caused by an adverse reaction between the molten metal surface and the mould surface it is prudent to investigate the type of reactions that can occur within this domain. The removal of a variable casting atmosphere, and the complexity of the alloy composition creates a situation where a simple metal can be reacted with the individual mould components in a controlled environment. Commercial aluminium-lithium alloys contain many minor additions to improve the processability of the alloy. Copper, magnesium, zirconium, silicon and iron are the usual additions. All other aluminium alloys contain these elements in varying amounts and metal-mould reaction is not evident. Assuming that these minor additions do not contribute to the reaction in any way, they can be removed from the aluminium-lithium alloy for these preliminary reactions. Aluminium can be treated in the same way, even though it is the major element in the alloy, it does not directly contribute to the defect. The casting atmosphere can be controlled by removing all oxygen, hydrogen, nitrogen and water vapour.

A series of experiments were carried out detailing the reactions between lithium metal and the individual components of sand moulds and investment moulds. A tube furnace was commissioned for this purpose. A steel tube of 22 mm internal diameter was inserted into the cavity of the furnace and a small steel boat (fig 2.1) was manufactured to fit intimately in the steel tube. The boat contained the materials to be reacted and was inserted into the middle of the steel tube. The tube was blocked at each end and an inlet and an outlet attached to allow the passage of argon which had been dried through two columns of silica gel and two columns of 4Å molecular sieve. Cooling coils were then attached at each end of the steel tube as a safety precaution. A thermocouple was inserted into the gap between the furnace and the steel tube and following a calibration experiment the temperature inside the tube was known to $\pm 5^{\circ}\text{C}$.

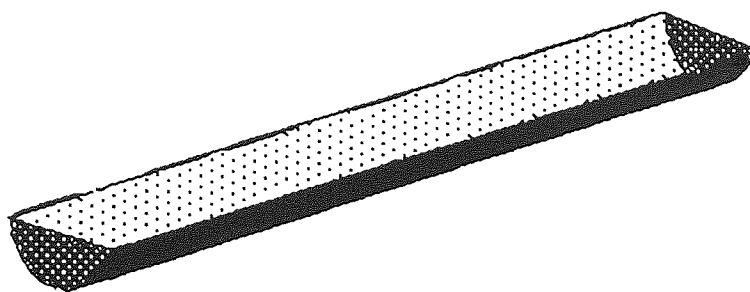


Fig 2.1 - A steel reaction boat

The mould materials to be tested were as follows : - silicon dioxide, aluminium oxide, 60 grade Buckland sand, 110 grade Redhill sand, sand binders (alphaset and betaset plus curing materials), molochite and zircosil (refractory materials used in investment shells).

The silicon dioxide was powdered α - quartz and the aluminium oxide was powdered α - corundum and they were used in a control capacity. Quartz was used primarily for its purity, but also for its superior mixing qualities with respect to sand. Aluminium oxide had been used as a mould surface wash in a previous attempt to combat the defect⁵³ and was included in the series of experiments to assess its effect. The sand used was supplied by Industrial Precision Castings Ltd (I.P.C.), Rochester, Kent. The binders had to be prereacted before they could be included in the series. Two resins were supplied by I.P.C., Alphaset and Betaset, manufactured by Bordens Ltd, North Baddesley, Southampton. Alphaset is a delayed cure resin and Betaset is an instant cure resin. Alphaset was reacted with a 10% w/w quantity of the hardener and betaset was cured using methyl formate vapour transported by a nitrogen carrier gas. The cured binders were then ground to a size of 500 μ after cooling below their glass transition temperature with liquid nitrogen.

The lithium used was finely divided by adding 3cm lengths of rod to a flask of liquid paraffin, preheated to 185°C in a silicon oil bath. After 10 minutes the flask was agitated vigorously to disperse the lithium. Spheres of approximately 500 μ were formed which were filtered from the hot liquid and stored under liquid paraffin for future use. When required, the lithium was prepared by removing the excess paraffin with petroleum ether.

Approximately 3.0 grammes of mould material was placed into the steel boat. The boat was then inserted into the steel tube in the furnace which had been preheated to 400°C. The boat remained in the tube for 30 minutes to reach ambient temperature. This procedure was to pre-dry the materials. An exception had to be made for the binders as they begin to decompose at temperatures below 400°C. After 30 minutes the boat was removed to a desiccator and allowed to

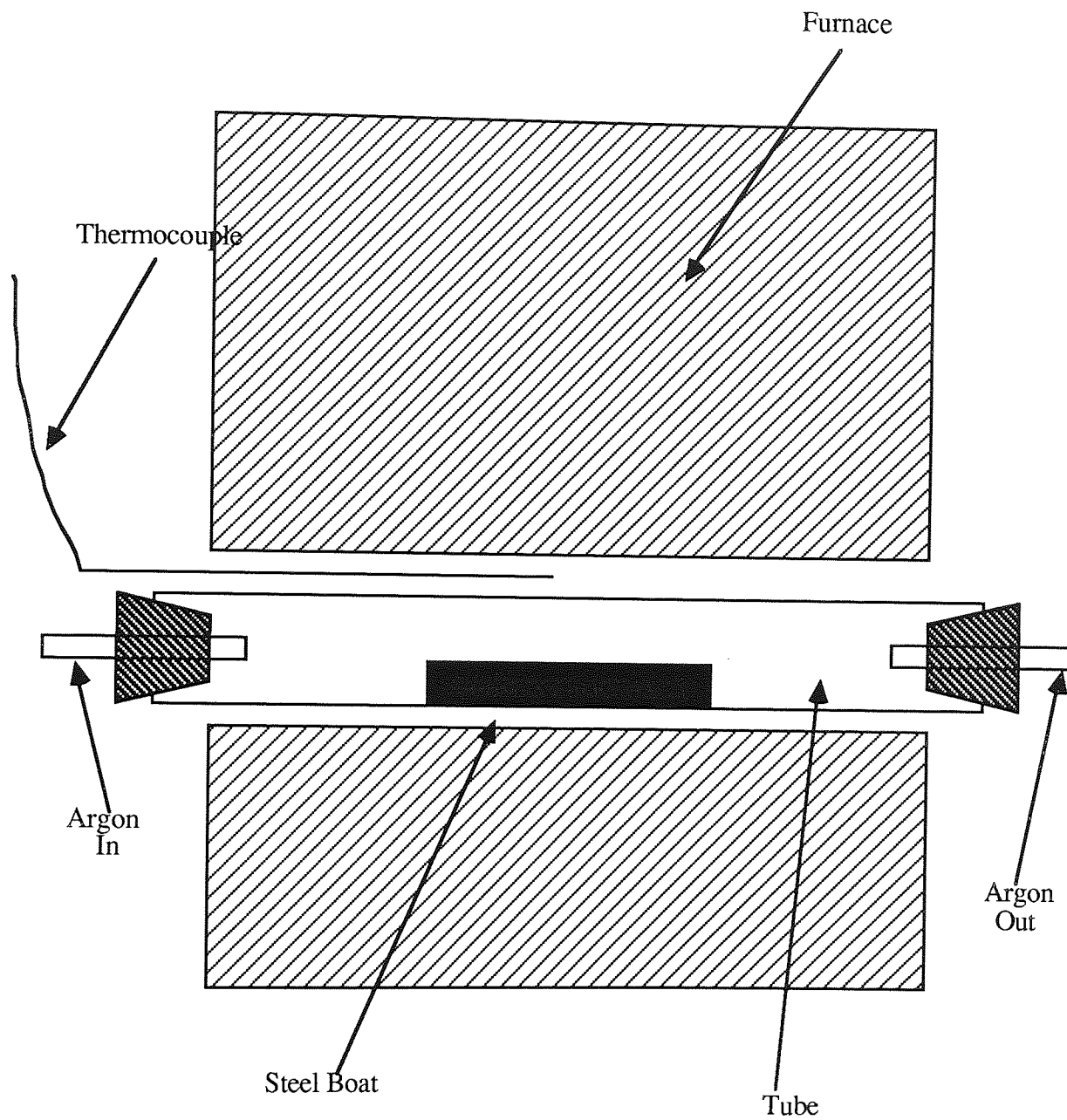


Fig 2.2 - Cross-section of the tube furnace arrangement

cool. Once room temperature had been reached the finely divided lithium was thoroughly mixed with the mould component and the boat returned to the steel tube. The dry argon flow was turned on and the reaction was allowed to proceed for 10 minutes after which the furnace was turned off and the boat was allowed to return to 20°C under argon. The boat was removed from the furnace and the product was ground, bottled and stored under desiccation for future analysis.

2.3 Analysis of Tube Furnace Products

Analysis of the reaction products was carried out using powder X-Ray diffraction and solid state magic angle spinning nuclear magnetic resonance spectroscopy (M.A.S.N.M.R.). X-Ray diffraction was performed on a Phillips X-Ray diffractometer using cobalt K_{α} radiation and the M.A.S.N.M.R. spectra were measured using a Bruker AC(E) 300 MHz spectrometer. The 'magic angle' was set with KBr and samples were packed into Delrin rotors and spun at approximately 5 kHz. The observation frequencies were 44.168MHz (^6Li), 59.628Mhz (^{29}Si) and 78.205MHz (^{27}Al). Apparent chemical shifts for ^6Li were measured with respect to a saturated solution of LiCl, ^{29}Si with respect to tetramethylsilane (TMS) and ^{27}Al with respect to a saturated solution of $\text{Al}(\text{NO}_3)_3$.

2.4 Results and Discussion

Table 2.1 shows a listing of the experiments undertaken in this study. Early reactions were carried out using lithium pieces (cube of side *ca* 4mm). Reaction was inhibited due to surface oxidation and low surface area. Finely divided lithium was introduced with the effect of gaining a more complete reaction. Typical reaction times for a finely divided lithium / silica reaction were approximately one minute and these were measured by monitoring the level of fine silica particles in the exhaust gas. The boat was left in the furnace for up to ten minutes to ensure the reaction had gone to completion. The one minute reaction time was taken as an arbitrary standard to compare the reactions of other mould constituents. When silica was replaced by alumina the reaction failed to go to completion at 400°C and the product consisted of a black flowery deposition the surface of the finely divided lithium balls. The inner parts to the lithium were unreacted and essentially recognisable as the original reagent. This contrasts to the silica reaction where the product was a grey / brown glassy material that had no defined shape and on investigation of the melting points of the lithium silicates and aluminates it can be seen that the silicates melt at approximately 1200°C, 800°C lower than the lithium aluminates. It can be concluded that as reaction occurs between the lithium and the silica the newly formed silicate material is in the molten state and able to move away from the reaction centre to allow fresh reactants to come together. In contrast the reaction between the lithium and alumina fails to create a hot enough reaction centre and the

aluminate phases form on the surface of the newly molten lithium, creating a crust that acts as a barrier between the alumina and the lithium and effectively terminating the reaction.

Reaction of the cured, ground binder resins with finely divided lithium resulted in a very violent reaction at 400°C. Throughout the reaction, which lasted approximately 30 seconds, the reactants 'crackled' continuously and an orange and purple flame was observed at the exhaust outlet. The black, charred product contained no trace of the lithium and the previously purple binder had decomposed to an amorphous ash. The flammable byproduct was either lithium vapour or hydrogen gas expelled from the decomposition of the binder. Lithium produces a carmine red flame on ignition and the flame observed was mainly orange with a purple component suggesting the cause was hydrogen. Reactions were carried out using lithium, silica and several

Reactants	Temp/°C	Atmosphere	Comments
Li + SiO ₂	400	Dry Argon	Li not fine divided
Li + SiO ₂	400	Comp Air	Violent Rn Mass increase
f.d. Li + SiO ₂	400	Dry Argon	More efficient reaction
f.d. Li + Al ₂ O ₃	400	Dry Argon	Reaction incomplete
f.d. Li + Al ₂ O ₃	450	Dry Argon	
f.d. Li + Al ₂ O ₃	500	Dry Argon	
f.d. Li + Al ₂ O ₃	550	Dry Argon	
f.d. Li + Al ₂ O ₃	600	Dry Argon	
f.d. Li + Al ₂ O ₃	700	Dry Argon	Rn compares to SiO ₂
f.d. Li + SiO ₂ + Mont	400	Dry Argon	Simulates greensand mould
f.d. Li + SiO ₂ + Hect	400	Dry Argon	
f.d. Li + SiO ₂ + Lap RD	400	Dry Argon	
f.d. Li + Redhill Sand	400	Dry Argon	Rn similar to SiO ₂
f.d. Li + Buckland Sand	400	Dry Argon	
f.d. Li + (Al) + 10% TH9	400	Dry Argon	Flammable exhaust gas
f.d. Li + (Al) + 10% TH8	300	Dry Argon	" "
f.d. Li + (Al) + 10% TH8	325	Dry Argon	" "
f.d. + (Al) + 10% TH10	325	Dry Argon	" "
f.d. + (Be) + 10% MF	325	Dry Argon	" "
f.d. Li + 30/80 Molochite	400	Dry Argon	Rn similar to Al ₂ O ₃
f.d. Li + 50/80 Molochite	400	Dry Argon	
f.d. Li + Zircosil 200	400	Dry Argon	Rn similar to Al ₂ O ₃

Table 2.1 - Pyrolysis reactions carried out in the tube furnace

types of clay to simulate the environment of a greensand mould. Montmorillonite, hectorite and laponite (a synthetic clay) were used for this purpose. The reactions took place with similar vigour to the silica and lithium only reactions. Clays are aluminosilicates in structure and hence reactions are unlikely to differ from the silica or alumina reactions. Silica was initially used as a replacement for sand to ensure intimate mixing and ideal reaction conditions, and having achieved successful reaction, sand was reintroduced to assess the affect of a larger particle size. Reaction time was again comparable to the silica reactions and the product was equally glassy. The original silica used was α -quartz and the sands were Redhill and Buckland. α -quartz is easily transformed into β -quartz at 573°C which in turn transforms slowly to β -tridymite at 867°C. It is possible and even probable that these components were formed during the reaction but to form the glass, the silica must vitrify. It is possible to melt β -quartz (1550°C) and β -tridymite (1703°C) if they are heated rapidly but it is unlikely that this occurred and it is more probable that localised vitrification resulted from the exotherms caused by reaction of lithium and silica. X-ray diffraction traces gave no evidence for the presence of α -tridymite suggesting that the reaction temperature was such that the vitrification of silica occurred without the transformation to β -quartz or tridymite, or more probably the non crystalline product was due to the vitrification of the newly formed lithium silicates.

The reaction of the investment mould constituents and lithium proceeded with less vigour than that of lithium and silica. The reaction of lithium with the molochites was slow at 400°C compared to silica and the reaction lasted for approximately two minutes. The reaction products were very similar to those of the lithium alumina reaction as were those of the zircosil reaction. The lithium balls were reacted on their surfaces with the inner metal left unreacted.

The final analysis of all the reactions carried out using lithium and the mould constituents gave the order of reaction as follows:

Organic Reagents >> Silicate Reagents > Aluminosilicate and Alumina Reagents

Powder X-ray diffraction analysis (see appendix) for the lithium / silica and the lithium / sand reactions revealed the presence of lithium silicates. Three different species were recorded, lithium metasilicate $[(Li_2SiO_3)_x]$, lithium orthosilicate (Li_4SiO_4) and lithium disilicate ($Li_6Si_2O_7$). Lithium orthosilicate exists as a series of discrete silicate tetrahedra with lithium occupying sites of co-ordination number 4, the disilicate contains a $(Si_2O_7^{2-})$ discrete unit which has a Si - O - Si link between the two tetrahedra and the metasilicate contains units of (SiO_4) sharing two oxygens with contiguous tetrahedra. The silica tetrahedra align themselves into chains with the repeat after every second tetrahedron. The ^{29}Si M.A.S.N.M.R. results confirm these findings where upfield shifts

are observed at - 107.94, -83.96, -81.46 and -16.50 ppm. Lippmaa and co workers⁵⁴ discovered whilst investigating aluminosilicates that ²⁹Si chemical shifts fell into relatively clear ranges depending on the number of further silicon atoms attached to the vertices of a given SiO₄ tetrahedron. The current nomenclature for the five possible silicon environments is Q⁰, Q¹, Q², Q³, Q⁴ where the superscript indicates the number of attached silicons. The line of greatest shift represents silicon in a Q⁴ environment and is characteristic of the original silica used as a reagent. The two lines at approximately -83 and -81 ppm are indicative of the silicon in a Q¹ environment and represents the Si₂O₇⁻ units in the disilicate. Lithium can occupy sites of co-ordination number 4 and 6 and it is this that causes the slight differences in the chemical shift values for the disilicate. The line observed at -16 ppm is that given by a Q⁰ species, a silicate containing discrete silica tetrahedra and is characteristic of the lithium orthosilicate species identified in the X.R.D..

The product of the reaction between lithium and alumina (α -corundum) at 700°C was analysed by powder X-ray diffraction (see appendix). Evidence of α -LiAlO₂ and γ -LiAlO₂ phases was observed. ²⁷Al M.A.S.N.M.R. results show a shift of some of the aluminium from the octahedral sites occupied in the corundum to tetrahedral sites in the lithium aluminates. γ -LiAlO₂ has been shown to have a tetragonal crystal structure⁵⁵ consisting of an infinite three-dimensional array of distorted tetrahedra, with aluminium and lithium atoms at the centres and oxygen atoms at the vertices. α -LiAlO₂ is reported to be trigonal^{56,57}. Each cation (aluminium or lithium) is surrounded by a distorted octahedron of oxygen ions. Every edge of each octahedron is shared with another octahedron and of the twelve edges, six are shared by octahedra of the same type and six of the opposite type. This arrangement can be considered as a slightly distorted superlattice of an NaCl structure. This structural assessment is in agreement with the ²⁷Al M.A.S.N.M.R. results showing peaks indicating Al atoms in tetrahedral (60 ppm) and octahedral positions. ⁶Li M.A.S.N.M.R. reveals the presence of a single lithium site shifted downfield to 0.724 ppm. The ⁶Li spectrum was obtained several months after the ²⁷Al spectrum and after the pyrolysis experiment was carried out. It would be expected that two distinct lines would be seen for the two lithium environments in the α and γ aluminates but it has been suggested that the LiAlO₂ phase that forms at lower temperature⁵⁶ (and there is dispute over which phase this is) is metastable at room temperature. Therefore over a period of time the lithium atoms in the lower temperature phase may migrate and a structural change may be evident. This phenomenon has been observed in Laponite, a synthetic clay containing trioctahedral structural lithiums. When the clay was ion exchanged with lithium ions it was possible to distinguish between the structural and the interlamellar lithiums by ⁶Li M.A.S.N.M.R.. Over a three month period the structural lithiums migrated to a common environment. This observation is explained in detail in chapter five.

Several cases were noted for both lithium / alumina and lithium / silica where resonances in the lithium spectra were shifted far downfield and outside the recognised chemical shift range.

Shifts of this magnitude can only be explained by paramagnetic behaviour and in this case is due to the conduction electrons of the metal itself. This type of shift is known as a Knight shift. A study of these results is given in section 5.6

Analysis of the reactions between the organic binder products and lithium proved to be difficult. The reaction product recovered from the tube furnace was a charred, amorphous mass and hence powder X-ray diffraction was of no use. ^6Li M.A.S.N.M.R. spectra gave single resonances for each binder combination but the samples proved difficult to spin and the resulting resolution is poor. Downfield chemical shift values were obtained at approximately 0.5 ppm relative to a saturated solution of LiCl. Precise values of the chemical shift should be used only with caution due to the poor resolution but values in the region of 0.5 ppm are in line with the shift values obtained for the lithium aluminates and also for values obtained for lithium / silica reactions and hence this indicates the presence of Li - O species.

Analyses of the products from the investment mould components gave similar results to the products of the lithium / silica and lithium / alumina reactions where applicable. X-ray diffraction traces gave information suggesting the presence of lithium silicates and aluminates and the N.M.R. spectra confirmed these results.

2.5 Conclusions

Under controlled conditions lithium was found to react with silica in the form of powdered quartz and sand, alumina in the form of powdered corundum, organic binder materials in the cured and powdered form, molochite and zircosil in varying degrees. Powder X-ray diffraction and M.A.S.N.M.R. analyses showed that various types of lithium silicates and aluminates are formed with the inorganic constituents and suggest that lithoxo species are formed with organic materials. The overall order of reaction was found to be:

Organic Reagents >> Silicate Reagents > Aluminosilicate and Alumina Reagents

The vigour of the reaction observed between the lithium and the binder components indicated that the primary reaction taking place on the surface of a sand mould was between alloy and binder. Secondary reactions may be occurring between the alloy and sand, but since the lithium concentration in the alloy is much reduced relative to that experienced by the sand in the pyrolysis experiments, these reactions will occur with a much reduced frequency.

The reaction observed between lithium and alumina shows that coating the surface of a sand mould with an alumina wash will only succeed in preventing the lithium / binder reaction. A metal

- mould reaction will still occur and a defect will still be observed as was noted in test castings carried out at Industrial Precision Castings Limited⁵³.

Some ^6Li M.A.S.N.M.R. spectra obtained throughout this study gave resonance lines far outside the accepted chemical shift range. These shifts were recognised as Knight shifts. They were investigated by M.A.S.N.M.R. and the results are reported in section 5.6.

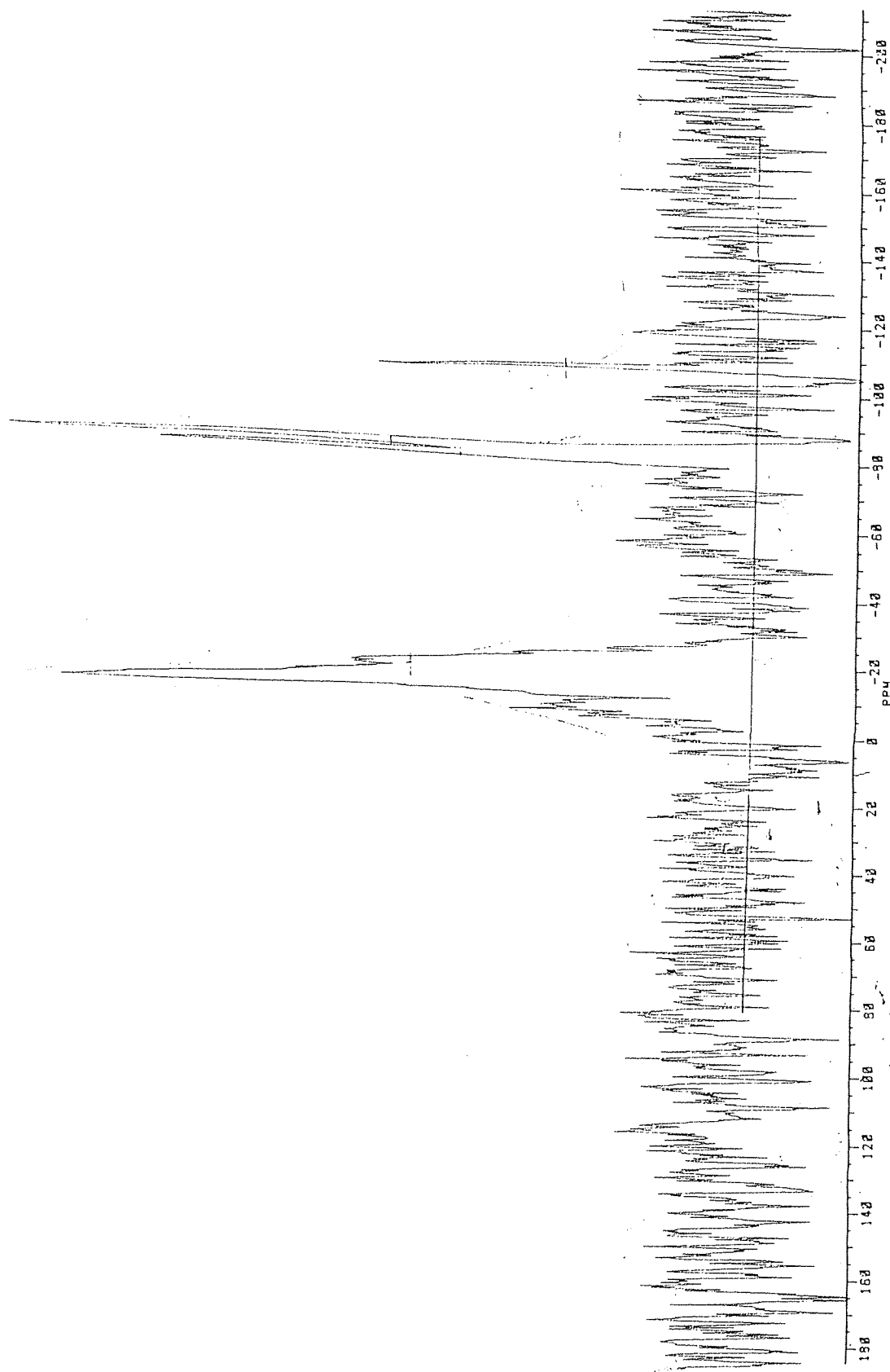


Fig 2.3 - ^{29}Si M.A.S.N.M.R. spectrum of a lithium / silica reaction showing the four different resonances revealing the presence of lithium silicates

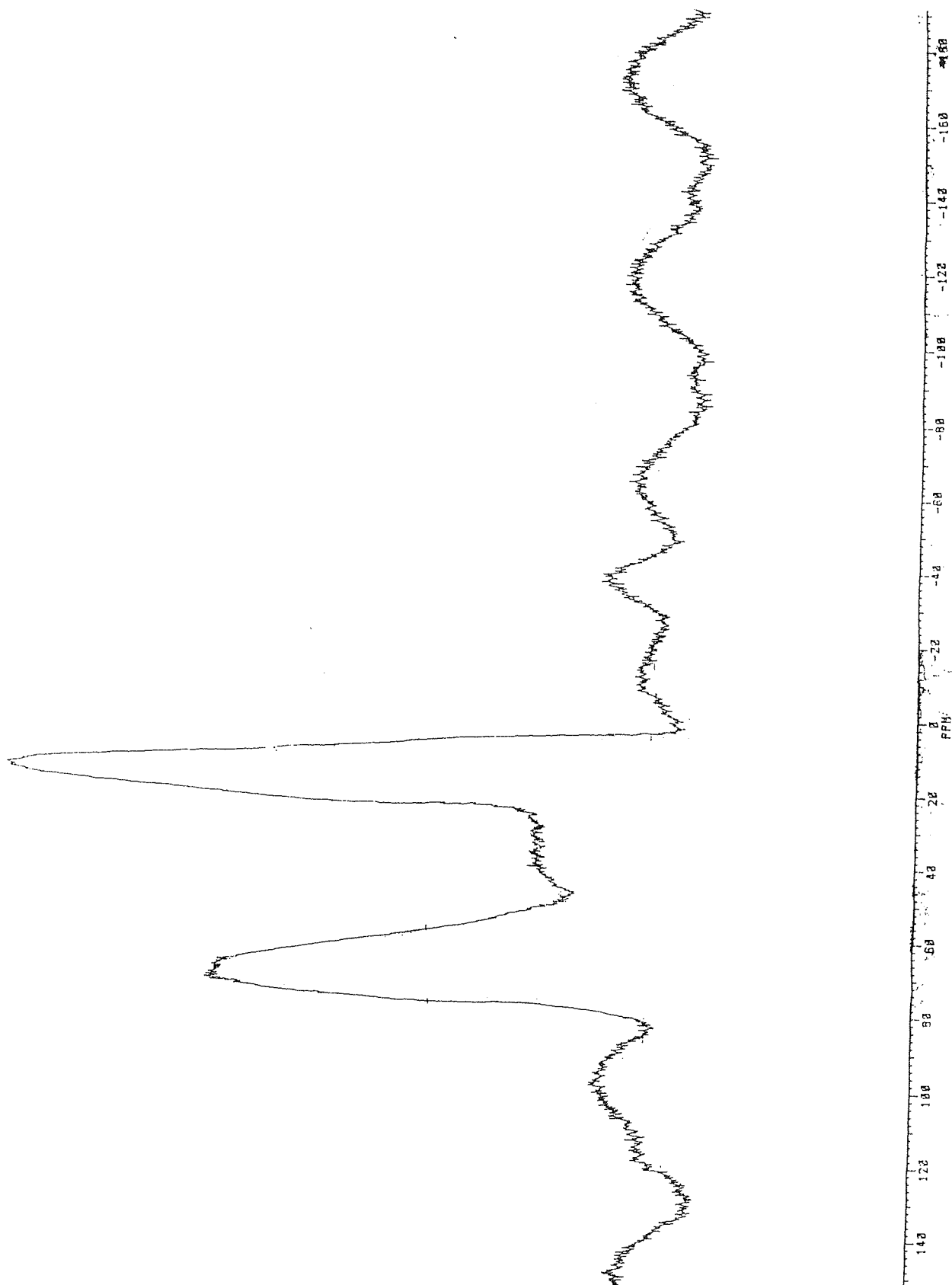


Fig 2.4 - ^{27}Al M.A.S.N.M.R. spectrum of a lithium / alumina reaction showing the peak at 70 ppm revealing aluminium in a tetrahedral environment

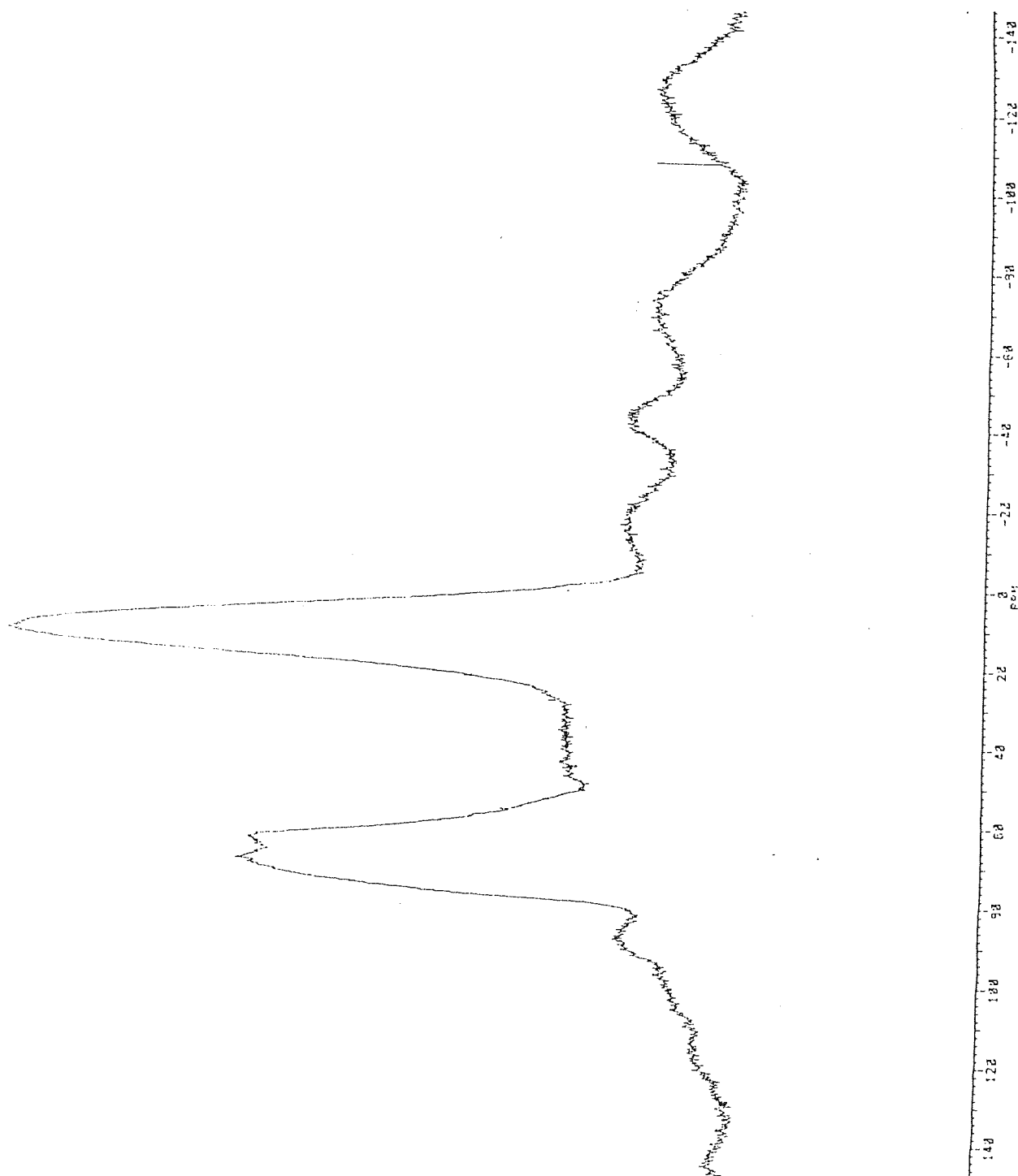


Fig 2.5 - A second ^{27}Al M.A.S.N.M.R. spectrum of a lithium / alumina reaction

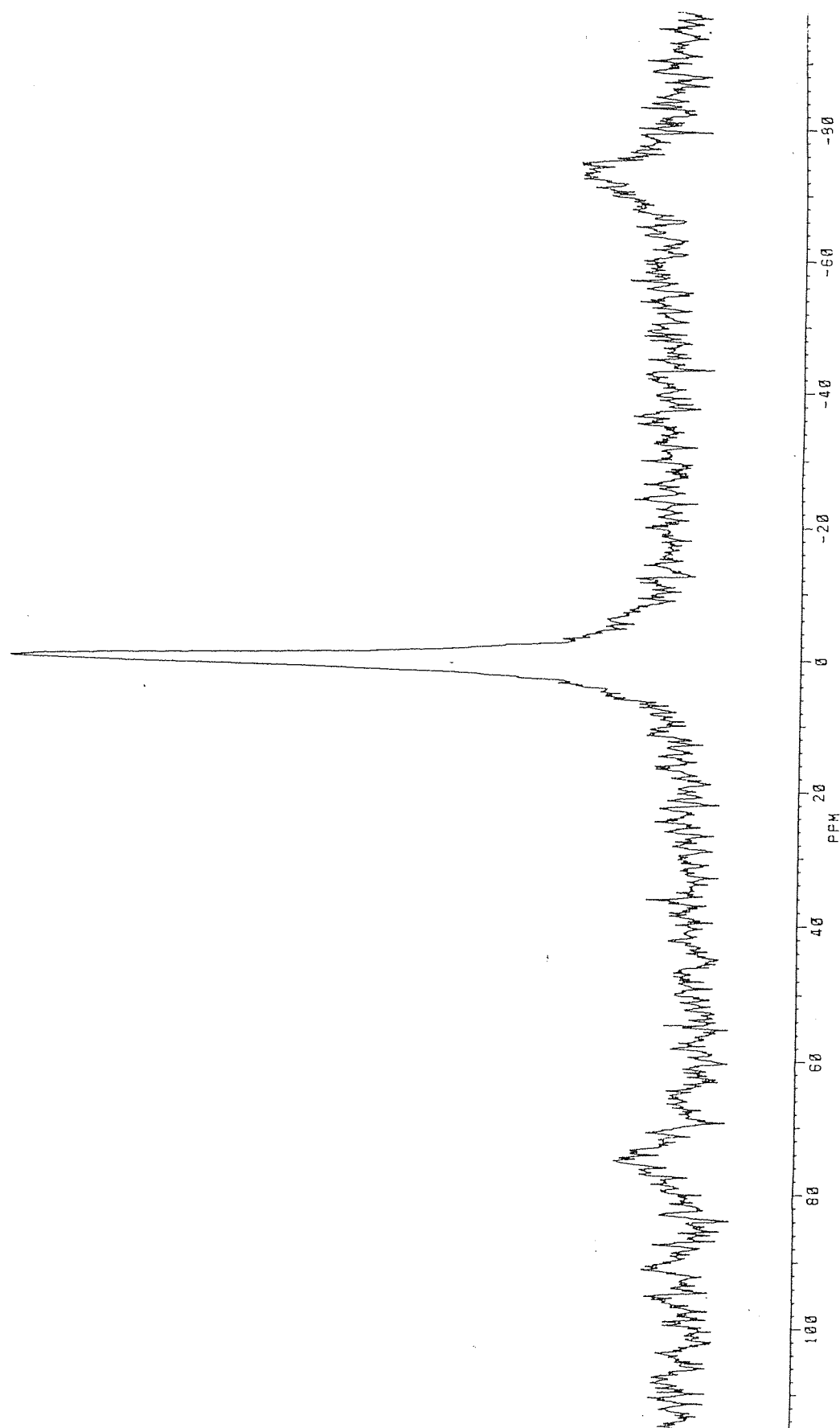


Fig 2.6 - ${}^6\text{Li}$ M.A.S.N.M.R. spectrum of a lithium / alumina reaction showing a single resonance

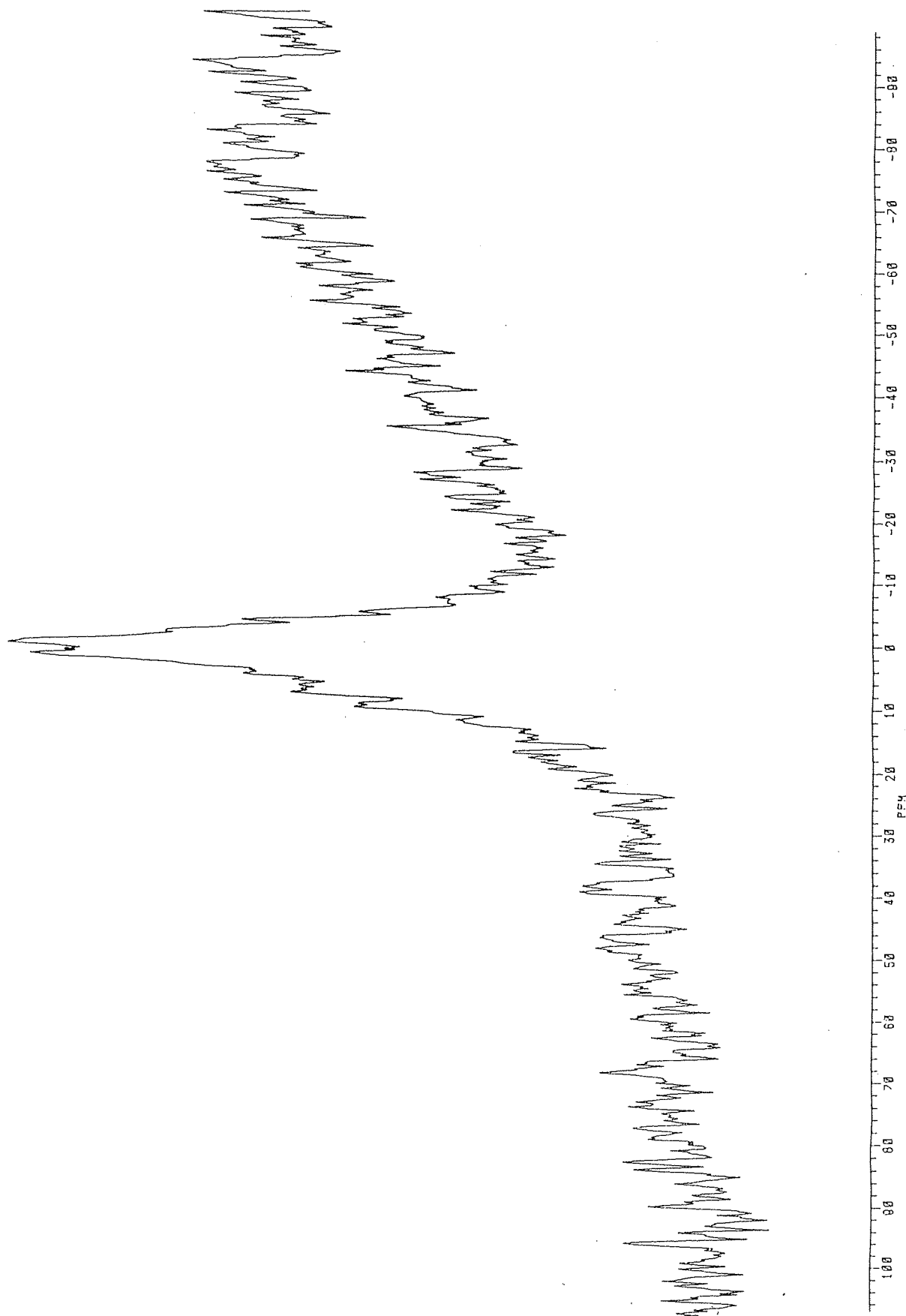


Fig 2.7 - ${}^6\text{Li}$ M.A.S.N.M.R. spectrum of a lithium / alphasat reaction showing a single resonance

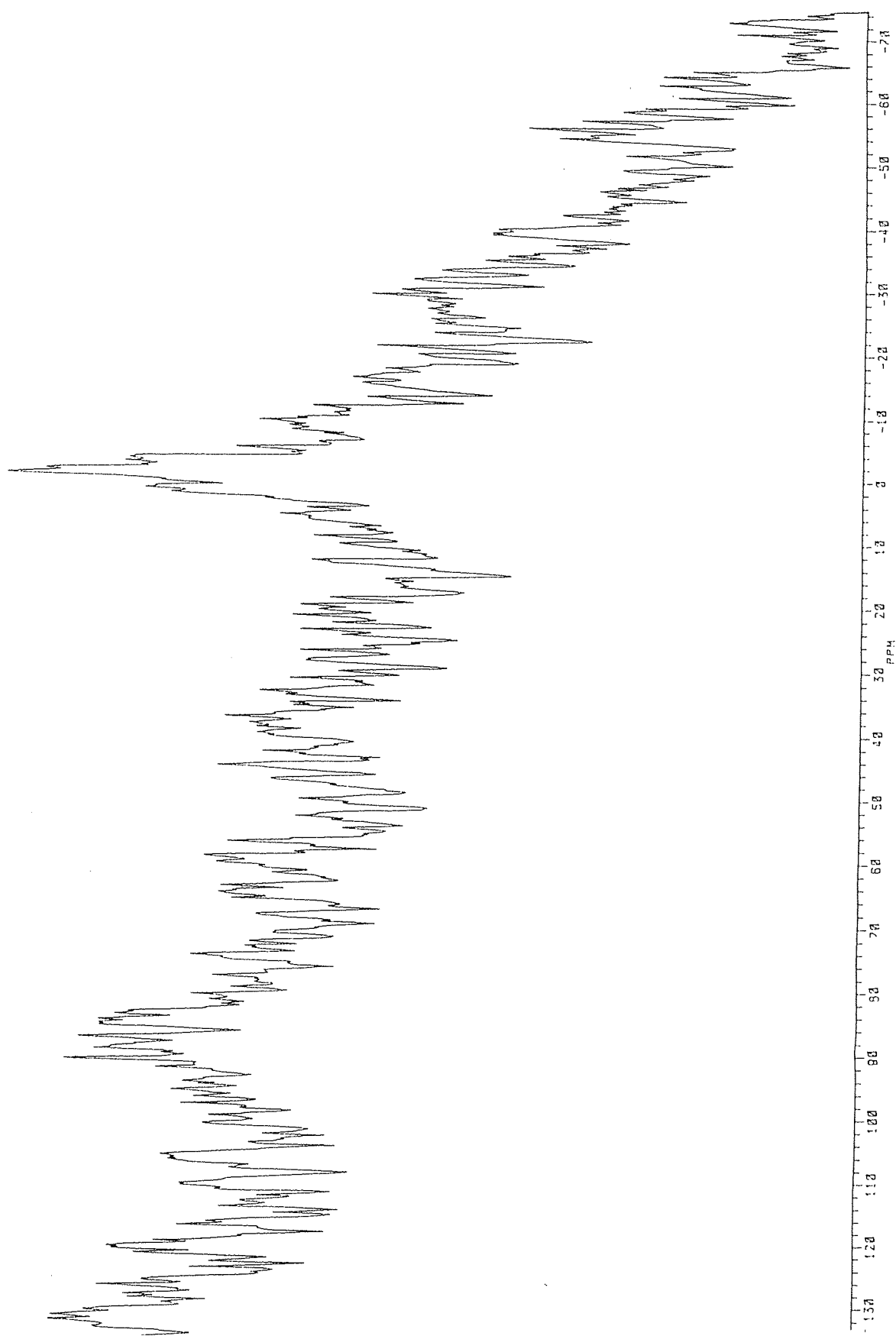


Fig 2.8 - A second ^6Li M.A.S.N.M.R. spectrum of a lithium / alphaset reaction

Chapter Three

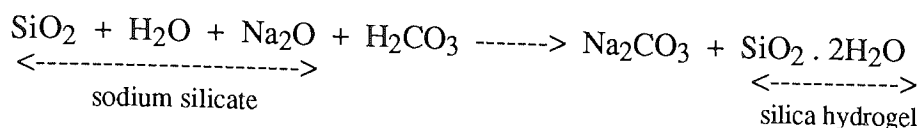
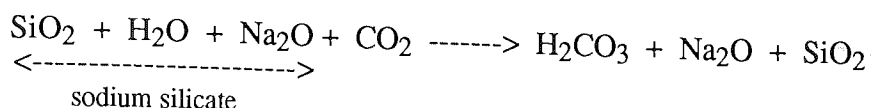
**STUDIES INTO THE
BINDER MATERIALS**

3.1 Introduction

Casting can be carried out in a number of ways e.g. die casting, investment casting and shell moulding but the most common method is sand casting. In order to cast into sand it must maintain the desired shape for sufficient time to pour the metal and allow it to cool. Therefore any material capable of holding the sand grains together during the casting process can be classed as a binder. Binders suitable for foundry use must exhibit additional properties than merely holding the grains together. They must be sufficiently resistant to temperature so as not to collapse before the metal has solidified but after solidification and cooling they must completely collapse to allow the sand to be easily removed from the casting leaving its surface smooth.

Binders can be divided into two groups; inorganic and organic. In modern foundries inorganic binders are clays and sodium silicates. Clays⁵⁸ are natural binders and function on their ability to swell on addition to water. Clays are aggregates of minute sheets having length, breadth but minimal thickness. There are two basic sheets that build into clay structures, silica sheets and alumina sheets. The arrangement of these sheets determines the properties of the clay. The sheets build into layers and these layers stack to form the clay. In theory, the charges of the silicons and the aluminiums should balance with the associated oxygens but in practice some aluminiums are replaced by magnesiums resulting in a negative charge on the layer. The interlayer region contains water molecules and those clays with excess negative charges have associated positive ions, usually sodium or calcium to electrically balance the clay. On addition of water the counter balancing ions within the interlayer region become hydrated and leave the associated negative charge on the clay layers. There is a repulsion between the layers and they are forced apart allowing more water between the layers which swells the clay. The layers will become dispersed if there is sufficient water present. Some clays are better than others for this property and illites and montmorillonites are widely used within the foundry industry. In practice the clay is mixed with the sand and a set amount of water added which 'gels' the sand. This gelling has an associated strength known as the green strength, hence the title greensand moulds for moulds with clay binders. Green strength is now a standard term applied to all binders used for sand moulds in the precured state.

Sodium silicates⁵⁹ are used as binders in association with CO₂ and ester curing systems. Sodium silicate is a ternary system comprising of SiO₂ - Na₂O - H₂O. It is essential that the silicate is a homogeneous liquid and only sodium silicates with a SiO₂/Na₂O ratio between 1.0 and 4.0 fall into this category and those used in foundries between 2.0 and 3.3. The cure is effected by forming a silica hydrogel network around the sand. The CO₂ process hardens the binder using the following mechanism:



When CO₂ is passed through the sodium silicate coated sand the gas dissolves in the water of the silicate solution forming carbonic acid. The acid then reacts with the disodium oxide to form sodium carbonate and silica hydrogel which bonds the sand grains together. The bond strength formed depends on the flow rate of the gas used.

The ester set process utilises the same chemical pathway as the CO₂ process. The ester is mixed with the sodium silicate and the alkalinity of the silicate solution causes a reversal of the esterification reaction. In conjunction with the water in the silicate solution the original alcohol and acid are formed. The acid then reacts with the disodium oxide in the same manner as the carbonic acid forming silica hydrogel. Blending several esters can give curing systems with variable setting times, a factor that can be important for moulding.

Organic binders can be divided into oils and resins. Oils are used only in a small capacity as they have been superseded by resins but small and old foundries still use them. Oils used are naturally occurring esters of glycerol and fatty acids such as linseed, perilla, tung and dehydrated castor oils. These oils dry and harden on standing and this is due to the degree of unsaturation in the oils. The more unsaturation, the greater the drying power. Once the oils are mixed with the sand the hardening can be effected using three processes. (1) stoving - where the oil bonded sand is heated to 200°C, (2) cold setting / hot curing where after initial cold setting, the final hardening occurs with a short time stove at 220°C, (3) cold curing where the final strength is obtained without heat.

Over the last 40 years oils, silicates and clays have been replaced by resins for foundry binders. This is because resins give 'in box' curing, do not have the breakdown limitations of silicates and require less skill in the production of the moulds than hand rammed greensand. Resins are more expensive than all the other binder materials but this is offset by its ease of use and lower rates of addition, 2% as opposed to greater than 3% for the inorganic binders. There are four types of resin, phenolics, ureas, furans and a specialist resin made from polyols.

Phenolic resins are a wide range of resins produced from phenol and formaldehyde and are used in several moulding processes such as shell moulding, hot box and cold box processes. There are two types of phenolic resin, Novolaks and Resoles. Novolaks are two stage resins used

primarily for shell moulding and are made by kettling or refluxing phenol and formaldehyde with a formaldehyde to phenol (F/P) ratio of less than 1. The resin produced is thermoplastic and can be melted and cooled several times without altering its properties. But when the resin is reacted with hexamethylene tetramine the resin becomes thermosetting. Resole resins are single stage resins produced under alkaline conditions from a F/P ratio of greater than 1 but less than the theoretical maximum 1.5. During kettling the resin will partially polymerise and will continue to do so in its container so it has a limited shelf life. Curing of the resin is brought about by heat or acidic conditions or a mixture of both depending on the moulding process. Where acid conditions are used the rate of cure is approximately proportional to the pH.

Urea resins bond sands using the same mechanism as resole resins. Urea is kettled with formaldehyde at a F/U ratio of 1.5 to produce dimethylol urea. This can then be polymerised using heat or acidic conditions to produce dimethyl urea with some cross-linking

Furan resins are based on the five membered heterocyclic ring furan. This is again kettled with formaldehyde to form a methylol group on the ring producing furfuryl alcohol. This used to be produced by processing oat husks but synthetic plants are now in operation. Curing is again by heat or acids producing methylene bridged polymers with some cross-linking via double bonds in the ring.

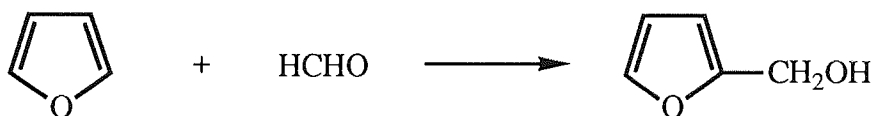


Fig 3.1 - Reaction of Furan and Formaldehyde

3.2 The Binder System

Two binder systems were used in this study. They were supplied by Industrial Precision Castings Limited (I.P.C.), Rochester, Kent and manufactured by Borden (U.K.) Limited, North Baddesley, Southampton.

- | | | |
|----------|---|--|
| Alphaset | - | A cold set phenolic resole resin. It is alkaline in pH, water soluble and contains no nitrogen or sulphur |
| Betaset | - | A cold set gas hardened phenolic resole resin. It is alkaline in pH, water soluble and contains no nitrogen or sulphur |

Betaset is cured by methyl formate a volatile ester and alphaset has a series of hardeners depending on the size of mould to be made and the length of cure time required. They are designated TH8, TH9, TH10 and cure from 15 minutes to 40 minutes respectively.

3.3 Analysis

Infrared spectra were obtained of the binder constituents using a Perkin Elmer FT1710 spectrometer. Samples of the binder products were placed between two sodium chloride plates and these were scanned from 4000cm^{-1} to 600cm^{-1} . ^1H N.M.R. spectra were obtained using a Varian 30Mhz spectrometer. Samples were prepared using no solvent in a quartz tube with tetramethyl silane as an internal standard. Mass spectral data were produced on a AE1 MS9 mass spectrometer.

3.4 Results and Discussion

Figures 3.2, 3.3 and 3.4 show the ^1H n.m.r. spectra of TH8, TH9 and TH10 respectively measured at 20°C . There are similarities between all three spectra, particularly figures 3.2 and 3.3. Both show prominent peaks at 2.1δ and 4.3δ . TH9 is a much purer mixture than TH8 as can be seen by the lack of peaks surrounding the 2.1δ resonance in figure 3.2. This is confirmed by infrared data which show a single strong resonance at 1740cm^{-1} for TH9 in contrast to two peaks at ca 1750cm^{-1} for TH8. Figure 3.4 shows a similar single resonance at 2.1δ but together with a multiplet at 4.3δ with two added multiplets at approximately 3.8δ and 5.3δ . The presence of an ester group is evident in all three hardeners due to the singlet resonance at 2.1δ and also an ether linkage due to the 4.3δ resonance.

Compound	Chemical Shift / δ	Integral value / mm
TH8	2.1 sing	67
	4.3 sing	47
TH9	2.1 sing	47
	4.3 sing	32
TH10	2.1 sing	50
	3.8 sing	23
	4.3 mult	32
	5.3 mult	-

Table 3.1 - N.M.R. Data for Alphaset Hardeners

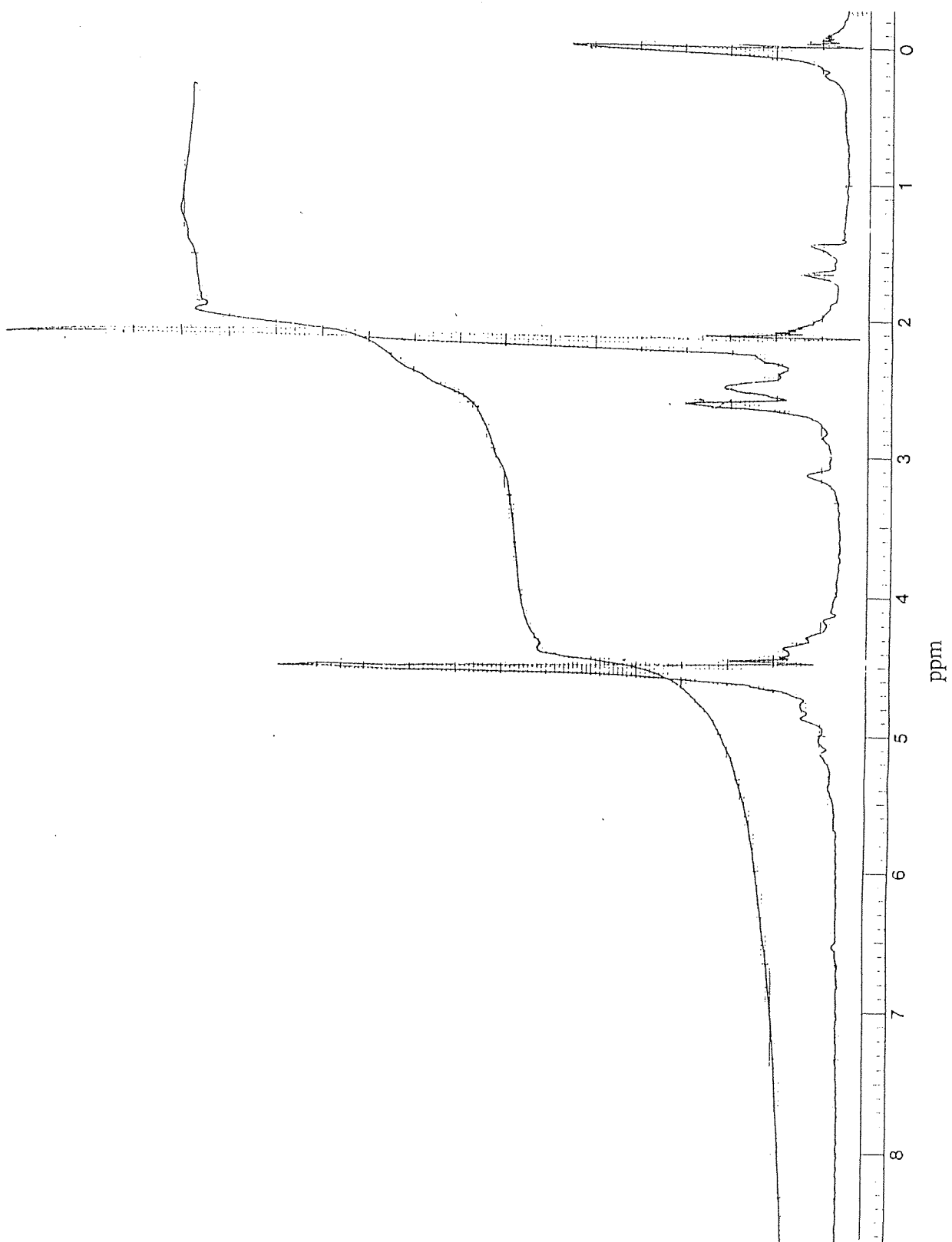


Fig 3.2 - ^1H N.M.R. for curing material TH8

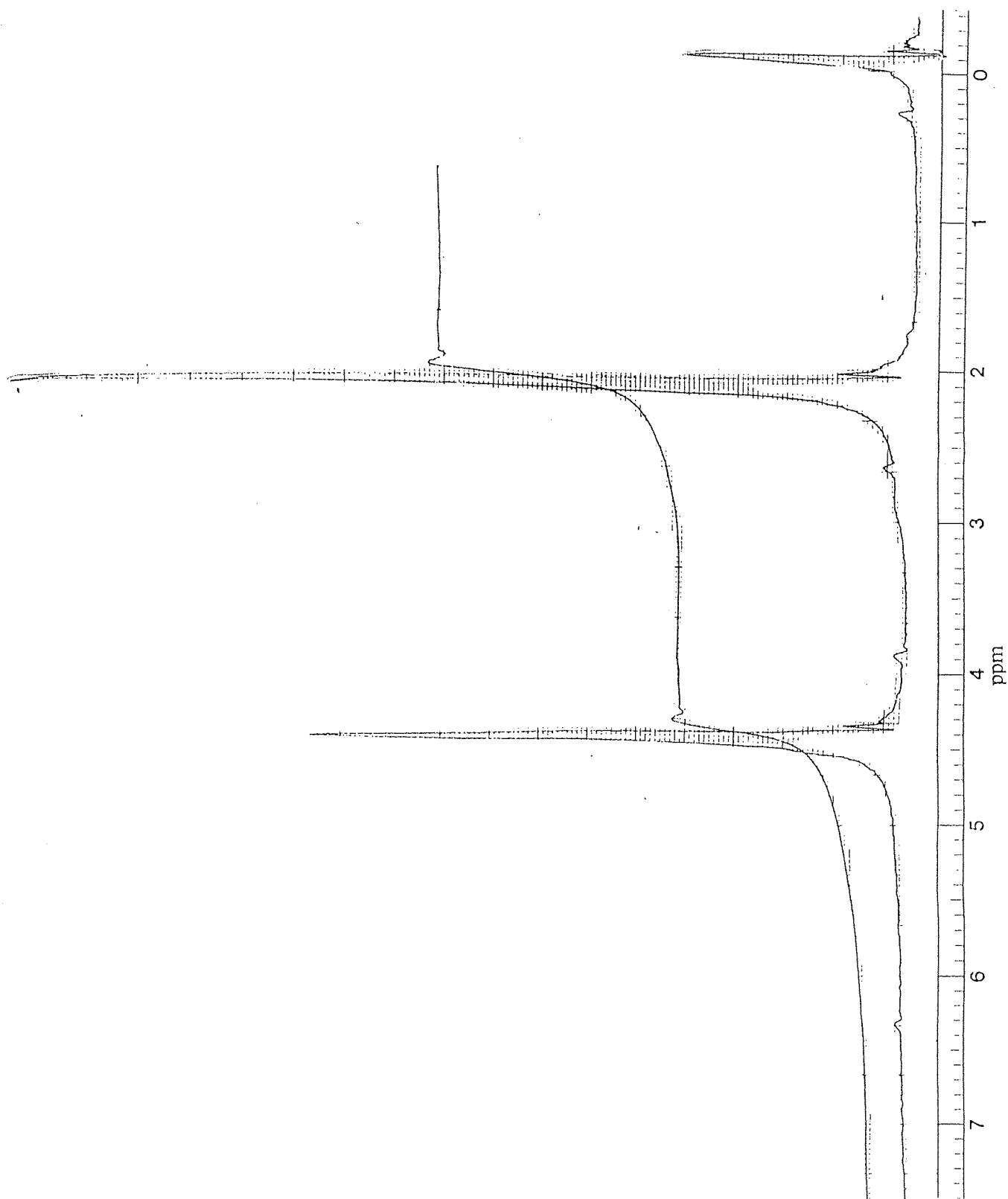


Fig 3.3 - ^1H N.M.R. for curing material TH9

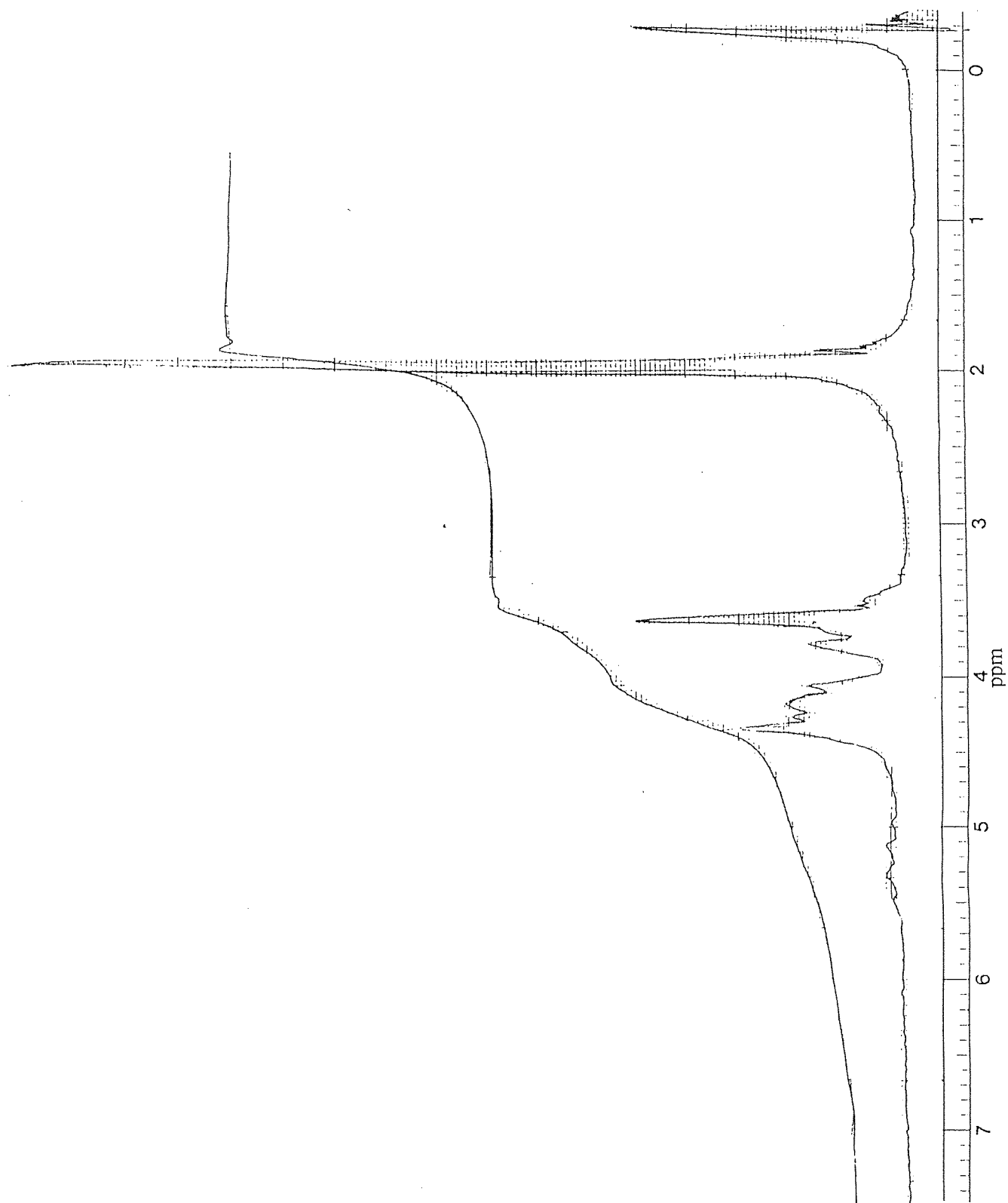


Fig 3.4 - ^1H N.M.R. for curing material TH10

Infrared gives evidence of a carbonyl group along with the carbon-carbon stretch, carbon-oxygen stretch and carbon-hydrogen stretch. Analytical data point very strongly towards an acetate group and mass spectra confirmed this with spectra matching closely to 1,2 ethane diol diacetate. Boiling point measurements were in line with that of the diacetate and hence TH9, as the pure compound, can be confirmed as 1,2 ethane diol diacetate. TH8 and TH10 both contain the diacetate in some capacity but also contain other compounds to regulate the curing time.

Compound	Infrared Frequencies / cm ⁻¹
TH8	Weak 2900 - 3000 Strong 1740 Strong 1770 Strong 1220 Medium 1165
TH9	Weak 2900 Strong 1740 Strong 1220 Sharp 1105 Sharp 1135
TH10	Weak 3000 Weak 2920 Strong 1760 Strong 1230

Table 3.2 - Infrared Data for Alphasets Hardeners

Figure 3.4 provides a spectrum that contains evidence of 1,2 ethane diol diacetate but it also provides information that is consistent with the presence of triacetin (1,2,3 glycerol triacetate). A higher boiling point in the order of 270°C indicates that this is correct.

Mechanistically it can be said that the curing reaction is identical to that of the ester / silicate binder system. The ester is added to the phenolic resin and the presence of water in the resin facilitates a reversal of the esterification forming 1,2 ethane diol (ethylene glycol) and acetic acid from the 1,2 ethane diol diacetate. The pH of the mixture is decreased below 7.0 and the condensation polymerisation of the resole begins (see fig 3.5). The speed of cure is governed by how fast the mixture becomes acidic.

Analysis of the final bonded resin was undertaken by intimately mixing a quantity of alphaset resin with a 10% w/w quantity of TH9 for a 24 hour period in order to ensure complete reaction. The product was then leached with methanol for 30 minutes to remove any excess starting material. Finally the reaction product was washed with fresh methanol and dried in vacuo. To facilitate grinding, the cured resin (a pliable polymer), was cooled below its glass transition temperature by cooling in liquid nitrogen. Infrared data produced from a KBr disc of the resulting powder provided clear evidence of hydroxide activity within the molecule, this being primarily from the phenolic hydroxide groups but some aliphatic activity will contribute from unreacted ortho methoxy groups (see fig 3.5).

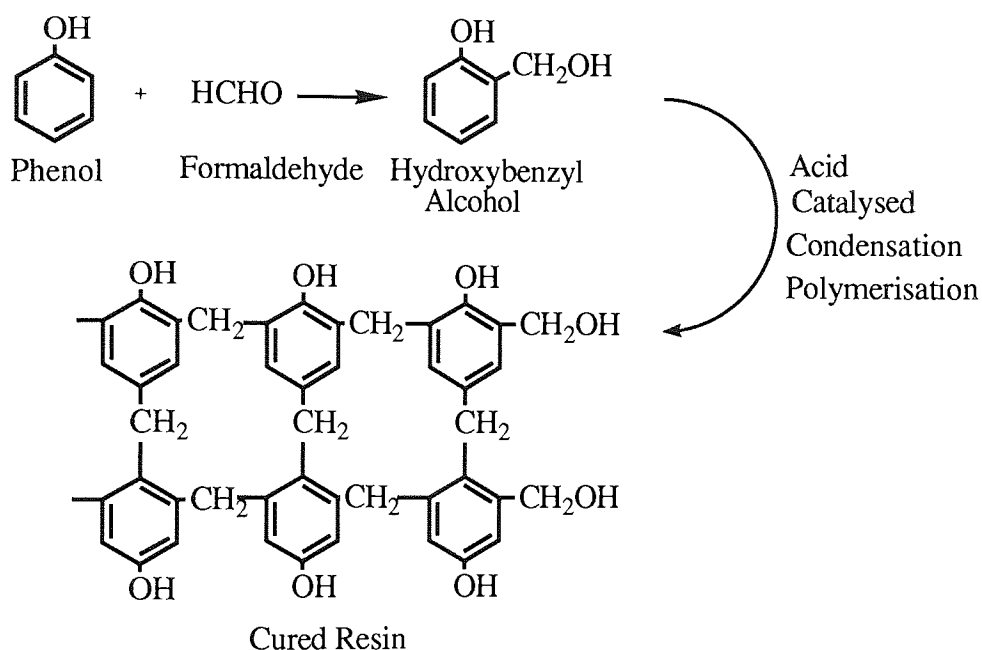


Fig 3.5 - Mechanism for Curing the Alphaset / Betaset Binders

The reactivity of the cured binder and the finely divided lithium described in the previous chapter can be explained by the presence of the hydroxide groups in the cured binder. Within a standard resin bonded sand mould the internal surface is thinly coated with the resin and hence there is a proliferation of hydroxide groups present on this surface. On the introduction of a lithium containing alloy there will be a redox reaction between the lithium and the hydroxyl groups producing hydrogen as a product. This gaseous product will be forced into the molten metal where localised supersaturation occurs and porosity is observed within the finished casting. The electropositivity of the metal is instrumental in the vigour of such a redox reaction. With lithium having an electronegativity value on the Pauling scale of 1.0, the promotion of this reaction is self-evident, yet aluminium has a Pauling electronegativity of 1.5 and in most cases evidence of the metal-mould reaction is not observed. The reasons for this are twofold. Firstly, the introduction

of lithium to aluminium increases the hydrogen 'pick up' rate by a power of ten. The result is a molten lithium alloy containing much more dissolved hydrogen than the equivalent standard aluminium alloy. The control of this is more difficult, and on pouring a lithium aluminium alloy there is a smaller margin for the dissolution of hydrogen before the saturation limit is reached. Secondly, aluminium forms a thin, impenetrable oxide coating on cooling which protects the remaining molten metal from reaction with the mould surface. The introduction of lithium breaks the oxide coating and allows reaction to take place.

In order to prevent reaction from taking place a separate protective coating must be applied between the internal mould surface and the surface of the incoming metal. This could be either physical or chemical. Industrial Precision Castings Limited applied washes to the surface of moulds in order to physically block the reaction. This was successful in part but only reduced the metal mould reaction. The slurries used for the washes were ceramic based and it was ascertained in the previous chapter that lithium reacts with alumino-silicate based ceramics to form lithium silicates/aluminates. To prevent any reaction occurring the contact of lithium with hydroxide groups, be they organic or inorganic, must be prevented and in order to do this chemical protection is the desired route.

Chapter Four

**METAL-MOULD
DEFECT EXPERIMENTS**

4.1 Introduction

Casting is as much an art as a science with practices being handed down through generations and development is made through trial and error. This is reflected in the common practices employed within foundries to combat defects and inconsistencies. Mould dressings, washes and coatings are physically placed onto the surface of the mould in an attempt to prevent the metal coming into contact with the 'real' surface of the mould. Chemical modification of the mould surface is not a technique that is employed mainly due to the training and experience of the personnel involved in the casting process. Two techniques are available at present to inhibit metal mould reaction. Aluminium - magnesium alloys are prone to metal mould reaction due to the aluminium oxide skin being broken by the reactive magnesium. The addition of small amounts of beryllium to molten aluminium - magnesium alloys acts as an oxygen scavenger and creates an alternative oxide film to that of the Al - Mg oxide coating. Methods of inhibition such as this belong in the realm of the metallurgist and hence will not be followed up in this volume. Metal mould reactions in other light alloys are commonly suppressed by the addition of boric acid and ammonium bifluoride which replace the oxide film with an alternative compound film. This method is not applicable to Al - Li alloys nor Al - Mg alloys and it is considered wasteful as the whole mould is treated when only the surface is active.

Surface treatment was chosen as the protective method because it is area specific and silicon containing groups were used for the following reasons :

- (i) They are widely used as hydroxide protecting groups in organic chemistry.
- (ii) The Si - O bond formed is very strong and is able to withstand the heat of the incoming metal without being burnt off instantly. Several silicones are baked onto the surface of some substances for better performance.
- (iii) Silicon groups have a relatively low coefficient of friction and this can aid the stripping of the casting.
- (iv) The compounds are easily available although the cost is not always favourable.

4.2 Preparation of Alloys

Prior to the casting trials several test alloys were prepared. Commercial aluminium of purity 99.9% was obtained from Alcan Ltd, Kitts Green, Birmingham. Lithium was to be added in order to obtain four alloys ranging from 1 weight percent to 4 weight percent. Four, one kilogram samples of aluminium were melted individually in a gas powered crucible furnace using a clay graphite crucible. The aluminium was heated to a temperature of 750°C before being degassed with hexachlorethane and cleaned with Coverall 2, a proprietry dry flux. The crucible was then removed from the furnace. Measured quantities of lithium rod were encased in aluminium foil and

were introduced to each melt under an argon atmosphere in small quantities to avoid the hazard of explosion and fire. The melts were mixed in between each addition. When the lithium addition was complete and thoroughly mixed the metal was poured into steel ingot moulds again under argon and the alloys were allowed to cool before being knocked out.

In order to confirm the lithium concentration, measured quantities of each alloy were dissolved in 1.18 S.G. hydrochloric acid and the resulting solution diluted to 1 ppm. Atomic absorption spectroscopy was used to ascertain the amount of lithium in each solution. Atomic absorption measurements were carried out using a Perkin Elmer 373 atomic absorption spectrometer with a hollow cathode lamp set at 670.8nm and using an air / acetylene flame. Spectroscopy grade lithium chloride was used as the standard and the linear working range of lithium is $2\mu\text{gml}^{-1}$. Table 4.1 shows the theoretical lithium concentrations based on the lithium additions to the aluminium melt and the actual concentrations calculated from the atomic absorption results.

Theoretical Concentration	Actual Concentration
1 %	0.94 %
2 %	1.89 %
3 %	2.77 %
4 %	4.55 %

Table 4.1 - Theoretical and actual lithium concentrations in the binary lithium aluminium alloys prepared at Aston.

4.3 Preparation of Moulds

4.3.1 Preparation of Sand Moulds

Sand moulds were prepared using two binders, Alphaset and Betaset, supplied by Industrial Precision Castings Limited, Rochester, Kent and manufactured by Bordens U.K. Limited, North Baddesley, Southampton and a furan resin, Furatec, kindly supplied by Foseco International Limited, Nechells, Birmingham at short notice. Two sands were used in the production of the moulds, 110 grade Redhill sand and 60 grade Buckland sand, also supplied by Industrial Precision Castings Limited.

Sand Moulds using Alphaset.

The casting box used for the mould was made from thin sheet 3004 aluminium alloy (1.0Mn - 0.8Mg - 0.7Fe - 0.3Si - 0.25Cu - 0.25Zn). It was circular in design with an internal diameter of 64mm and a height of 70mm. A B19 ground glass stopper commonly used in quickfit apparatus was used as the pattern for its ease of removal from the sand and its simple shape, allowing uncomplicated casting without the problems of pattern design related defects. 350 grammes of sand was mixed with 2% (by weight of sand) of alphaset manually until the mixture was homogenous. 10% (by weight of alphaset) of hardener was added to the sand and alphaset mixture. The ternary system was then mixed thoroughly manually until the hardener was well dispersed. Half the sand mixture was put into the casting box and rammed by hand with a second ground glass stopper. When the box was half full with compact moulding sand the pattern was placed in the centre of the box and more sand added around the pattern. The sand was rammed again with a ground glass stopper. Sand was continually added and rammed until the surface of the sand was flush with the edge of the pattern. The complete mould was then covered with a glass beaker to prevent drying out. The pattern was removed from the mould after 45 minutes when the binder had cured. The mould was then ready for the introduction of the molten metal.

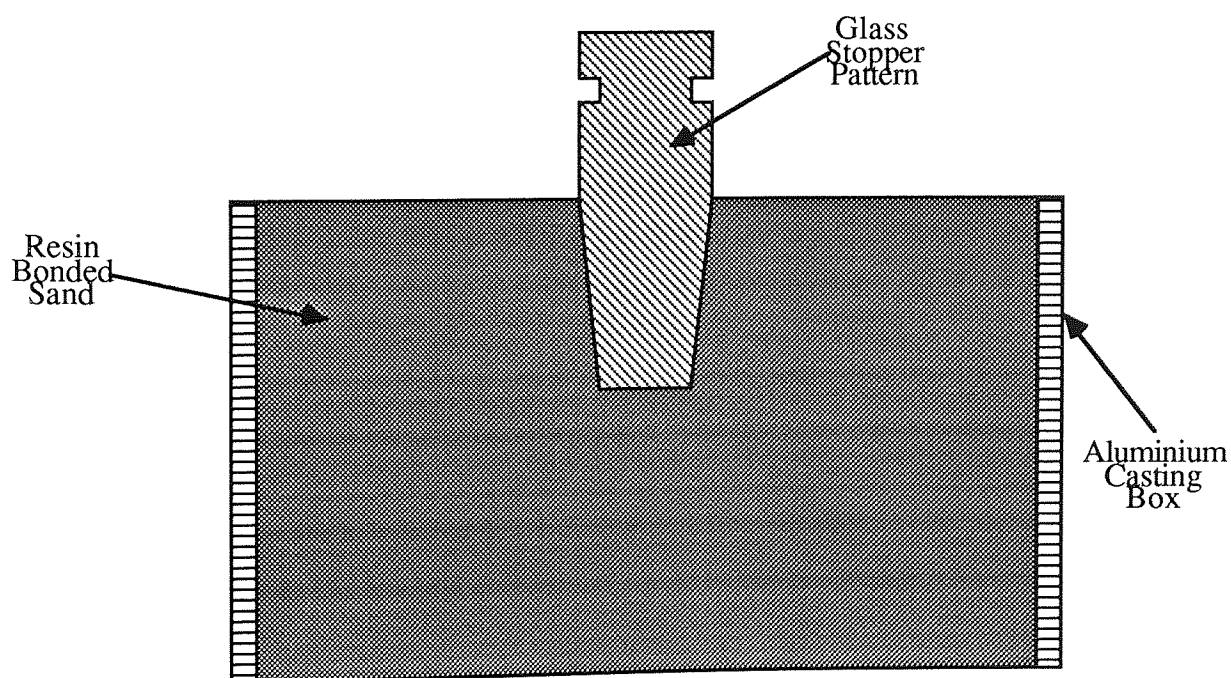


Fig 4.1 - Cross Section of a Typical Sand Mould

Sand Moulds using Betaset

The casting box and pattern used with the alphaset binder was also used with the betaset binder. 350 grammes of sand was mixed with 2% (by weight of sand) of betaset manually until

the mixture was homogenous. Half of the sand mixture was put into the mould and rammed with the ground glass stopper. When the mould was half full the pattern was introduced to the box. More sand mixture was added around the pattern and was rammed to compaction. This procedure was done until the sand was flush with edge of the pattern. Four small holes were put into the sand around the pattern to a depth of approximately 50mm with a 1mm diameter steel rod. Nitrogen gas was bubbled through the methyl formate hardener and then introduced to each of the holes for approximately 30 seconds. The methyl formate vapour cured the resin instantly. The pattern was then removed from the mould, which was then ready to receive the molten metal.

Sand Moulds using Furan Resin

350 grammes of sand was mixed with 1.3 % (by weight of sand) of furan resin manually until the mixture was homogenous. 40 % (by weight of resin) of para-toluene sulphonic acid was added to the sand mixture. Half the sand mixture was put into the mould and rammed with the ground glass stopper. The pattern was then placed in the box and sand added around it. This sand was rammed to compaction and the process repeated until the compact sand mixture was flush with the top of the pattern. The mould was then covered with a glass beaker for 45 minutes to prevent it drying out. After this time the pattern was carefully removed from the mould which was then ready to receive the molten alloy.

4.3.2. Preparation of Investment Moulds

Investment casting or lost wax casting as it is better known is completely different to sand casting. The pattern is made from wax and is coated in ceramic materials to create a shell. The wax is then melted out leaving a cavity for the metal to be poured into.

Casting wax, provided by Industrial Precision Castings Limited was melted at a temperature of approximately 80°C, and was poured into a glass tube of internal diameter 15mm. When the wax had cooled and solidified completely it was removed by heating the outside of the tube to melt the surface of the wax rod. The rod could then be pushed out of the tube. The rod was sectioned into lengths of 15mm. An 80mm length of copper wire was inserted into the top of the each wax rod to act as a hanger. To create the investment shell, the wax pattern had to be dipped several times in ceramic based slurries. The primary coat was made up of 200 grammes of zirconium silicate dispersed in 40ml of colloidal silica. Prior to dipping the pattern surface had all traces of oils and greases removed by washing in carbon tetrachloride. After air-drying the pattern was dipped into the slurry leaving the top surface with the copper wire clean. The pattern was then air dried before being dipped for a second time. This dipping procedure was carried out three times using the primary coat. Once the third primary coat had dried, back-up coats were added. Three

back-up coats were used and each differed by the grade of molochite included. The back-up coats were made up from 30 grammes of zirconium silicate and 70 grammes of molochite dispersed in 48ml of 'laksil', ethyl silicate solvated in ethyl alcohol. The three grades of molochite used were classified by their sizes in microns; 120 grade was the finest through 50/80 grade to the coarsest 30/80 grade. The pattern with primary coat added was dipped in each back-up coat three times commencing with the 120 grade and concluding with the 30/80 grade with each coat being allowed to air dry before applying the next. In all, twelve coats were added. The large number of coats was required for insulation purposes. Problems were encountered with the casting cooling too fast. This was due primarily to the pattern being too small and not enough coating was applied at each dipping. With the casting cooling too fast, the trial was not sufficiently similar to the industrial situation and the problem was not being reproduced.

Once the final coat had air dried the pattern plus shell was oven dried at 60°C for 1 hour. The temperature was then slowly raised to 250°C to melt the wax out. When the bulk of the wax had been removed the investment shell was taken out of the oven and stored until it was required for casting. Prior to any casting operation each investment shell must be fired at 900°C for 1 hour in order to burn out all traces of the wax and to remove any residual water or ethanol from the slurries to allow the silica gel binder to form from the colloidal silica used in the back-up coats. After firing the mould was placed in dry sand to provide extra insulation and a stable base to cast into.

4.4 Melting and Pouring the Binary Alloys

Salamander crucibles constructed from graphite obtained from Thomas Sutton Limited, Birmingham, were used to melt the binary alloys. The crucibles had to be preheated to the operating temperature of 750°C in order to slowly remove any water taken into the crucible structure from the atmosphere. If this procedure was not undertaken then the risk of an explosion was high. Approximately 50 grammes of the desired alloy was placed into the preheated crucible. Commercial purity argon that had been dried through silica gel and 4Å molecular sieve was passed through the furnace cavity to provide an inert atmosphere. The alloy was monitored at regular intervals and when the alloy was molten the crucible was removed from the furnace and a cleaning agent of a 30 : 70 mix of potassium chloride/lithium chloride was added to the melt. The cleaning agent was left for approximately one minute before the dross and slag formed on the alloy surface was removed. Before the cleaning process is undertaken the alloy is normally degassed with argon to remove any dissolved hydrogen, but because the quantity of metal used was so small, this procedure had to be forgone due to the fact that it caused the solidification of the alloy. All casting carried out in these trials use alloys that are not degassed. Once clean, the metal was introduced to the mould. After pouring, the mould was allowed to cool and the metal to solidify.

The casting was knocked out as soon as possible after pouring and it was then ready for sectioning and polishing.

4.5 Mould Treatment

All moulds were treated with agents in the liquid form. This was done either with compounds that were naturally liquid or with solids that were dissolved in a relevant solvent. Treatment of the sand moulds was carried out using two methods. Firstly the sand mould was placed in an enclosed chamber with a gas inlet and outlet. The treatment agent had dry nitrogen bubbled through it and the resulting vapour was introduced to the chamber via the inlet valve. All exhaust gases were released through the outlet valve and bubbled through an ammonia solution. The agent was able to react with the surface of the mould to create the protective chemical barrier. After treatment was complete the mould was removed from the chamber and was ready for casting. The second method was to put the sand mould into direct contact with the protective agent. The agent was able to react directly with the surface and any excess material could evaporate. Application was in this case by dripping the agent on to the surface because the mould was so small, but it is anticipated that on using larger industrial moulds a spraying technique will be employed.

Treatment of the investment moulds was carried out by immersing the complete mould into the liquid agent for a period of approximately 10 seconds. The mould was then removed and allowed to air dry for approximately two minutes. This procedure was again used because of the unusually small size of the mould but an investment mould is a one piece mould unlike sand moulds and spraying may be an unproductive technique. The mould would have to be partially filled with the treatment agent and then rotated to ensure complete coverage of the inner mould surface. Investment moulds were treated after they had been fired at 900°C and allowed to cool to 25°C before they were loaded into the insulating sand.

4.6 Experimental

All chemicals used for modification of moulds were purchased from standard chemical suppliers and were used as purchased. The chemicals used in the study of both the sand moulds and the investment moulds are listed below:-

tri-methyl chlorosilane (T.M.C.S.)
N,O-bis-trimethyl silyl acetamide (B.S.A.)
hexamethyl disilazane (H.M.D.S.)
triphenyl chlorosilane (T.P.C.S.)
trimethyl bromosilane (T.M.B.S.)

tri-isopropylsilyl chloride
t-butyl dimethyl silyl chloride

4.6.1 Preparation of Polished Macrosamples

All castings were dissected laterally using a hacksaw. One section was mounted in bakelite using a Meta-Serv automatic mounting press. The section was placed in the centre of the heating chamber and was covered with a measured amount of bakelite granules. The lid was then fastened down on the chamber and the sample and bakelite raised to meet the lid under a pressure of 32psi / 2.2 bar. The temperature of the chamber was raised to 140 -160°C for 8 minutes and then the sample was water cooled for 2 minutes. The 'macro' was removed from the heating chamber and was ready for polishing. The polishing of the sample was undertaken using a series of rotating emery paper discs (see fig 4.5). They were mounted on a Struers rotary polisher and were continually sprayed with water to aid smooth grinding and to remove all polishing waste. The

Casting No.	Type of Mould	Treatment Used	Alloy Conc.	Comment
BOB C1	1% Sand Mould	-	1% Alloy	
BOB C2	1% Sand Mould	-	2% Alloy	
BOB C3	1% Sand Mould	-	3% Alloy	
BOB C4	1% Sand Mould	-	4% Alloy	
BOB C5	2% Sand Mould	-	3% Alloy	
BOB C6	3% Sand Mould	-	3% Alloy	
BOB C7	4% Sand Mould	-	3% Alloy	
BOB C8	5% Sand Mould	-	3% Alloy	
BOB C9	2% Sand Mould	-	3% Alloy	
BOB S1	2% Sand Mould	TMCS Dripped	3% Alloy	
BOB S2	2% Sand Mould	TMCS Gassed	3% Alloy	
BOB C10	2% Sand Mould	-	3% Alloy	
BOB S3	2% Sand Mould	BSA Dripped	3% Alloy	
BOB S4	2% Sand Mould	BSA Gassed	3% Alloy	
BOB C11	2% Sand Mould	-	3% Alloy	Betaset
BOB S5	2% Sand Mould	TMCS Dripped	3% Alloy	Betaset
BOB S6	2% Sand Mould	TMCS Gassed	3% Alloy	Betaset
BOB S7	2% Sand Mould	TMCS Gassed	3% Alloy	No Hardener

Table 4.2 - Table Showing Sand Casting Experiments

Casting No.	Type of Mould	Treatment Used	Alloy Conc.	Comment
BOB I1	Investment	-	3% Alloy	No Sand
BOB I2	Investment	-	3% Alloy	No Sand
BOB I3	Investment	-	3% Alloy	-
BOB IS1	Investment	TMCS Dripped	3% Alloy	-
BOB IS2	Investment	TMCS Sub	3% Alloy	-
BOB I4	Investment	-	3% Alloy	-
BOB IS3	Investment	TMCS Sub	3% Alloy	-
BOB I5	Investment	-	3% Alloy	-
BOB IS4	Investment	TMCS Sub	3% Alloy	-
BOB I6	Investment	-	4% Alloy	-
BOB I7	Investment	-	2% Alloy	-
BOB I8	Investment	-	1% Alloy	-
BOB I9	Investment	-	3% Alloy	Larger Mould
BOB IS5	Investment	TMCS Sub	3% Alloy	Larger Mould
BOB IS6	Investment	TPCS in Ether	3% Alloy	-
BOB I10	Investment	-	Aluminium	-
BOB I11	Investment	-	3% Alloy	-
BOB IS7	Investment	TMCS sub	3% Alloy	5hrs to casting
BOB IS8	Investment	TMCS sub	3% Alloy	24hrs to casting
BOB IS9	Investment	TMBS Sub	3% Alloy	-
BOB IS10	Investment	TIPSC Sub	3% Alloy	-
BOB IS11	Investment	t-but DMSC Sub	3% Alloy	-
BOB I12	Investment	-	3% Alloy	Perlite Based
BOB I13	Investment	-	3% Alloy	-
BOB IS12	Investment	TMCS Sub	3% Alloy	-
BOB IS13	Investment	TMCS Sub	3% Alloy	Cast at 400°C
BOB IS14	Investment	TMCS Sub	3% Alloy	Cast at 400°C
BOB IS15	Investment	TMCS Sub	3% Alloy	Cast at 400°C
BOB IS16	Investment	TMCS Sub	3% Alloy	-
BOB IS17	Investment	TMCS Sub	3% Alloy	Cast at 300°C
BOB IS18	Investment	TMCS Sub	3% Alloy	-
BOB IS19	Investment	TMCS Sub	3% Alloy	Cast at 200°C
BOB IS20	Investment	TMCS Sub	3% Alloy	-
BOB IS21	Investment	TMCS Sub	3% Alloy	Cast at 100°C
BOB IS22	Investment	TMCS Sub	3% Alloy	-

Table 4.3 (previous page) - Table Showing Investment Casting Experiments

sample was ground on successively finer papers starting with 240 grit and going through 400 and 600 to 1200 grit. After grinding on each wheel the sample was rinsed under water to remove all grit and grinding dust. Following grinding on the 1200 grit wheel the macro was polished using two Meta-Serv universal diamond polishing wheels of a 6 micron diamond spray on a paper pad and a 1 micron diamond spray on a felt pad. The procedure for diamond polishing is more rigorous as it is essential that no contamination of the wheels occur. Polishing at this level can be ruined by one piece of grit, dust or even skin getting onto the wheel. The sample is cleaned using a 5% solution of Decon 90 in an ultrasound bath. This removes all contamination from any holes or porosity arising in the sample that standard cleaning cannot remove. After 30 seconds in an ultrasound bath the sample is removed, rinsed with methanol and dried on a hot air drier. The sample was then polished on the 6 micron diamond wheel. The cleaning regime was carried out prior to any subsequent diamond polishing.

4.6.2. Analysis of Macrosamples

All analysis of the macrosamples was carried out using optical microscopy and examination by naked eye. Optical microscopy was carried out using a Reichert and Jung Polyvar optical microscope.

4.7 Discussion

Figure 4.2 shows photographic examples of polished macrographs cast in a sand moulds with alphasert binder and no mould treatment. The porosity defect can be seen as the series of dark 'holes' circumnavigating the edge of the section interspersed with several smaller elongated slits. The hydrogen formed on the contact of the molten alloy with the mould surface is projected into the rapidly solidifying metal surface forming the slits. The holes are formed by several jets of hydrogen agglomerating in metal that is solidifying at a much slower rate allowing the shape to become defined. In order to discover whether this defect is affected by the lithium concentration of the alloy (1-4%) or the rate at which the binder was added to the sand mould a preliminary study was carried out. The results of this study are depicted in figure 4.2 and figure 4.3. Figure 4.2 shows four castings increasing from left to right in lithium concentration. The binder rate remained constant at 1% and it can be clearly seen that the porosity increase is a function of lithium concentration. In comparison figure 4.3 shows four castings increasing from left to right in binder addition. The lithium concentration remained constant at 3%. Again it can clearly be seen that there is little variation between the four macros. The assumption can be made that on the surface

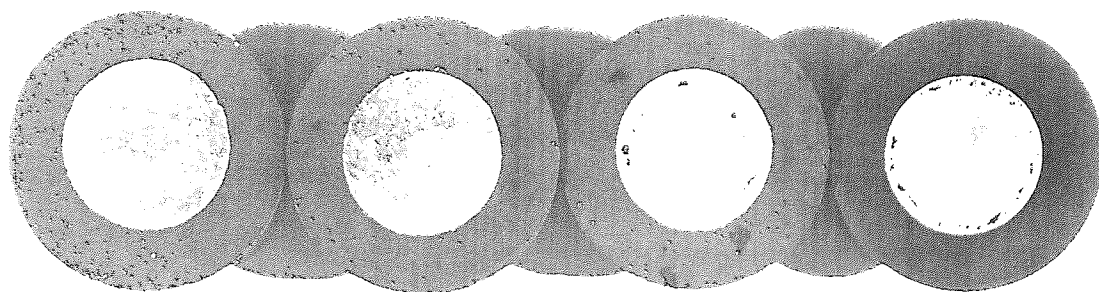


Fig 4.2 - Photograph showing a series of castings in 1% Alphasets moulds.
1% alloy(left) - 4%alloy(right)

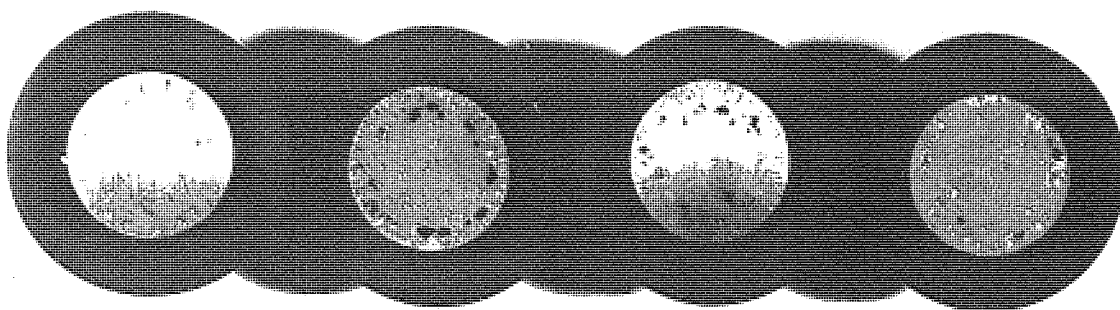


Fig 4.3 - Photograph showing a series of castings using a 3% Al/Li alloy in Alphaset moulds. 1%(left) - 4%(right)

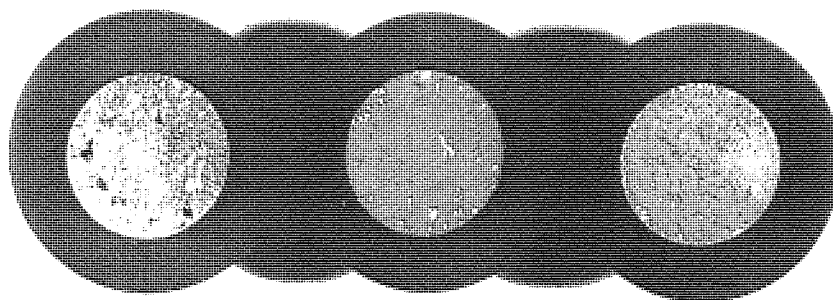


Fig 4.4 - Photograph showing castings in a 'gassed' Alphaset mould(right) and an untreated mould(left)

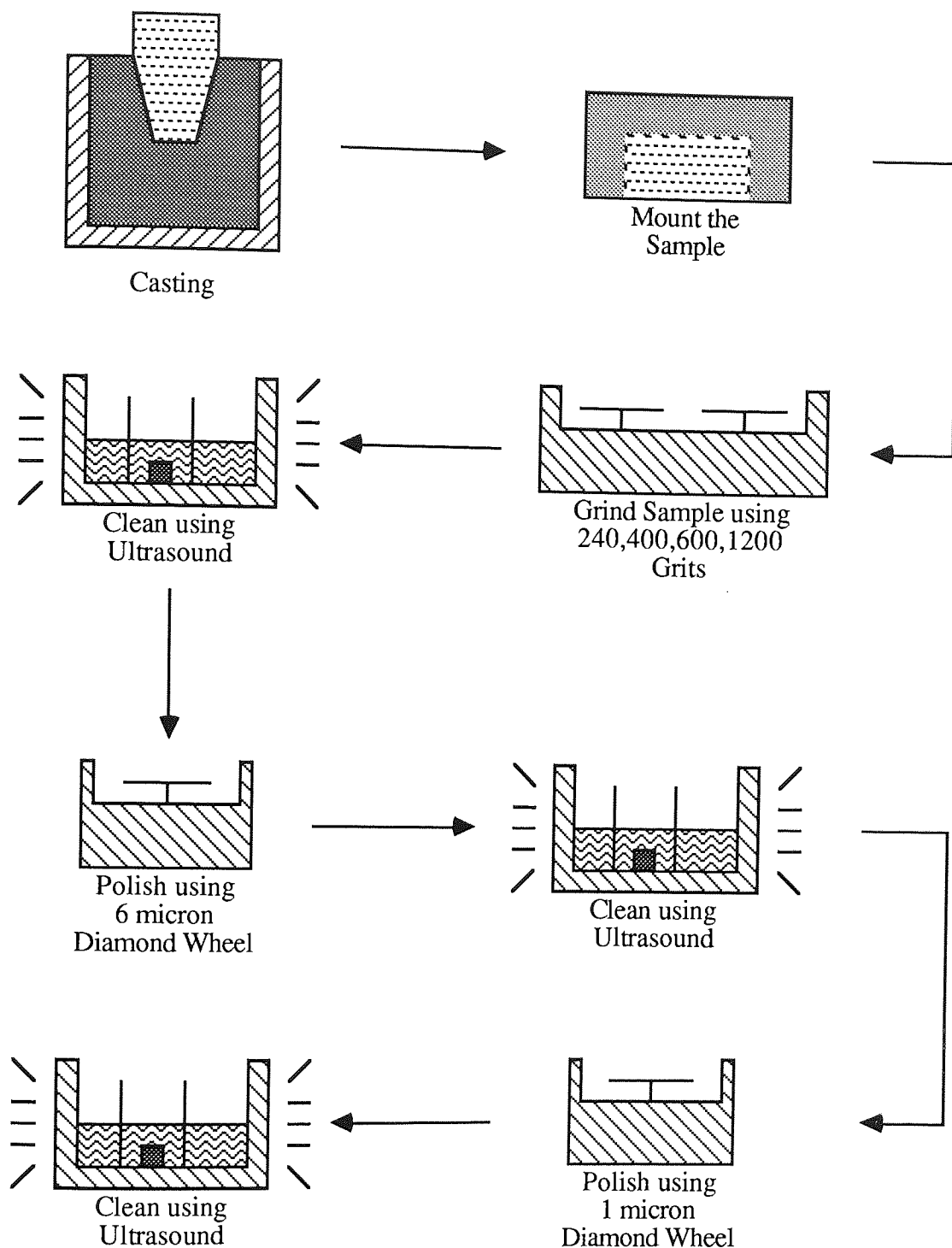


Fig 4.5 - Flow Diagram Showing Polishing Regime of Casting Sample

of any commercial lithium aluminium casting alloy (2-4% Li) there is sufficient lithium activity to create the porosity defect provided that the conditions are favourable. It can also be assumed that on the surface of any commercially resin bonded sand mould there is hydroxide activity in excess of that required to react with the lithium atoms on the surface of a commercial alloy.

In order to combat the metal-mould reaction the contact between the lithium in the alloy and the hydroxide groups on the binder must be removed. This can be done either physically by coating the mould with a slurry, or chemically by functionalising the surface hydroxide groups. Industrial Precision Castings Limited have worked with a limited degree of success on coating the mould with a standard alumina based mould coating slurry. The severity of the defect was reduced but not removed. Experiments described in chapter 2 provide an explanation for these findings. Lithium was shown to react with alumina but relative to the resin binders a much higher energy input was required to initiate reaction and if the slurry coating is not thoroughly dried before casting, residual water will create an added problem by forming hydrogen gas from the redox reaction between the water and lithium in the alloy. Most ceramics contain aluminosilicate groups in large quantities and it is inconceivable that lithium will not react with any of them and therefore a physical barrier of this kind will not eliminate the defect.

Chemical protection is subject to several conditions. Application must be of a simple nature i.e. chemical reaction must take place between agent and hydroxide within the temperature constraints of the casting industry and the reaction must be rapid so as not to delay the casting process. The reaction must produce a product in high yield since surface coating is the desired outcome and no gaps must be evident. Byproducts must not interfere with the protecting agent and should be easily removable without causing harm to operating personnel. The removal or stabilisation of active hydroxides is commonly carried out in organic chemistry by silylation and the use of trimethylchlorosilane (TMCS) was an excellent starting material. It was first used by Sauer⁶⁰ in 1944 who silylated methanol and ethanol with TMCS and pyridine. The pyridine was used as an acid acceptor to prevent the expulsion of hydrogen chloride into the atmosphere. The use of TMCS ramified in the following years as it was used for silylating amines⁶¹ and metal salts of acids^{62,63}. The use of TMCS as a powerful silylating agent had now been established and it was able to be used on its own without the need of a catalyst. This was the ideal basis for its use as a hydroxide protecting agent for the phenolic groups within the resin binder. The production of trimethylsilyl ethers on the surface of the mould will convey a water repellency to the resin which will aid in preventing the water produced as a byproduct in the condensation polymerisation of the resin from leaching out of the mould via the internal mould surface. Any water that was already present on the surface of the mould would have been converted to hexamethyldisiloxane on contact with TMCS.

The choice of methods of application was influenced by treatments used for other solid substrates. Conferring water repellency to mud bricks⁶⁴ was carried out by passing steam, into which 25% w/w methyltrimethoxysilane had been trained, through a chamber containing the brick for 15 to 20 minutes. After testing, the water repellency was said to be excellent. This method was modified into the nitrogen/TMCS gassing method used in this work. Shrinkproofing cellulose fibres⁶⁵ is carried out by spraying dried fabric with aerosols containing organic substituted silicon halides or halogenated silanes from 1 second to 5 minutes at 24°C. Spraying TMCS directly onto the mould resulted from this process.

On gassing, the mould took on a yellow hue in contrast to the purple colouring it exhibited when first prepared. The gassing process took approximately of 3 hours to be 'complete', i.e. for the mould to look completely yellow to the naked eye. Once the gassing process had been completed the mould was removed from the gassing chamber and was cast into immediately. The results of this casting can be seen in figure 4.4. In comparison to the untreated mould (shown left in figure) the improvement in castability is excellent. The number of large spherical holes found nearer to the centre of the casting has been reduced to zero but the smaller elongated holes have been unaffected and have increased in number. This suggests that the surface treatment has

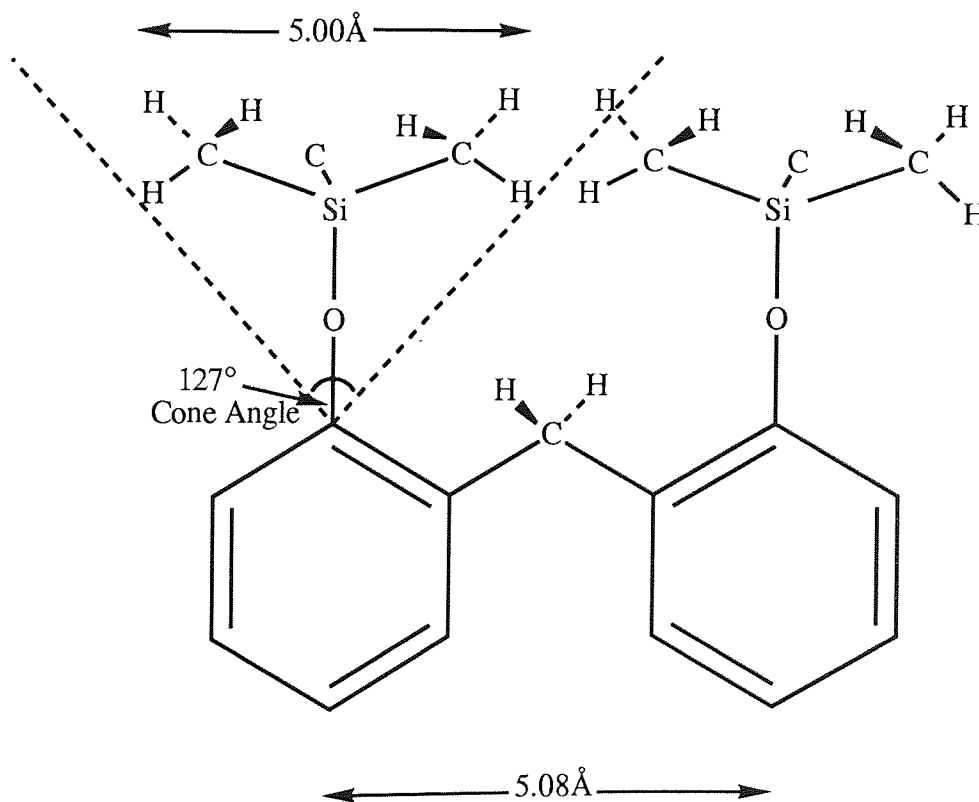


Fig 4.6 - A Functionalised Resin in Diagrammatic form Showing Cone Angle, Inter-Oxygen Distance and Maximum Cone Diameter

removed large concentrations of hydroxide sites in any one area and reduced the number of sites for lithium attack by giving a coverage of 50-60%. There is now a more thinly spread series of hydroxide groups all over the mould surface interspersed with a network of silyl ethers. Figure 4.8 shows the polished result of a casting carried out using the 'spraying' method. Due to the size of the mould, spraying was replaced by dripping the TMCS onto the internal surface of the mould. This method has the advantage of being area specific, i.e. the applicator can define the area of the mould they wish to treat unlike the gassing method where the whole mould surface is treated as it comes into contact with the agent. Again the large spherical holes have been removed but the smaller porosity has been significantly reduced as well. The amount of silylation that can occur along the length of a resin will be a function of the size of the silylation group. Sterically hindered reaction sites will have a reduced activity towards such groups as trimethylchlorosilane. Tolman⁶⁶ carried out an extensive piece of work assessing the effects of changing ligands on phosphine molecules. This work introduced cone angles, a term that gives some reference for the size of a substituent. Tolman's definition for the steric parameter θ for symmetric ligands (all substituents the same) is the apex angle of a cylindrical cone centred 2.28\AA from the P atom, which touches the Van der Waals radii of the outermost atoms of the substituent groups. From this definition Tolman produced a cone angle for $\text{P}(\text{Me})_3$ of 118° .

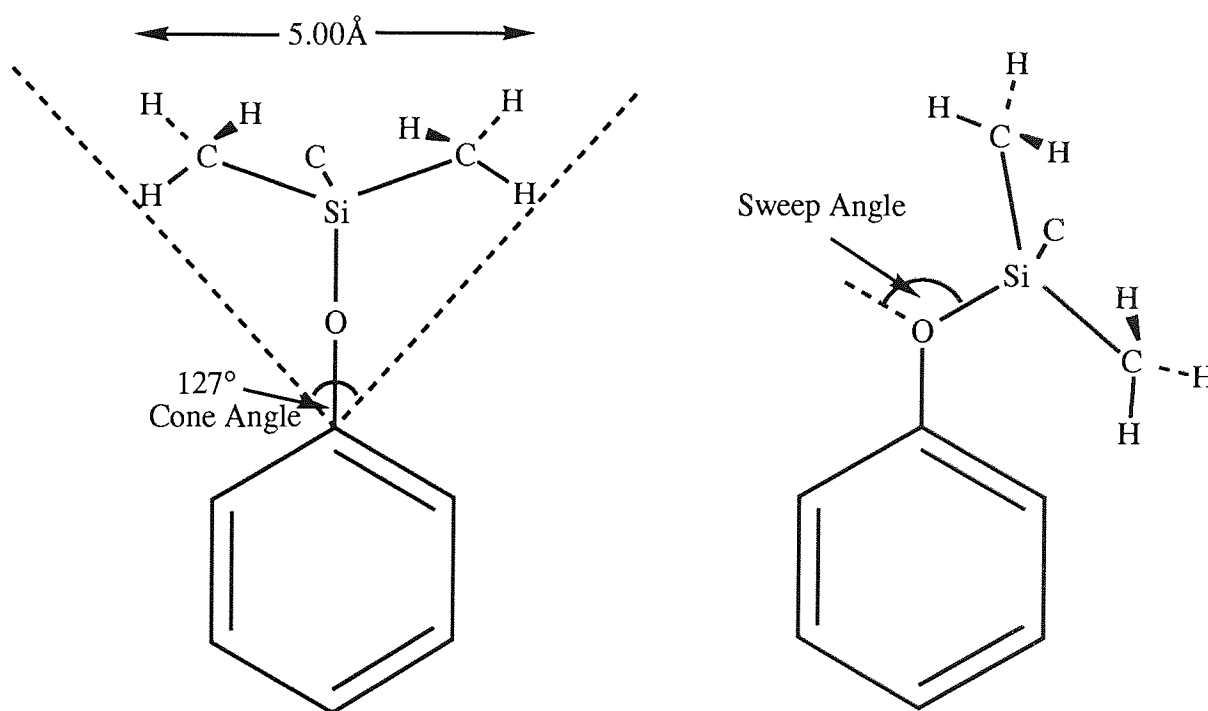


Fig 4.7 - Representation of the Cone Angle / Sweep Angle difference

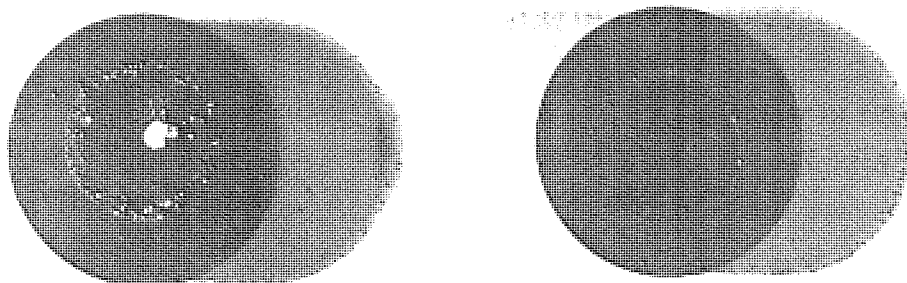


Fig 4.8 - Photograph contrasting castings from a TMCS spray treated
mould(right) and an untreated mould(left)

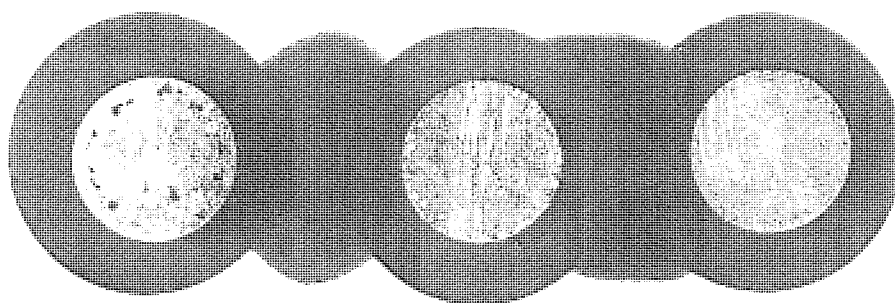


Fig 4.9 - Photograph showing three castings poured simultaneously. Untreated(left),
TMCS 'gassed'(middle) and 'TMCS 'sprayed'(right)

Using standard bond lengths, angles^{67,68} and trigonometry a cone angle was calculated for $\text{Si}(\text{Me})_3$ of 127° (see fig 4.6). Although these two groups are similar in size the phosphine group has a lone pair of electrons which reduces the C-P-C bond angle. This feature is not present in the silicon equivalent and the cone angle is correspondingly larger. Using a simple model of a standard phenolic resin and literature bond lengths and angles, the intramolecular distance between adjacent hydroxide oxygens is calculated as 5.08\AA . Using the precalculated cone angle and an assumption that the C-O-Si bond angle is 180° , the base of the cone at its widest point is 5.00\AA . Two $\text{Si}(\text{Me})_3$ groups could co-exist on adjacent hydroxides with 0.08\AA separating the two. This model is unrealistic in two ways : (i) the C-O-Si bond is $< 180^\circ$ and (ii) the use of quoted bond lengths does not take into account the Van der Waals radius of each atom in the same way as the Tolman model. The revised model would create a slightly larger cone with a sweep angle of $2(180 - \alpha)$ where α is the angle of the C-O-Si bond (see fig 4.7). The $\text{Si}(\text{Me})_3$ group will now introduce a steric factor into the bonding characteristics of the adjacent hydroxide groups. This concept can now be used in the interpretation of the experimental results (see fig 4.10). On using the gassing method, the first incoming trimethylchlorosilane group will have considerable mobility and no restriction on hydroxide site attack.

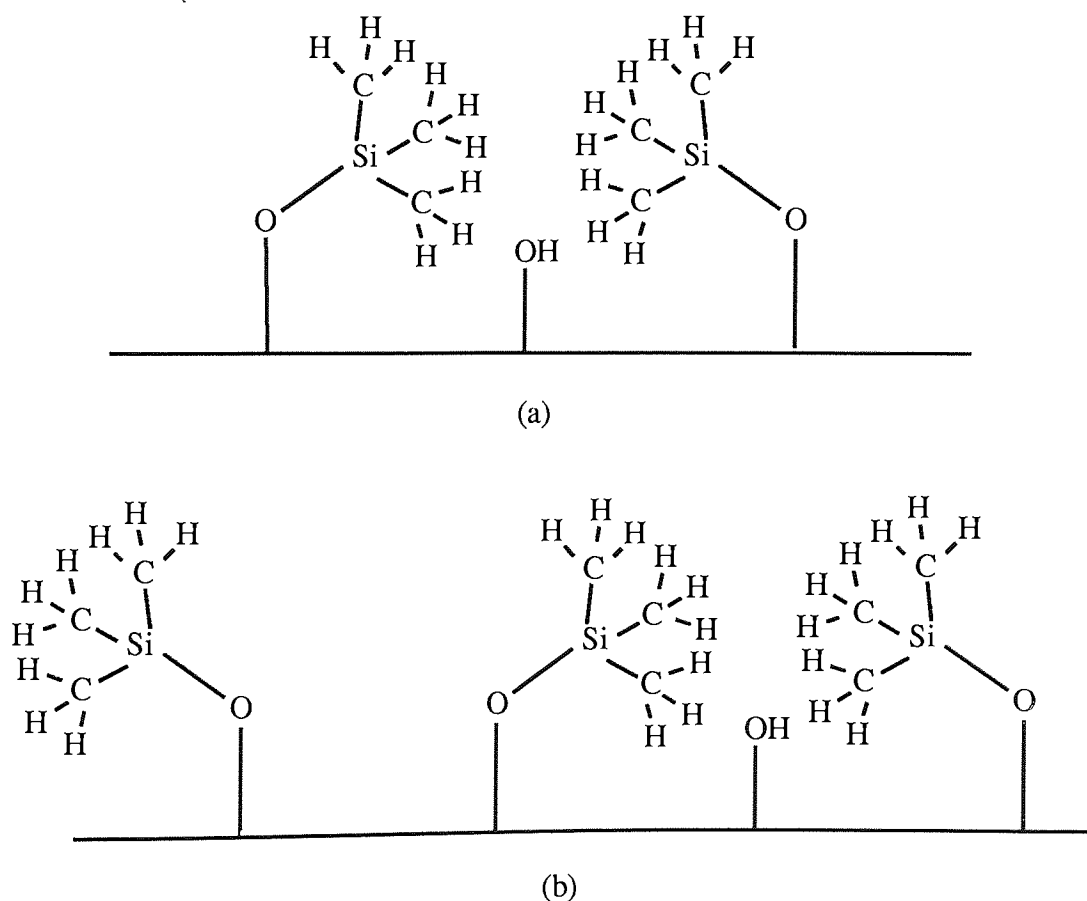


Fig 4.10 - Figure Showing the Difference in Functionalisation Characteristics
Between (a) the Gassing Method and (b) the Spraying Method

When the initial silyl ether has been formed a steric factor is introduced into the reactivity of the hydroxides adjacent to the ether group. This factor will make attack unfavourable to the incoming groups which will still have considerable mobility. Reaction is therefore more likely to occur two hydroxides along from the initial ether group. Alternate hydroxides will be functionalised and overall this will give a 50% coverage to the surface of a mould. Analysis of the spraying method shows that an excess of trimethylchlorosilane groups will be present at the mould surface as the first silyl ether is formed. In this case mobility is considerably reduced and the steric hinderance will be overcome by the first ether group rotating away from the adjacent hydroxide to allow reaction to occur. The two groups will now be 180° out of phase with each other and both rigidly protecting the free hydroxides next to each reacted group. In this way two out of every three hydroxides can be functionalised and an overall coverage of 66% is achieved. In both these systems complete coverage is not achieved and infrared evidence shows this is the case, with broad OH stretching frequencies prevalent at 3300 cm^{-1} . I.R. samples were prepared by drying the treated resin particles in an oven at 60°C prior to disc preparation in order to minimise the pick up of stray OH groups from the atmosphere.

The castings shown in figures 4.4 and 4.8 were cast separately but, since casting is not a particularly reproducible event, it can be suggested that the two castings cannot be compared directly. Figure 4.9 attempts to overcome the problem by comparing three castings carried out simultaneously using the same melt. The outcome shows the same result as the individual castings with an improvement in the gassed sample (middle in diagram) and further improvement in the sprayed sample (right in diagram).

TMCS is an antiquated reagent with regards to hydroxide group protection. More modern methods suggest the use of compounds such as hexamethyldisilazane (HMDS) and N,O-bis-trimethylsilyl acetamide (BSA). These compounds are derivatives of TMCS and are preferentially used by organic synthetic chemists to gain higher yields in hydroxide conversion. HMDS is a liquid boiling at 125°C . It can be used alone, i.e. with no catalyst and has been successful in this mode with aliphatic alcohols and phenols but its more common usage is with an acid catalyst in particular TMCS up to 50%. TMCS is not strictly a catalyst in the defined sense of the word but is classed as one in this case as the reaction is more rapid when it is employed. BSA is also a liquid with a boiling point of $71\text{--}73^\circ\text{C}$. It is known to be a very powerful silylating agent being used to convert alcohols, amides, amino acids, phenols and carboxylic acids at low temperature⁶⁹.

HMDS was mixed with a 25% w/v quantity of TMCS. The mix was placed into the gassing unit and a 2% alphaset mould was gassed with a nitrogen carrier gas for 3 hours. A second mould

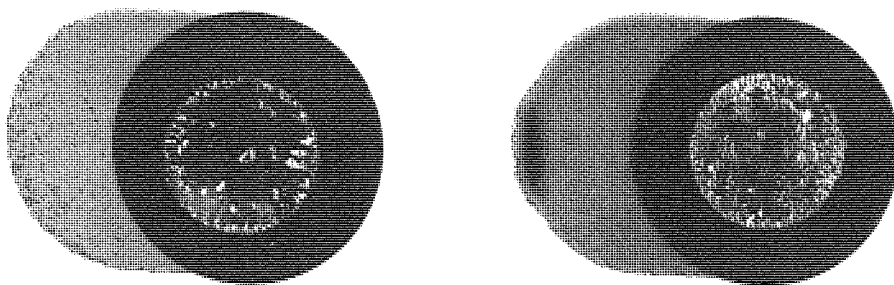


Fig 4.11 - Photograph showing castings from a HMDS/TMCS 'gassed' mould(right)
and an untreated mould(left)

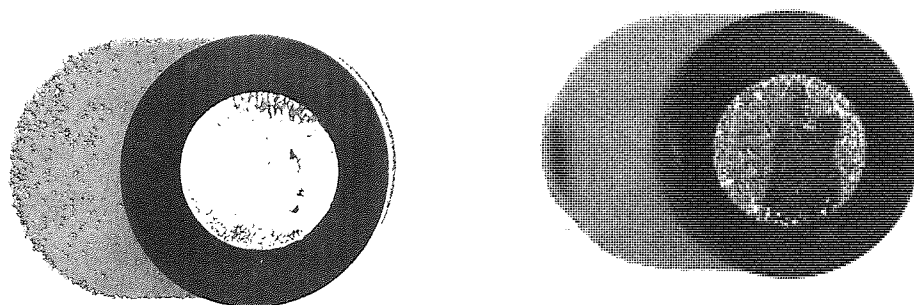


Fig 4.12 - Photograph showing castings from a HMDS/TMCS 'sprayed' mould(right)
and an untreated mould(left)

was treated by the spraying method and after treatment both moulds were allowed to dry in a desiccator. The moulds were cast independantly of each other but both were compared with a casting from an untreated mould. The results of these casting trials are given in figures 4.11 and 4.12 with the treated mould on the right. The gassed mould exhibits no improvement over the untreated mould and the 'holes' are severe. The sprayed mould does show a degree of improvement with respect to the untreated casting but the level of protection afforded by the mixture is negligible compared to the 100% TMCS treated moulds.

BSA was applied to two 2% sand moulds in the methods described for TMCS. The moulds were simultaneously cast into immediately after treatment and were compared to a TMCS treated mould (left in diagram). The results can be seen as polished macros in figure 4.13. The sample that underwent the gassing procedure shows very little improvement over an untreated mould and the sprayed sample (right in diagram) shows minor improvements by way of reduced large holes. The smaller porosity is still very severe and there is no improvement on an untreated mould.

The use of HMDS and BSA as effective silylating agents depends very much on the object of silylation. Pierce⁷⁰ shows that using similar procedures for different substrates can yield widely varying results. It is true to say that for the conversion of simple hydroxy groups i.e. those that are not neighboured by strongly electron donating groups, or are grossly sterically hindered, BSA is a superior converting reagent to the others and this is probably the case for many other compounds as well, but for more complex molecules one cannot necessarily predict the outcome of a silylation reaction. Solvent effects also play a large part in a silylation reaction e.g. the silylation of acetamide⁷⁰ using TMCS and benzene as a solvent produces a very low yield yet the same reaction with triethylamine produces an 83% yield and also the conversion of cholesterol⁷¹ using HMDS in pyridine and THF produces a less than 10% yield but TMCS with pyridine and THF gives greater than 90% conversion. Such happenings occur in the relatively controlled atmosphere of the organic chemist's glass flask and predicting the effects of silylating compounds used neat without the aid of catalysts and solvents in such an uncontrolled environment as the surface of a sand mould is a difficult task. The results of the casting trials carried out on sand moulds suggests strongly that HMDS and BSA are unsuited to this type of reaction, even though the substrate is not a particularly complex molecule in terms of silylating the hydroxide group and that TMCS has a high conversion rate and a good resistance to the heat effects caused by the incoming metal.

The treatment and casting of a betaset mould gave results consistent with the alphasbet experiments. The results shown in figure 4.14 show an untreated mould (left), a gassed mould and a sprayed mould (right). The gassed macro shows there was a good covering around the mould cavity with the exception of one area which is due to insufficient mixing of the sand and resin initially. This left a relatively large concentration of resin on the casting surface, something

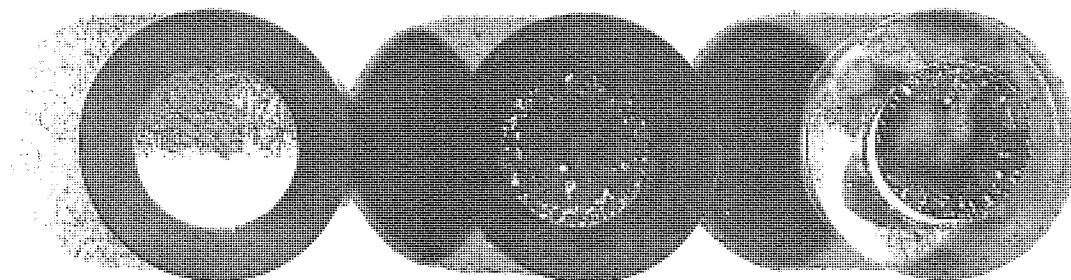


Fig 4.13 - Photograph contrasting three castings poured simultaneously. A TMCS mould (left), a BSA 'gassed' (middle) and a BSA 'sprayed' (right)

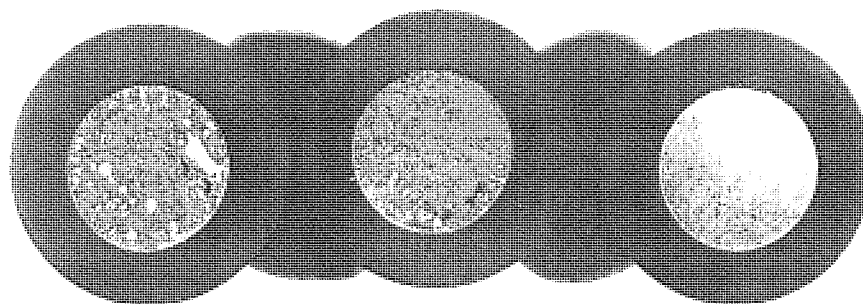


Fig 4.14 - Photograph showing three castings poured simultaneously into TMCS treated Betaset moulds. Untreated (left), 'gassed' (middle) and 'sprayed' (right)

that the gassing method is unable to combat and a problem that is unlikely to arise in a foundry due to the efficient modern mixing techniques. In effect a betaset mould is identical to an alphaset mould, the difference being the curing method. The final mould is still a sand mould bonded by a phenolic resin with an excess of hydroxide groups on the mould surface and hence the chemical treatment will take an identical form to that of an alphaset mould. This is not the case for an investment mould. Investment shells, as they are also known, are ceramic based and do not contain any organic binders. The shells are built up slowly around a wax pattern from ceramic slurries containing colloidal silica as the binding agent. After having been dipped into several grades of slurry and the shell has reached its desired thickness, the wax is melted and removed from the mould cavity. The shells are then fired at 900°C for approximately 1 hour to remove all traces of water and other organics used in the slurries and also to 'cure' the colloidal silica binder by forming a silica network around the ceramic. Post fired shells are removed to a holding furnace at 400°C to be chill cast into at temperature. This casting procedure is wholly different to that of the sand moulds and modifications had to be made to the treatment procedure.

Initially the cause of the metal-mould defect had to be ascertained. Since no phenolic binders or any hydroxide containing organics were being utilised in the moulding process there had to be a different mechanism occurring for essentially an identical defect to be manifested. In the initial study of the interactions occurring between lithium and the individual mould constituents the reactions of molochite and zircosil were of similar vigour to those with silica and alumina. Concentrating on the mould building procedure it can be seen that the initial layers of ceramic are 100% zircosil and hence the molochite is only being used for bulking and insulatory purposes. In terms of metal-mould reaction only zircosil and silica, the binder, need be considered. Investigation of materials such as silica and silicates reveals structures built up from the basic SiO_4 units into chains, multiple chains, rings, sheets and 3 dimensional networks. Zircosil is a structure built from discrete SiO_4 units interconnected by eight co-ordinated zirconium atoms, in contrast silica is a 3 dimensional structure where all four of the oxygens are shared. Independent of the way the units are built up, there is a point where the structure is broken, i.e. at an edge, and at these points the termination sites are completed by inorganic hydroxide groups. In effect the surface of an investment mould is also covered in hydroxide groups but of an inorganic nature and are less reactive than the phenolic hydroxides of the sand moulds. A polished macrograph of a 3% binary alloy cast into an investment mould at room temperature is shown in figure 4.15. The macrograph is shown besides a casting made with 99.9% aluminium and a macrograph of a foundry casting in order to contrast the laboratory sample against both its industrial equivalent and a defect free casting. The lithium alloy casting is very similar to a sand casting in its representation of the porosity defect yet it is distinctly different from the foundry sample. The industrial casting shows the defect as large holes close to the edge of the section with little or no fine porosity. This can be explained in terms of the precasting treatment of the metal. As explained earlier the metal in

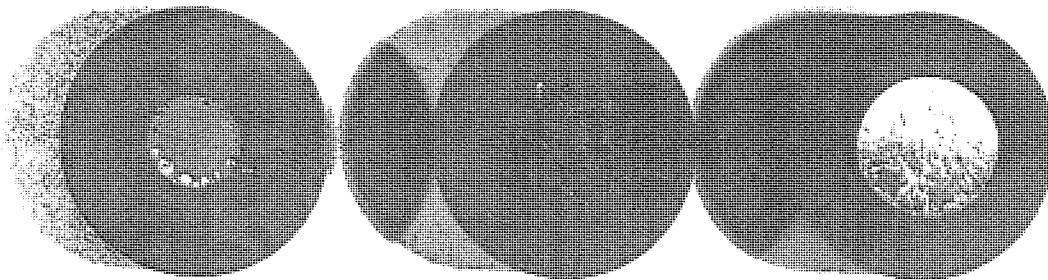


Fig 4.15 - Photograph showing polished micrographs of a foundry casting(left),an aluminium investment casting(middle), and an untreated Al/Li investment casting(right)

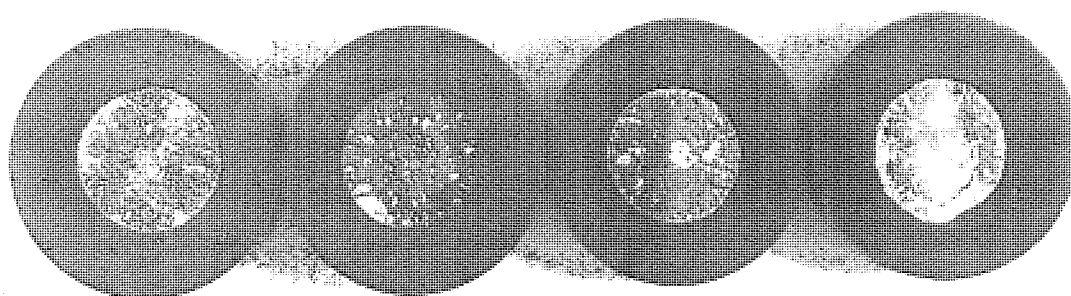


Fig 4.16 - Photograph showing a series of castings from untreated investment shells using alloys with an increasing concentration of lithium. 1%(left) - 4%(right)

a commercial crucible is degassed to lower the amount of dissolved hydrogen, but due to the quantity of metal used in a laboratory casting this procedure is impractical. The effect of the degassing on the casting would be to remove the initial effect of the metal-mould reaction and all hydrogen produced would dissolve into the metal until the saturation level was reached, at which point the defect would manifest itself. During this time delay the outer part of the casting would be solidifying and the projection of hydrogen into the body of the casting would be prevented and a gaseous build up would ensue nearer the casting surface.

A series of castings were made to assess the effect of the increasing concentration of lithium in the alloy on the severity of the defect. The results of this study can be seen in figure 4.16. The alloy concentration increases from 1% to 4% in 1% intervals and is exhibited in this order from left to right. Investigating the macrographs qualitatively shows there is no variation in the incidence of the porosity which is in direct contrast to a similar investigation on the sand moulds. In that case the porosity increased noticeably from 1% to 4%. The reason for such a difference is due to the regularity of the internal surface of the mould. The investment shell is very smooth and regular and therefore the incoming alloy will gain a more intimate contact with the surface allowing a better contact with the available hydroxyl groups. There is sufficient hydroxide activity on an investment shell to manifest the porosity defect in the 1% alloy in some quantity.

It has been established that investment casting will exhibit metal-mould reaction at any commercial aluminium-lithium alloy concentration. Treatment of glassy and ceramic materials by siloxylation is a well known technique and is used to improve their water repellent qualities, their electrical and mechanical properties and to aid the adhesion of plastics and glass by the formation of an intermediate layer. Investment shells were treated with TMCS using methods similar to those utilised for sand moulds. This provided an insight into the suitability of the material for this high temperature application. Initial attempts to carry out castings in untreated moulds were hampered by the lack of insulation provided by the investment shell and misrun was encountered due to the early solidification of the alloy. This problem was remedied by the use of a sand bath to provide the extra insulation. Using this technique two trial castings were made using treated moulds. The macrographs are pictured in figure 4.17. The first was made using the spraying procedure used on the sand moulds and the second was made by complete submersion of the mould in the siloxylating agent. The results of this trial were very promising with the latter application method producing a better casting. It was therefore decided to employ this technique for subsequent applications. It would be unlikely that a commercial foundry could use this technique due to the high cost factor of the TMCS and also there would be difficulty in containing the treatment agent due to high volatility. Spraying would be preferable for the larger mould size.

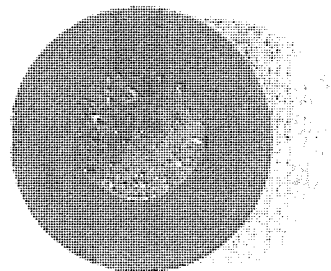
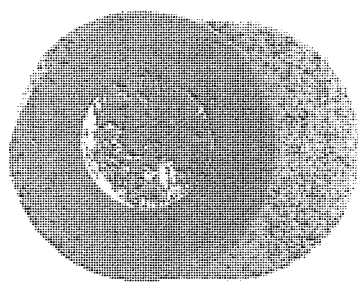


Fig 4.17 - Photograph showing the castings from two TMCS treated investment moulds using a sand insulating bath

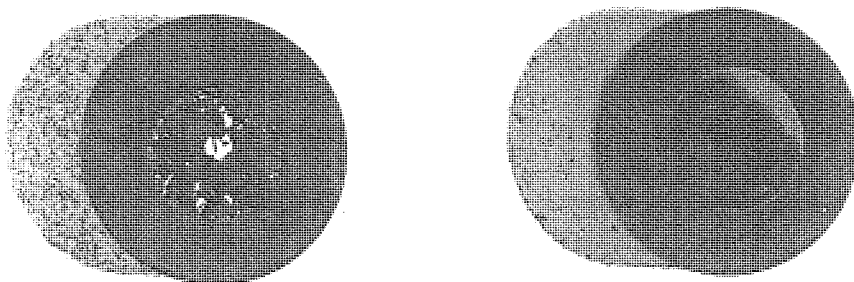


Fig 4.18 - Photograph of two investment castings, one untreated (left) and one TMCS treated(right)

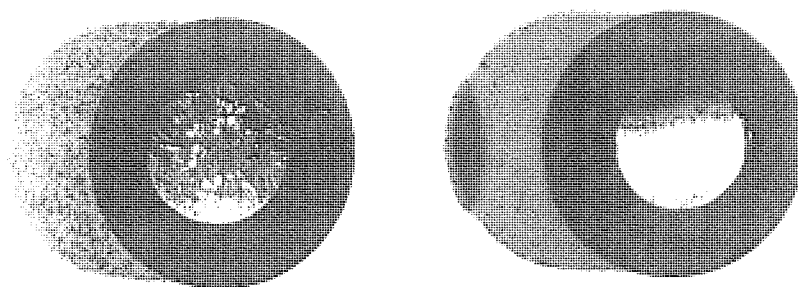


Fig 4.19 - Photograph showing a repeat run of the casting experiments shown in fig 4.18

For comparison purposes it was considered prudent to cast a treated mould with the same melt as an untreated mould. A 3% aluminium - lithium alloy was used for this purpose. Figure 4.18 shows the macrographs of this experiment and figure 4.19 represents a repeat trial to figure 4.18 to establish consistency. The casting from the untreated mould is the macrograph on the left in both diagrams. The porosity is severe for the untreated mould in both cases and the castings show examples of the fine porosity and the coarse 'holes'. The casting from the treated mould in figure 4.18 shows considerable improvement over its contemporary but does exhibit two small areas of fine porosity. The treated casting in figure 4.19 shows no porosity to the naked eye and examination under an optical microscope at a magnification of 200x provides no evidence for any porosity as shown in figure 4.21. Figure 4.20 shows a similar magnified photograph of a casting from an equivalent untreated mould. Improvement of the treated casting can be seen in two ways: (i) there is a distinct lack of holes of any size within the body of the casting (light area) and (ii) the surface of the casting is uniform suggesting that there has been limited or no attack on the casting by hydrogen gas. Under similar conditions to those used for sand casting the protection against the defect in the investment shell is superior and again this is due to the surface smoothness. Investment casting is a precision casting technique and therefore no post-cast treatment is necessary to regulate the casting dimensions and so by definition the mould must not contain any irregularities that will be conveyed to the casting. The internal surface of the investment shell contains minimal crevices and cracks which allows the TMCS and other agents to coat the surface more effectively providing better protection.

Several different silanes were tested to ascertain their performance against TMCS. Triphenyl chlorosilane (TPCS) is a solid at room temperature and its ease of transportation and storage were attractive properties. Its use as a mould treatment agent could only be established in the presence of a solvent. The solvent used for this purpose was di-ethyl ether which has a low boiling point for ease of removal but its use in a foundry environment must be circumspect due to its low flash point. A 10% w/w solution of TPCS in sodium dried ether was made up and the mould submerged into it for 10 seconds. The mould was removed for air drying and a crystalline deposit could be seen on the surface of the mould. A casting was carried out in the mould by the method previously described and the resulting macrograph can be seen in figure 4.22 (right) with a casting carried out in an untreated mould. The two castings were cast separately. The TPCS has increased the castability of the metal to a similar extent to the TMCS. The crystalline deposit had no adverse affect on the finished casting but the use of TPCS is unattractive due to cost and solvent flammability problems.

Trimethylbromosilane (TMBS) was used as an alternative to the chloride due to bromide being a better leaving group. The compound provided a colourful acknowledgment of the siloxylation by turning the liquid a yellow colour as HBr was given off. The resultant treated

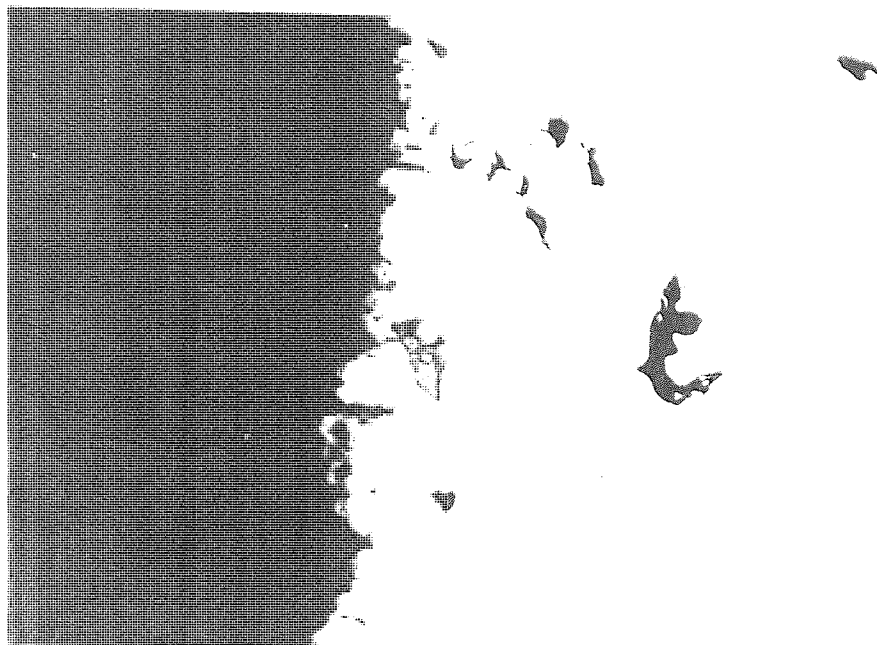


Fig 4.20 - Photograph magnified 200x of the edge of an untreated investment casting

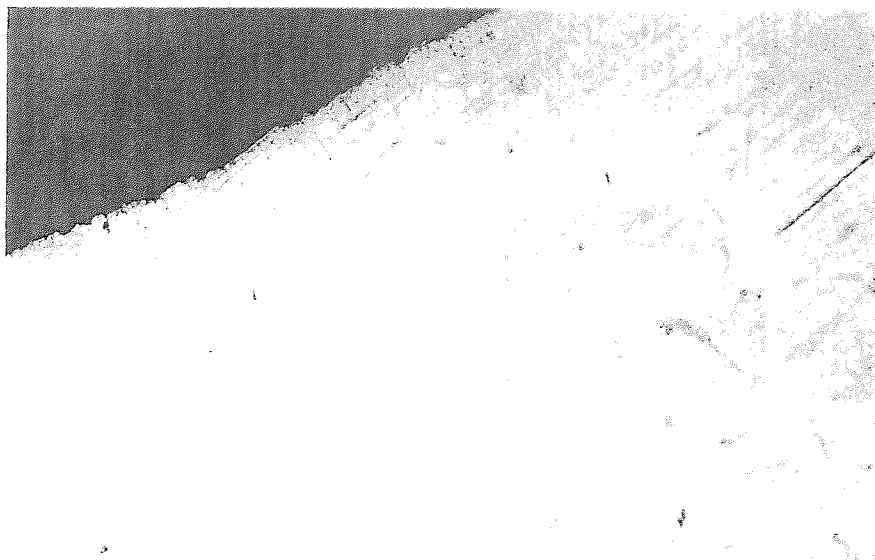


Fig 4.21 - Photograph magnified 200x of the edge of a TMCS treated investment casting

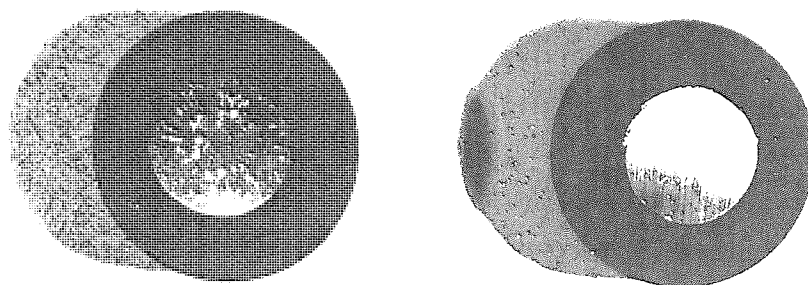


Fig 4.22 - Photograph showing castings from a TPCS treated mould(right)
and an untreated mould(left)

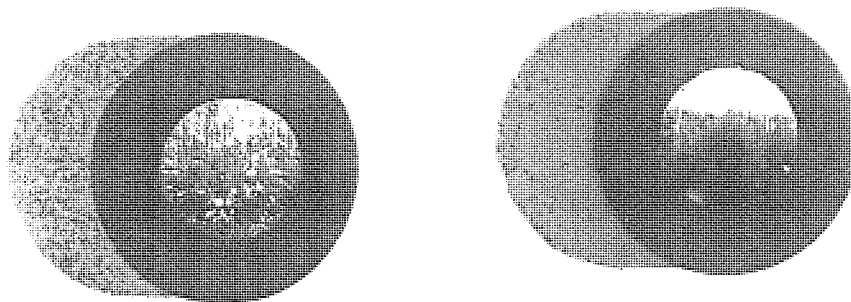


Fig 4.23 - Photograph showing castings from a TMBS treated mould(right)
and an untreated mould(left)

mould took considerably longer to dry as the bromo derivative of TMCS is less volatile with a boiling point of 79°C in contrast to 57°C for the TMCS. When the mould was cast into there was a small fire on the top of the mould that burned for several seconds. This was due to TMBS vapour being present in the mould cavity as TMBS has a much increased density over TMCS. The flammability of the treatment agents could be a problem when the procedure is scaled up. No fires were encountered during the TMCS trials. The macrograph produced from the casting can be seen on the right in figure 4.23. It is shown against an untreated mould and the two were cast separately. The casting exhibits no porosity and is equal to both the TMCS castings and the TPCS casting. This result was expected but the chloro derivative would be used in preference for volatility, density and cost reasons.

Tri-isopropylchlorosilane and tert-butyldimethylchlorosilane were used as siloxylating agents to test the protection given by larger aliphatic groups. On casting into the isopropyl treated mould there was again the incident of a fire that was more severe than that of the bromo derivative. This is not necessarily due to the density of the compound which is only slightly higher than that of TMCS, but more likely due to the volatility factor. The boiling point of tri-isopropyl chlorosilane is 198°C and the mould had not dried sufficiently and the excess coating was burnt off. This could be remedied by heating the mould to remove the excess treatment agent. The resulting casting is shown in figure 4.24 (right) again alongside an untreated casting carried out separately. The macrograph reveals the incidence of porosity spread evenly around the casting. The tert-butyl methylchlorosilane is a solid at room temperature so a 10% w/w solution was made up in dry diethyl ether. The mould was treated in the same way as the TPCS mould. There were no problems encountered on casting. The macrograph is represented in figure 4.25 (right). There is considerable porosity in this casting and on a quantitative basis it can be said there is no improvement on the untreated casting.

The performance of TMCS as a mould coating on a series of moulds subject to a time delay between treatment and casting can be seen in figure 4.26. In theory a mould should be surface treated immediately prior to casting but unforeseen circumstances can cause delays therefore a series of three moulds were cast into 1 hour, 5 hours and 24 hours after treatment. Figure 4.26 shows these castings from left to right respectively. The effect of the TMCS does not significantly diminish over the time period as would be expected since the Si-O bond is resistant to hydrolysis. The mechanism by which this occurs is a cleavage of the Si-O bond (in preference to the O-C bond) due to the susceptibility of the silicon to nucleophilic attack. Hydrolysis of the silyl phenol ether is dependant on several factors including structure and steric arrangement. An acid medium is advantageous and the presence of HCl is usually sufficient to catalyse the reaction. Over a period of time the hydrogen chloride generated throughout the silylation and any excess TMCS

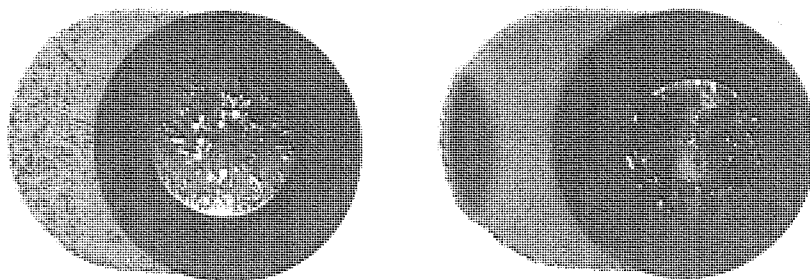


Fig 4.24 - Photograph showing castings from a TiPCS treated mould(right)
and an untreated mould(left)

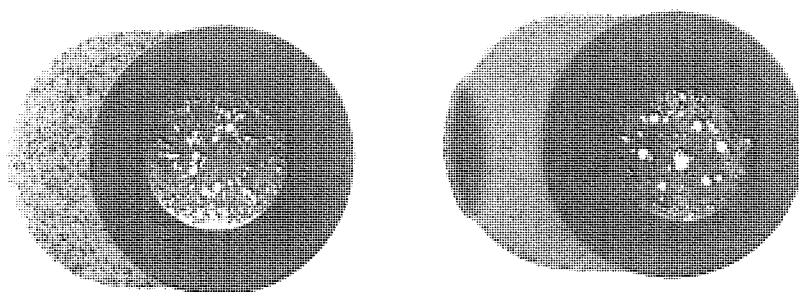


Fig 4.25 - Photograph showing castings from a TtertBCS treated mould(right)
and an untreated mould(left)

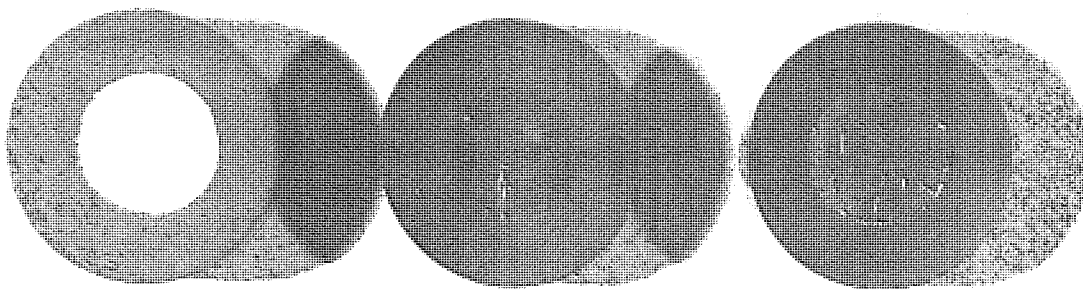


Fig 4.26 - Photograph showing a series of time delayed castings
1hr(left), 5hr(middle) and 24hr(right)

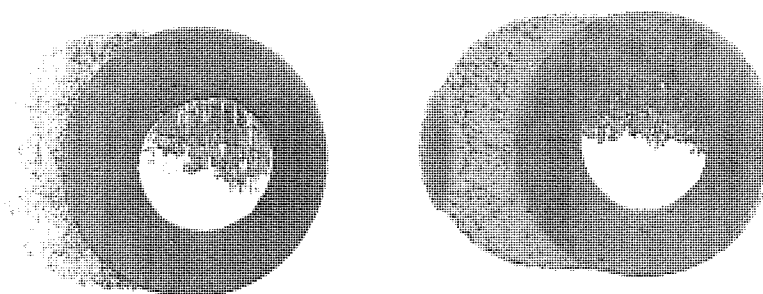


Fig 4.27 - Photograph showing two TMCS treated moulds. One cast
at RT(left) and one at approximately 400°C(right)

will be removed from the mould surface and hence an acid medium is no longer prevalent. Therefore hydrolysis of the silyl ether is retarded. Current practice in precision casting foundries is to chill cast investment moulds at a temperature of approximately 400°C. Chill casting was removed from the investment casting procedure for the experiments carried out previously in order to compare the results with the sand casting trials which were cast at room temperature. It was necessary however, to assess the protection of TMCS at mould temperatures of up to 400°C. The casting procedure had to be modified slightly to accommodate the change. Following the firing at 900°C the mould was cooled in a desiccator to room temperature. It was then treated as normal and allowed to air dry. It was placed in a sand bath which was placed inside an ashing furnace built within a CEM MDS 81 industrial microwave oven. The microwave power was set at 100%(650W) and the oven temperature was set to 400°C and the mould allowed to warm up. When the furnace had reached the desired temperature the mould was removed from the oven and cast into immediately. The results from this casting can be seen in figure 4.27 (right) alongside a treated mould cast simultaneously at room temperature. The casting was of good quality with no porosity and in this case is better than the casting at room temperature but there was a discrepancy between the furnace temperature in the microwave oven and the mould temperature. Adjustments had to be made and a second casting was poured at a mould temperature of 370°C. The macrograph is shown in figure 4.28. There is a marked increase in fine porosity around the edge of the section over a mould treated and cast at room temperature although there are no 'holes'. Once the temperature problems had been remedied a series of double castings was made. Pairs of TMCS treated moulds were cast into, one at raised temperature and one at room temperature. The temperature range used for the raised temperature castings was 100°C to 400°C in 100°C stages. This series of castings can be seen as the macrographs in figures 4.29 to 4.32 with the high temperature castings displayed on the right. The four castings poured at temperature show no correlation with regards to the occurrence of the defect. There is most porosity on the 400°C casting as may be expected yet there is a large manifestation on the 200°C with very little on the 300°C casting and some porosity on the 100°C casting. Few conclusions can be drawn from such results but they indicate that the moulds treated at higher temperatures are more susceptible to protective coating breakdown. Siloxanes and silicone oils are used effectively in the plastics and rubber industry as mould release agents by baking the coating onto the surface, and the use of these materials on investment shells may improve the coating performance. However the outcome of this study relies on more comprehensive trials being carried out in a foundry environment where more conclusive evidence could be obtained.

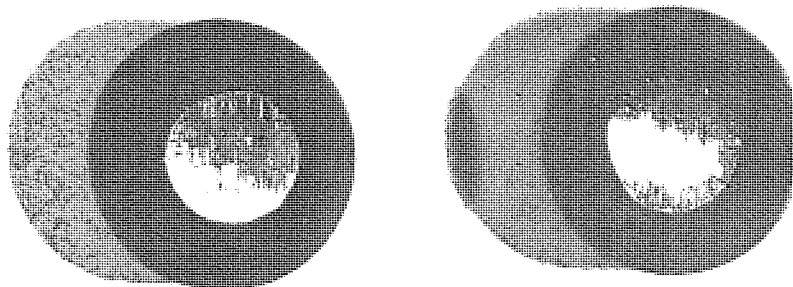


Fig 4.28 - Photograph showing castings from two TMCS treated moulds.
One at RT(left) and one at 370°C(right)

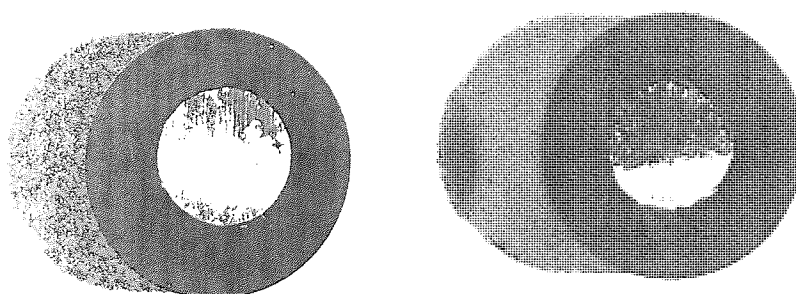


Fig 4.29 - Photograph showing castings from two TMCS treated moulds.
One at RT(left) and one at 400°C(right)

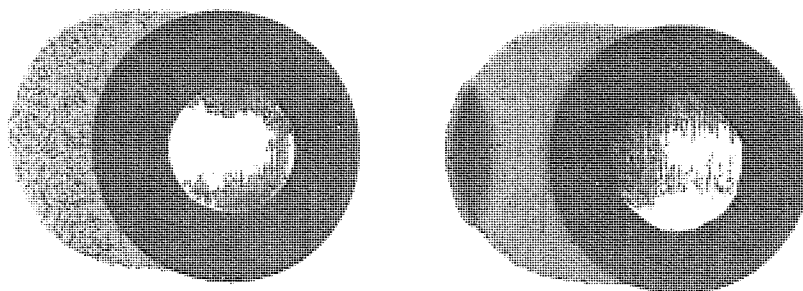


Fig 4.30 - Photograph showing castings from two TMCS treated moulds.
One at RT(left) and one at 300°C(right)

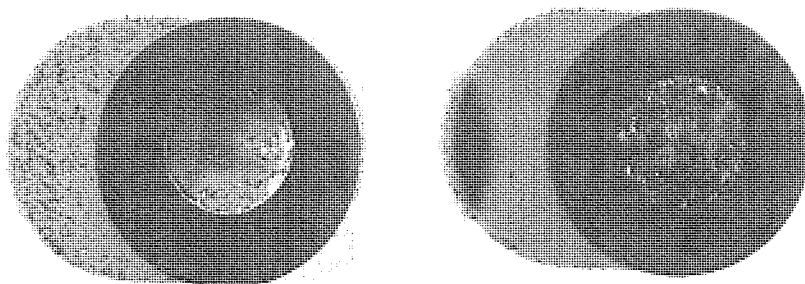


Fig 4.31 - Photograph showing castings from two TMCS treated moulds.
One at RT(left) and one at 200°C(right)

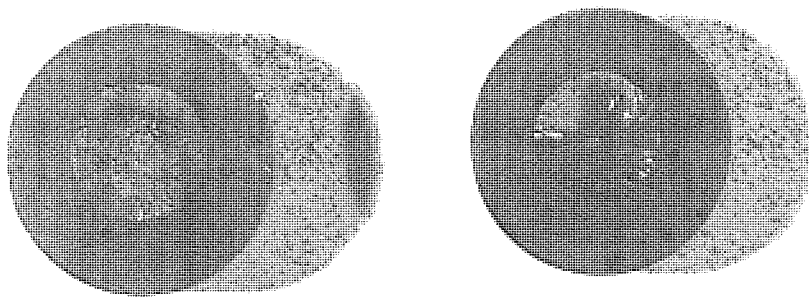


Fig 4.32 - Photograph showing castings from two TMCS treated moulds.
One at RT(left) and one at 100°C(right)

4.8 Conclusion and Further Work

Casting experiments have established that the metal mould reaction is caused by both the organic hydroxide groups present on the phenolic binders for the sand moulds and the inorganic hydroxide groups on the ceramic refractories used for investment shells. The vigour of the reaction is directly related to the concentration of lithium in the alloy but independent of the binder concentration for sand casting and independent of alloy concentration for investment moulds. Surface differences are responsible for this variation in the respective moulds. Treatment can take the form of physical or chemical coating but physical coating is normally ceramic based to cater for the heat generated by casting and it has been established that this does not remove the cause of the defect. Chemical coating must be effective and simple to use. Sand moulds are restricted to low temperature treatment due to the sensitivity of the organic binders to temperatures in excess of 70°C. Simple silanes were employed to carry this task out, primarily trimethylchlorosilane. The method of application that was utilised to greatest effect was spraying. Other, more complicated, hydroxide protecting agents were tested with poor results. Investment moulds require a different method for casting and hence a different protecting procedure could be used.

Trimethylchlorosilane was used as a standard and several other silanes were tested with mixed results. The triphenylchlorosilane and trimethylbromosilane gave excellent results but the silanes with larger organic groups gave poor castings. The conclusion that can be drawn is that simplicity is imperative. A substance that can be easily applied with the excess easily removed gives the best results. Should it be required a mould can be left for at least 24 hours before casting after being treated with TMCS without any decrease in hydroxide protection. Higher temperature castings were carried out using TMCS but the outcome was inconclusive and further work must be done to ascertain the value of TMCS at higher temperatures.

The testing of some of these materials in a foundry environment would be vital to the overall assessment of the casting problem. Experimentation of such processes as casting in a laboratory is false and real information can only be gained from real casting. The outcome of this trial gives a good indication as to the direction which the project should head in. Investment shells may benefit from the utilisation of silicone oils and polymers that can be baked onto the surface. This may give a more reliable coating with a semblance of permanence about it. Their use is well documented as mould release agents for the rubber and plastic industry and in the protection of masonry. Liquid polydimethylsiloxanes applied as a non toxic aqueous emulsion from a spray and baked onto the surface of an investment mould would seem the ideal route forward.

Chapter Five
N.M.R. STUDIES

5.1 Introduction

The use of ${}^6\text{Li}$ rather than ${}^7\text{Li}$ for solid state M.A.S.N.M.R. studies has not been widely explored. Information is presented in this chapter that supports the view that, for solid state work, ${}^6\text{Li}$ is the preferred nucleus for study because the narrower lines may enable resonances of similar frequency to be resolved using ${}^6\text{Li}$ M.A.S.N.M.R. when an apparent singlet may be seen in the ${}^7\text{Li}$ M.A.S.N.M.R. spectrum.

5.2 Solid State N.M.R. Spectroscopy

An element with a nucleus containing an uneven number of nucleons or an odd atomic number will exhibit nuclear (spin) angular momentum. This spin has an associated magnetic momentum which, when placed between the poles of a magnet, will align with the applied magnetic field and interact with neighbouring nuclei with similar magnetic properties. The nuclear spin thus behaves like a magnetic dipole and the potential energy E of this dipole is determined by the action of the magnetic moment μ in a magnetic field of strength B_0 and is defined as

$$E = - \mu \cdot B_0 \quad \text{.....eq (1)}$$

The nuclear angular momentum or 'spin' is represented by the vector \mathbf{I} and has a maximum value of $\hbar[I(I+1)]^{1/2}$, where I is the nuclear spin quantum number, \hbar is the reduced Planck's constant $h/2\pi$ and $I\hbar$ is the maximum observable component of \mathbf{I} in any direction. The observable components of \mathbf{I} are $M_I\hbar$ where M_I is the magnetic quantum number and take the values $I, (I-1), \dots, (-I+1), (-I)$ and hence the total number of observable components is $2I+1$. Nuclei such as ${}^{16}\text{O}$ with $I = 0$ are non magnetic and so cannot be observed by N.M.R., but those nuclei that do exhibit magnetic properties increase by half integral values of I ($1/2, 1, 3/2, 2, 5/2, \dots$) e.g. ${}^1\text{H}$ ($I=1/2$), ${}^{27}\text{Al}$ ($I=5/2$).

The magnetism of a nucleus can best be described in terms of its gyromagnetic ratio γ , the proportionality constant relating the magnetic moment μ to the nuclear spin angular momentum \mathbf{I}

$$\gamma = \mu/\mathbf{I} \quad \text{.....eq (2)}$$

this equates to

$$\gamma = \mu/\hbar [I(I+1)]^{1/2} \quad \text{.....eq (3)}$$

or

$$\gamma = \mu/I\hbar \quad \text{.....eq (4)}$$

By convention the magnetic field B_0 is applied in the z direction and the magnetic moment μ can align with it in any of $2I+1$ orientations at an angle θ to the field direction. A diagrammatic

representation of this can be seen in figure 5.1. Since the nucleus is spinning the magnetic moment precesses around the z axis at a frequency known as the Larmor frequency.

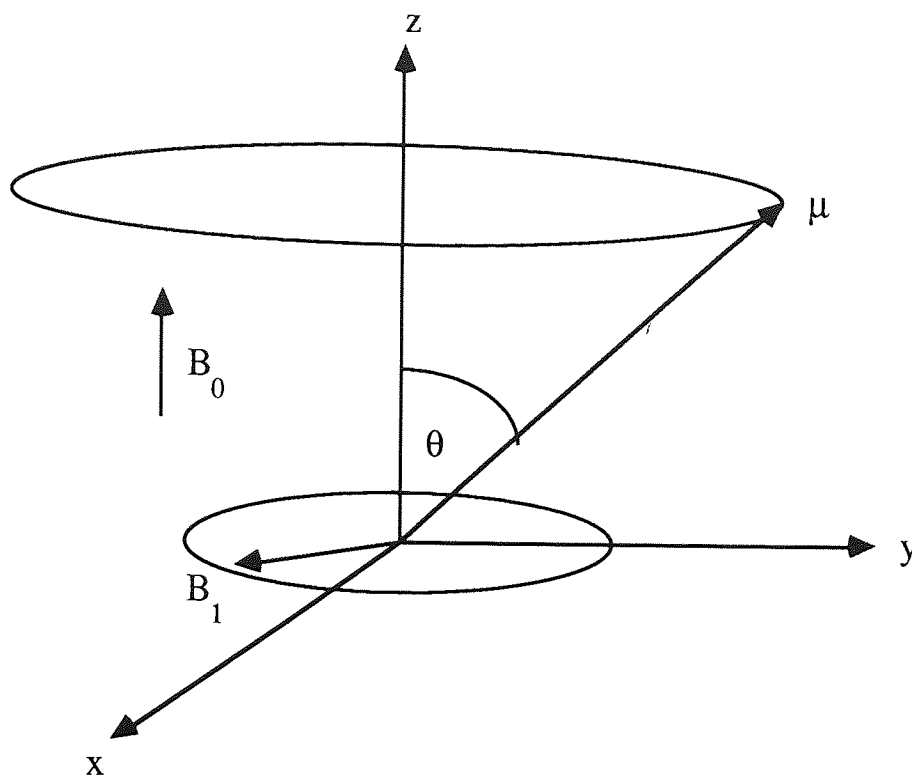


Figure 5.1 - Vectorial Representation of the Larmor Precession

The N.M.R. experiment is carried out by changing the orientation of the magnetic moment to another orientation, normally the mirror image, by applying a second magnetic field of strength B_1 in the xy plane rotating at the Larmor frequency.

Utilising equations (1) and (4) and the quantization of the vector I into observable components $M_I \hbar$ along the direction of B_0 gives

$$E = -\gamma \hbar M_I B_0 \quad \dots \text{eq (5)}$$

The $(2I+1)$ values of M_I ranging from $-I$ to $+I$ correspond to the different magnetic energy levels separated by Zeeman splitting as illustrated in figure 5.2. Changing the orientation, or flipping the spin of the nucleus, can be effected by supplying the energy quanta sufficient to induce a transition of the nuclear spin between energy levels. The selection rule is $\Delta M_I = \pm 1$ so that for a single bare nucleus all the transitions have the same energy ΔE

$$\therefore \Delta E = \eta \nu = \gamma \hbar B_0 = \mu B_0 / I \quad \dots \text{eq (6)}$$

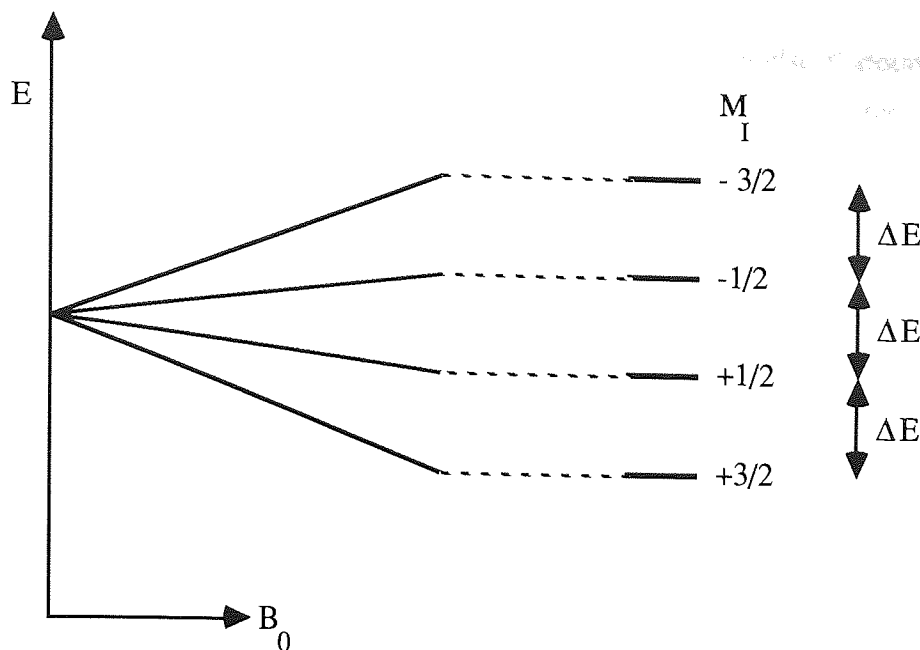


Figure 5.2 - The Energy Levels of a Nucleus with Spin $I = 3/2$ showing the Zeeman Splitting

The energy quanta required to cause a transition can be supplied by electromagnetic radiation of the correct frequency and this frequency can be obtained from the Bohr relation :

$$h\nu = \Delta E$$

$$h\nu = \mu B_0 / I \quad \text{.....eq (7)}$$

By combining equations 7 and 4 the above equation can be expressed in terms of the gyromagnetic ratio :

$$\nu = \gamma B_0 / 2\pi \quad \text{.....eq (8)}$$

Therefore the nucleus can interact with radiation whose frequency depends only upon the applied magnetic field and the nature of the nucleus.

The field strength of B_1 can be equated to $\gamma B_0 / 2\pi$ and the application of B_1 to the precessing nuclei will therefore cause absorption and emission transitions, but always resulting in a net absorption of energy. As B_1 is rotating at the Larmor frequency it appears stationary to the precessing nuclei and they will precess around B_1 . The precession cone, originally centred around the z axis, will shift. Since all the magnetic moments do not have the same component in the xy plane they no longer cancel out and a net magnetisation M_{xy} is experienced in the xy plane. M_{xy} is

now rotating about the z axis, causing a current to be induced in a coil placed around the sample. This electromagnetic current is the basic signal measured in the N.M.R. experiment.

Due to the exceptionally small splitting of nuclear energy levels, of the order of 10^{-25} J, the detected signal is very small making N.M.R. much less sensitive than other spectroscopic techniques, such as optical spectroscopy. In order to 'boost' the signal a series of repeated experiments must be carried out to gather sufficient information for a meaningful spectrum. This process brings its own set of problems. The signal to noise ratio increases only as \sqrt{n} where n is the number of experiments carried out but more importantly, in order to repeat the experiment the Boltzmann distribution must be re-established and the repetition time depends on the rate at which this occurs. When the population of the nuclear energy levels are equal, the system is said to be saturated and no more perturbation can occur. Unlike other systems though where molecular collisions can bring about the restoration of the Boltzmann distribution, the relaxation of nuclear spins can only be induced by local magnetic fields rotating at the Larmor frequency. The relaxation time, as it is known, can take from ms to hundreds of seconds meaning some N.M.R. experiments can take several hours if not days to produce a satisfactory signal to noise ratio. Cross Polarisation has been developed to overcome the problems associated with the extended relaxation times of some nuclei and this is described in section 5.3.4., however, some of the more well used nuclei ^1H , ^{19}F and ^{31}P have manageable relaxation times.

Since N.M.R. is an analytical tool based on perturbing the nuclear environment it is understandable that various nuclear parameters will affect the acquired spectrum but basic physical factors must be taken into account when carrying out an N.M.R. experiment on bulk samples. Factors such as chemical shift and spin-spin coupling (J) are factors that can divulge useful information to the user on the chemical system under study but other parameters such as dipolar and quadrupolar coupling can cause broadening of the signal that masks relevant chemical information. These factors are all attributable to interactions between neighbouring nuclei and it is important to minimise all negative influences in the experiment in order to achieve the best result.

Following Griffen⁷², a typical nuclear spin Hamiltonian \bar{H} can be considered :

$$\bar{H} = \bar{H}_{\text{cs}} + \bar{H}_J + \bar{H}_D + \bar{H}_Q \quad \text{.....eq (9)}$$

where \bar{H}_{cs} relates to the chemical shift, \bar{H}_J to the spin-spin coupling and \bar{H}_D and \bar{H}_Q to the dipolar and quadrupolar terms respectively.

5.2.1. Chemical Shift

The chemical shift interaction is derived from the local magnetic fields induced at the nucleus by the action of the electrons circulating within the applied field. If these induced magnetic fields are opposed to the applied field (B_0) then the nucleus is shielded from it and vice versa. The nucleus experiences an effective field given by :

$$B_{\text{eff}} = B_0 (1 - \sigma) \quad \text{.....eq (10)}$$

where σ is the chemical shielding tensor expressed in ppm. The resonance condition in equation (8) can now be expressed as :

$$\nu = \gamma B_0 (1 - \sigma) / 2\pi \quad \text{.....eq (11)}$$

The shielding tensor is derived from quantum mechanical calculations relative to a bare nucleus. This is obviously impractical and chemical shifts are quoted relative to a standard substance ie tetramethylsilane for ^1H , ^{13}C and ^{29}Si . The chemical shift can be defined as :

$$\delta / \text{ppm} \equiv 10^6 (\nu_s - \nu_{\text{ref}}) / \nu_{\text{ref}} \quad \text{.....eq (12)}$$

which can be related to the shielding difference in the limit $\delta \ll 1$. Then $\delta \approx \sigma_{\text{ref}} - \sigma_s$ where s refers to the sample and ref denotes the reference.

5.2.2. Dipolar Coupling

Direct intermolecular interactions are created by the coupling of any two magnetic moments μ_1 and μ_2 separated by a vector r . This dipolar interaction can be represented as :

$$\bar{H}_D = \gamma_1 \gamma_2 h^2 (\mathbf{I}_1 \cdot \mathbf{D} \cdot \mathbf{I}_2) / r^3 \quad \text{.....eq (13)}$$

where γ_1, γ_2 are the magnetogyric ratios for each spin, r is the distance between the two nuclei and \mathbf{D} is the dipolar coupling tensor. The effect of the dipolar interactions on the N.M.R. spectrum depends on the orientation of the dipole in the field and hence the angle θ contributes magnitude of the spectral change. From the $\mathbf{I}_1 \cdot \mathbf{D} \cdot \mathbf{I}_2$ interactions only two terms contribute in the first order and both have a factor $(3\cos^2\theta - 1)/r^3$. This has two implications (i) the interaction is strongly dependant on the internuclear distance and the interaction diminishes rapidly as r increases and (ii) a sample capable of rapid motion can average out all the θ values and hence the dipolar interaction will average to zero. This is a major distinction between solid state and solution N.M.R.. The

rapid tumbling afforded by the sample being in the liquid state is sufficient to remove the dipolar problem and the spectrum is unaffected. In solids or liquid crystals the nuclear positions are maintained relative to the field and hence the direct interaction of the magnetic dipoles will be observed in the spectrum. For a single crystal the interaction between two isolated spins can be evaluated. A magnetic nucleus X with spin I_1 has $2I_1+1$ orientations in the magnetic field and this would split the resonance of neighbour Y at a distance r into a $2I_1+1$ multiplet. The peak separation would depend on the term $\gamma_1\gamma_2h(3\cos^2\theta-1)/r^3$, where θ is the angle between the internuclear vector and the field. For any particular nucleus within a polycrystalline sample, though, pairwise interactions described above occur for all angles and all distances and the net result being a severe broadening of the spectrum which is field independent.

5.2.3. Quadrupolar Interactions

Any nucleus with a spin $> 1/2$ has the added complication of possessing a quadrupole moment. The quadrupole moment arises from the fact that the nucleus no longer has spherically distributed charge. The charge is now distributed ellipsoidally either prolate or oblate. The non-spherical charge distribution gives rise to an electric field gradient at the nucleus, and the interaction between the electric field gradient (EFG) and the nuclear spin gives rise to the quadrupolar interaction. When a molecule is placed in an applied magnetic field opposing forces start to act upon the nucleus.

- (i) The magnetic moment of the nucleus will tend to force all the nuclei to align with the applied magnetic field.
- (ii) The electric quadrupole moment will attempt to orient each nucleus with respect to the EFG and not the applied magnetic field.

The decisive factors in this competition are (i) the strength of the nuclear magnetic moment and its interaction with the magnetic field and (ii) the strength of the nuclear electric quadrupole moment and its interaction with the electric field gradient within the molecule. The stronger the quadrupolar interaction the broader the absorption line.

The effect of the quadrupolar interaction on the N.M.R. spectrum depends on the angle θ that the nuclear vector makes with the magnetic field B_0 , and again terms arise in the mathematics containing the $(3\cos^2\theta-1)$ factor. Therefore quadrupolar interactions are subject to similar rules to dipolar interactions in the fact that if the sample is in the liquid state then the molecules are tumbling rapidly and any orientations of the nucleus with respect to the parent will average to zero since in the N.M.R. timescale all orientations will be experienced. In the solid state such tumbling is not apparent and a single crystal would produce a $2I$ multiplet in the first order but in a poly

crystalline sample interactions over all orientations will produce a spectral broadening of typically several hundred hertz.

5.2.4. Indirect Spin-Spin Coupling

In both solution and solid state an indirect electron coupled spin-spin interaction can occur between two neighbouring nuclei I_1 and I_2

$$\bar{H}_J = h I_1 \cdot J \cdot I_2 \quad \text{.....eq(14)}$$

In contrast to the direct dipolar interaction this coupling does not average to zero in liquids, and therefore in isotropic phases only an average value of J is observed. Whereas D contains structural information in the form of internuclear distances which may be intermolecular, J contains intramolecular bond related structural information. The coupling is manifested as a symmetrical multiplet splitting which are independent of the applied field as expected for an intramolecular interaction.

There are three mechanisms for J coupling but the most important is the Fermi contact interaction of an s electron with the nucleus. Consider an HF molecule where both nuclei have $I=1/2$ and +ve magnetogyric ratio. The bonding electrons must have antiparallel spins ($\alpha\beta$) by the Pauli principle and their motions are correlated such that if the electron with the α spin is near one nucleus then the one with the β spin is likely to be near the other. Within each nucleus the magnetic moments of the nucleus and electron are more stable when parallel so that their spins are antiparallel (electrons have negative γ).

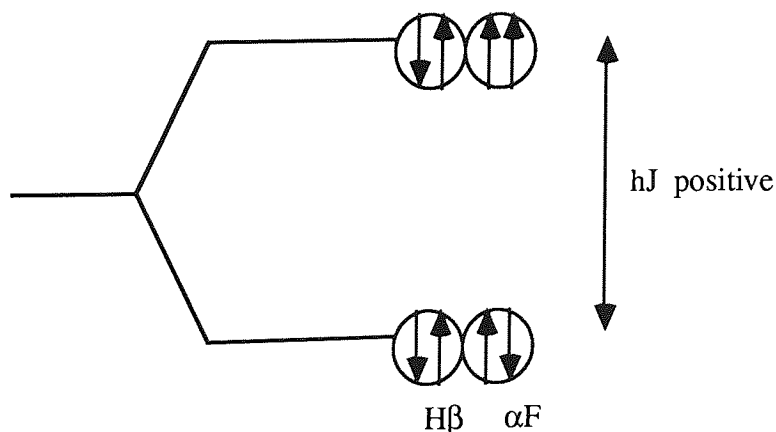


Figure 5.3 - Splitting of ^1H energy level in HF by spin-spin coupling to ^{19}F , mediated by the Fermi contact interaction

The nuclear spins are therefore coupled, having a lower energy when antiparallel than when parallel and the difference in energy hJ_{HF} is defined as positive (see figure 5.3). The interaction can be slightly different if taken over two bonds for example the coupling of ^{19}F and ^1H in CH_3F . The bonding electrons on the carbon are more stable when parallel i.e. $\text{H} \uparrow\downarrow \text{C} \uparrow\downarrow \text{F}$ by Hund's rule of maximum multiplicity. Thus the parallel configuration of the H and F is now the more stable. The energy difference this time $^2hJ_{HF}$ is denoted as negative.

The other spin-spin coupling terms⁷³ involves interactions mediated by p,d electrons. The orbital term J^o_{AB} arises from the perturbation of the magnetic field due to the electrons orbital motion by the nucleus A, this perturbation being experienced by nucleus B and vice versa. The spin-dipolar terms J^{sd}_{AB} arises from the direct interaction of the magnetic dipole of the nucleus A with that of the orbital electron which then interacts with the nucleus B and vice versa. The observed coupling constant is therefore the sum of all three terms $J^c + J^o + J^{sd}$.

The total number of interactions a nucleus can experience within an applied field have now been described and equation 9 is shown below with the appropriate magnitudes of each term in Hertz.

$$\bar{H} = \bar{H}_{cs} + \bar{H}_J + \bar{H}_D + \bar{H}_Q \quad \dots\text{eq}(15)$$

(0-10³) (0-10) (5*10⁴) (10⁵-10⁶)

The fundamental difference between solution and solid state N.M.R. spectra is that in the former case, the fast rotational and translational motion of the molecules averages the interactions. In the case of \bar{H}_D and \bar{H}_Q the tensors are traceless and their isotropic average values are exactly zero. These are not directly observed at all in solution N.M.R. spectra although they may contribute indirectly via relaxation mechanisms. In the case of \bar{H}_{cs} and \bar{H}_J non zero averages occur resulting in the isotropic chemical shifts observed in high resolution solution spectra.

The basic solution to obtaining high resolution solid state spectra is thus to implement experimental procedures which remove the dipolar and first order quadrupolar interactions completely.

5.3. Line Narrowing Techniques For Solids

5.3.1. Magic Angle Spinning (M.A.S.)

There are two ways of removing dipolar broadening. One is to manipulate the sample and the other is to manipulate the spins. Manipulation of the sample is carried out using the magic angle spinning technique and widths as narrow as a few hertz have been obtained. Spinning the sample

rapidly about an axis inclined at an angle θ to the field introduces the term $(3\cos^2\theta-1)/2$ into the time averaged N.M.R. Hamiltonian representing the dipolar interaction, the anisotropic chemical shift interaction, the anisotropic spin-spin coupling and the first order electric quadrupole interactions. If the sample were spun rapidly at an angle so as to make the term $(3\cos^2\theta-1)/2$ equal to zero then all the above interactions would vanish from the spectrum. This angle is $54^\circ 44'$ and is termed the 'magic' angle.

5.3.2. Multipulse Line Narrowing

Manipulation of the spin system can be carried out by multipulse line narrowing experiments. This is done by introducing a time dependence into the spin system by applying a train of rf pulses whilst the sample remains stationary. Pulse repetition rates can be made greater than the static dipolar line width so in effect line narrowing can be achieved with pulse spacings of a few microseconds equivalent to rotation speeds in excess of 100kHz. This method differs from M.A.S. in that (a) the pulse train affects interacting spins only if they have the same Larmor frequency (ie homonuclear broadening only is removed) and (b) the rotation of the spin does not affect the anisotropic chemical shift interaction, thus the components of shielding can be obtained.

5.3.3. High Power Dipolar Decoupling

In abundant spin systems, the most common being protons, there is a high density of nuclei of high isotopic abundance. In this case the dipolar interaction can be represented as :

$$\bar{H}_D = \bar{H}_{D(H-H)}$$

The dipolar term becomes dominant within the overall Hamiltonian and the solid proton spectrum generally shows only a broad featureless absorption. In order to decouple these strong interactions very powerful decoupling fields are necessary and their finite efficiencies combined with the small range of proton chemical shifts has rendered this technique impractical. Dilute spin systems are much simpler. In this case there is only a low concentration of the nucleus being observed due to either a low isotopic abundance or a low absolute concentration of the particular nucleus in the sample. The dipolar Hamiltonian is now as follows :

$$\bar{H}_D = \bar{H}_{D(H-X)} + \bar{H}_{D(X-X)}$$

The term H-X is used here to denote the hydrogen interaction with the chosen nucleus since hydrogen is abundant in many systems but most ceramic systems have little or no hydrogen and in this case the $\bar{H}_{D(H-X)}$ term is reduced to a negligible amount. However for systems that do

contain a considerable amount of hydrogen or other abundant N.M.R. active nucleus the $\bar{H}_{D(H-X)}$ term is dominant. This term can be removed by decoupling at the proton resonance (or other nucleus) frequency whilst observing at the X nucleus frequency.

5.3.4. Cross Polarisation

The three techniques described so far, are all concerned with improving the spectral resolution. Cross polarisation (C.P.) increases the signal to noise (S/N) ratio of the spectrum of the dilute nucleus without affecting the resolution.

The technique is based on enhancing the magnetisation of the dilute nucleus (S) from the magnetisation reservoir of the abundant proton (I) spin system. Initially the proton spin magnetisation is rotated by 90° to align it with the y-axis in the rotating frame. The phase of this on resonance pulse is now shifted by 90° so that it (B^I_1) and the proton magnetisation are both aligned along the y-axis. The proton spins will now precess around (B^I_1) and are said to be 'spin locked', the fast T_2 decay which would normally occur being prevented by the spin locking field (B^I_1). Simultaneous with the phase shift of the proton pulse, an on resonance RF pulse (B^S_1) is applied to the dilute nucleus X, the magnitudes of (B^I_1) and (B^S_1) being chosen so as to satisfy the Hartmann - Hahn condition :

$$\gamma_I (B^I_1) = \gamma_S (B^S_1)$$

The X nucleus magnetisation now grows by transfer of magnetisation (cross polarisation) from the proton reservoir during the contact time τ_c . The contact is provided by the dipolar interaction of the I - S spins. At the end of the contact time B^S_1 is turned off and the X nucleus decay is measured whilst the proton spins are simultaneously decoupled by the field B^I_1 . After a delay time τ_D the sequence is repeated.

The N.M.R. experiment for solids is now complete. It has been shown that, with the use of magnetic fields, transitions of the nuclear spin can be induced. It has also been shown how various inter and intra molecular interactions can affect these transitions causing the broadening of resonances and transforming the highly resolved spectrum as would have been seen in liquids to a broad featureless spectrum with little definition. Explanations of techniques derived to overcome these solid-state problems have been given and the solid state chemist is now capable of producing a highly resolved spectrum nearing solution quality in some cases.

Until recently the nuclei available to a solid state inorganic chemist wishing to carry out N.M.R. studies have been limited. Classical inorganic chemists could study the effects of metal

complexes through the ^{19}F and ^{31}P nuclei and geologists and mineral chemists were able to examine samples using ^{29}Si and ^{27}Al . The advent of line narrowing techniques, Fourier transform, and faster spinning speeds has brought a new array of nuclei into the grasp of the inorganic chemist, not least ^{13}C which has benefited considerably from the decoupling and cross polarising techniques. Lithium has become an increasingly important nucleus in recent times and the use of this nucleus in N.M.R. work has also increased. ^7Li N.M.R. spectroscopy is well established in solution studies. The nucleus has a high natural abundance (92.5%) and a favourable receptivity (1500, $^{13}\text{C} = 1.00$); however, the quadrupole moment ($-4.5 \times 10^{-30} \text{ e m}^2$) can give rise to broad lines in non-cubic environments. It is, therefore, sometimes profitable in solution studies to examine ^6Li spectra despite the lower abundance (7.5%) and less favourable receptivity (3.58, $^{13}\text{C} = 1.00$) as the quadrupole moment is also significantly lower ($-8 \times 10^{-32} \text{ em}^2$), and narrower lines can result⁷⁴⁻⁷⁷.

The use of ^6Li for solid state M.A.S. N.M.R. studies has been somewhat overlooked in favour of the more abundant and receptive ^7Li . Studies have been carried out on various undoped lithium containing materials utilising the ^6Li N.M.R. nucleus, and information is presented in this chapter that supports the view that ^6Li is the preferred nucleus for solid state work since the low receptivity and lower abundance of the ^6Li nucleus does not affect the N.M.R. experiment to the degree that was initially anticipated. The narrower spectral lines of ^6Li has enabled resonances of similar frequencies to be resolved when an apparent singlet may be seen in the ^7Li spectrum.

5.4. Experimental

Several lithium compounds were obtained and prepared for the study.

8-Lithoxoquinoline sesquihydrate

8-hydroxyquinoline (15g, 0.105 moles) was treated with an ethanolic solution of lithium ethoxide (0.103 moles). A precipitate was formed which was filtered from the yellow solution, and soxhlet extracted with ethanol. The resulting yellow solution was evaporated to afford yellow crystals, which were washed with cold ethanol and dried in vacuo. The product yield was 60%; and it had a melting point in excess of 300°C . Elemental analysis gave C, 67.4; H, 4.54; N, 8.62; O, 15.2% agreeing with the theoretical formula $\text{C}_9\text{H}_7\text{LiNO}_{1.5}$ which requires C, 67.5; H, 4.38; N, 8.76; O, 15.0%.

Laponite RD, which will be referred to as laponite, was obtained from Laporte Industries Limited. The thermal treatment, and rehydration ($200, 400, 600, 800, 1300^\circ\text{C}$) was carried out following the literature method⁷⁸ using a Carbolite furnace. The clay was ion exchanged with

lithium using both a conventional method⁷⁹ and by treating 1g of laponite with an aqueous solution (10cm^3) of 1mol dm^{-3} LiCl in a screw-capped Teflon container (Savillex Corporation, Minnetonka, Minnesota, U.S.A.) and heating for 5 mins in a Sharp Carousel domestic microwave oven (650W, med-high setting in five one minute bursts).

Other materials

Lithium compounds were also obtained from commercial sources e.g. LiCl, LiBr, LiI (Aldrich), Lithium Metesilicate (Pfalz and Bauer). All samples were used in their purchased state without further processing.

Li (12-Crown-4) Bromide

Li (12-Crown-4) Bromide was prepared by a literature method⁸⁰ entailing the preparation of a 1:1 molar ratio solution of LiBr and 12-Crown-4 in a 1:1 methanol ethanol mixture. The solvent was slowly evaporated to yield the product in a crystalline form. Li (12-Crown-4) Br was obtained in a 68% yield and has a melting point of $>300^\circ\text{C}$. Elemental analysis provided C, 36.5; H, 6.03% when $\text{C}_8\text{H}_{16}\text{BrLiO}_4$ requires C, 36.5; H, 6.08%.

5.5. Results and Discussion

The need for considering ^6Li M.A.S.N.M.R. as an analytical tool developed from work being carried out on the lithium containing materials synthesised from the pyrolysis work explained in chapter 2 and also from work being done on Laponite, a synthetic lithium containing smectite clay (the closest natural counterpart being hectorite). Little work has been reported on the use of ^6Li M.A.S.N.M.R. and it was considered prudent to survey some solid state ^6Li data for a variety of 'simple' compounds and hence the range of materials listed in table 5.1 was considered. Following this work Eckert et al⁸¹ reported their findings of N.M.R. studies on non oxide chalcogenide glasses. ^6Li solid state N.M.R. was used in conjunction with other N.M.R. nuclei to assess the structural and motional properties of the glasses. They observed that the ^6Li M.A.S.N.M.R. spectra were significantly better resolved than the corresponding ^7Li N.M.R. spectra, results that are in line with the findings of the work reported in this chapter.

It is necessary to point out, before any examination of experimental data can be made, that the comparison of ^6Li and ^7Li spectra is not simple.

Compound	δ (ppm vs. satd. aq. LiCl)
LiI	-2.312
LiBr	-2.152
	-0.359
laponite	-0.735
Li ₂ SiO ₃	0.200
Li(12-crown-4)Br	0.659
Li(C ₉ H ₆ NO).1/2H ₂ O	1.397

Table 5.1 - Some ⁶Li Chemical Shift Data obtained from M.A.S.N.M.R. studies of Lithium Compounds

⁷Li has a nuclear spin of 3/2. When the nucleus is located in a ligand field of less than cubic symmetry (ie when the electric field gradient (EFG) is >0), the maximum of the -1/2 <---> +1/2 transition does not correspond to the isotropic chemical shift since spinning at the magic angle does not average second order quadrupolar effects to zero. The situation for ⁶Li is different. The nuclear spin is integral (I=1) and the quadrupole effect would be expected to produce a doublet for an oriented ⁶Li sample. Since the use of ⁶Li in solid state work is a novel technique the effects of M.A.S. on such spectra are not well documented and this work has been carried out with a view to developing a better understanding of the subject.

In order to assess the use of ⁶Li M.A.S.N.M.R. as an analytical tool comparisons have been made between ⁶Li and ⁷Li and they are displayed in table 5.2. When Magic Angle Spinning is employed, dipolar broadening is eliminated and therefore any remaining effects can be attributed to quadrupolar interactions with ⁶Li and ⁷Li subject to the same EFG. If then, the samples are spun off the magic angle dipolar effects will be introduced to the spectrum, but as ⁶Li has a smaller gyromagnetic ratio than ⁷Li the resultant spectrum for ⁶Li will show reduced broadening in comparison to the ⁷Li spectrum. 8-Lithoxoquinoline sesquihydrate was used to investigate the above points. Although the structure of 8-Lithoxoquinoline sesquihydrate is unknown the symmetry of the lithium environment must be low. The ⁶Li M.A.S.N.M.R. spectrum (fig 5.4) shows a singlet of 128Hz full width at half maximum. On the removal of the the proton dipolar coupling, (fig 5.5) the peak width increases to 135Hz, a figure that is not inconsistent with the coupling of H₂O. Spinning the sample 'off angle' increases the peak width considerably to 750Hz due to the introduction of dipolar broadening (fig 5.6). The non decoupled ⁷Li M.A.S.N.M.R. spectrum is, as expected, broader than the ⁶Li equivalent in an identical chemical environment (fig 5.7). The increase in FWHM is 6.86 fold at 926Hz, (the ratio of the quadrupole moments ⁷Li : ⁶Li is 56.25). Removal of the spinning produces a 5.56 fold increase in the peak width for the ⁷Li spectrum.

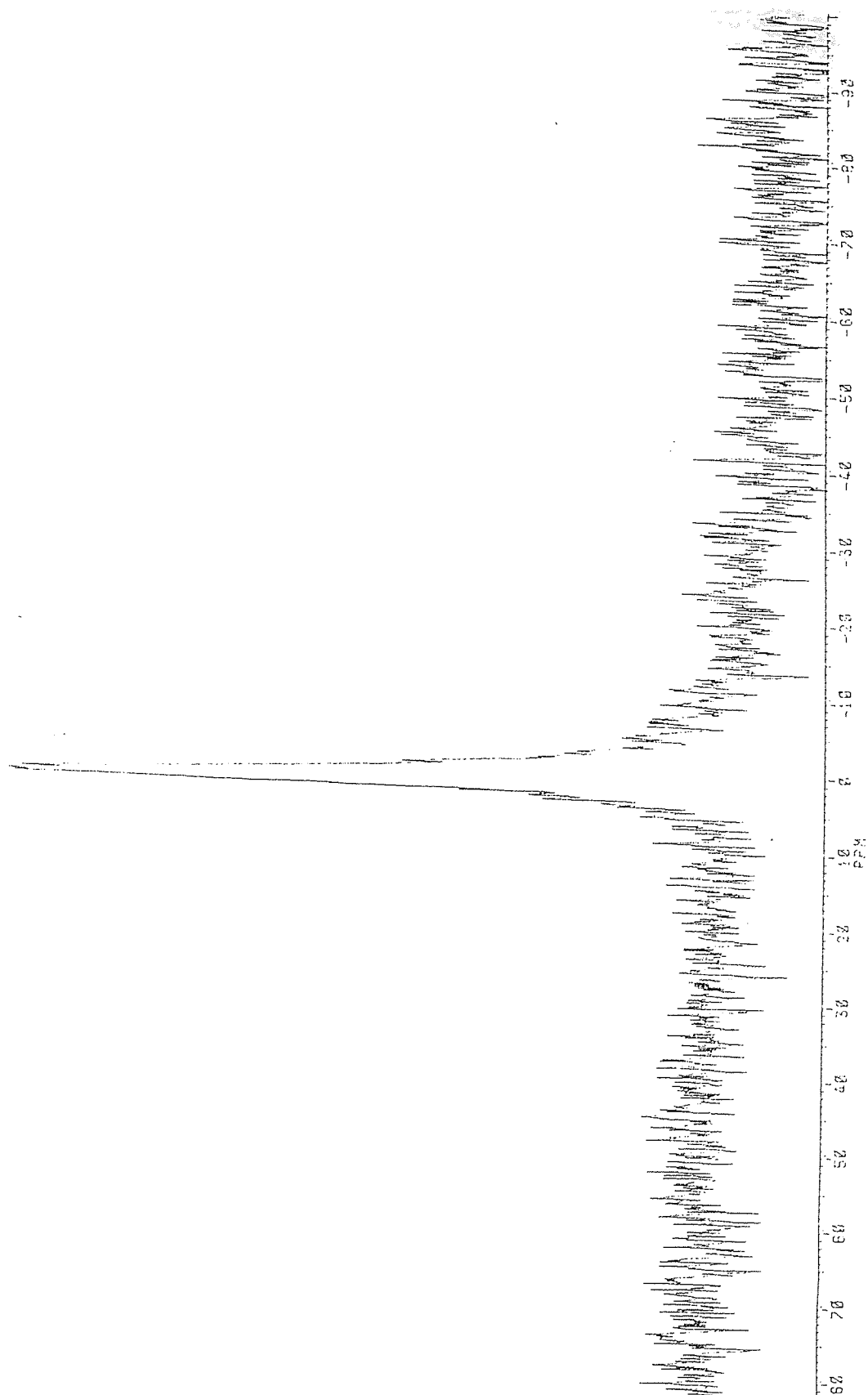


Fig 5.4 - ^6Li M.A.S.N.M.R. spectrum of 8-Lithoxoquinoline sesquihydrate showing a singlet of 128Hz full width at half maximum.

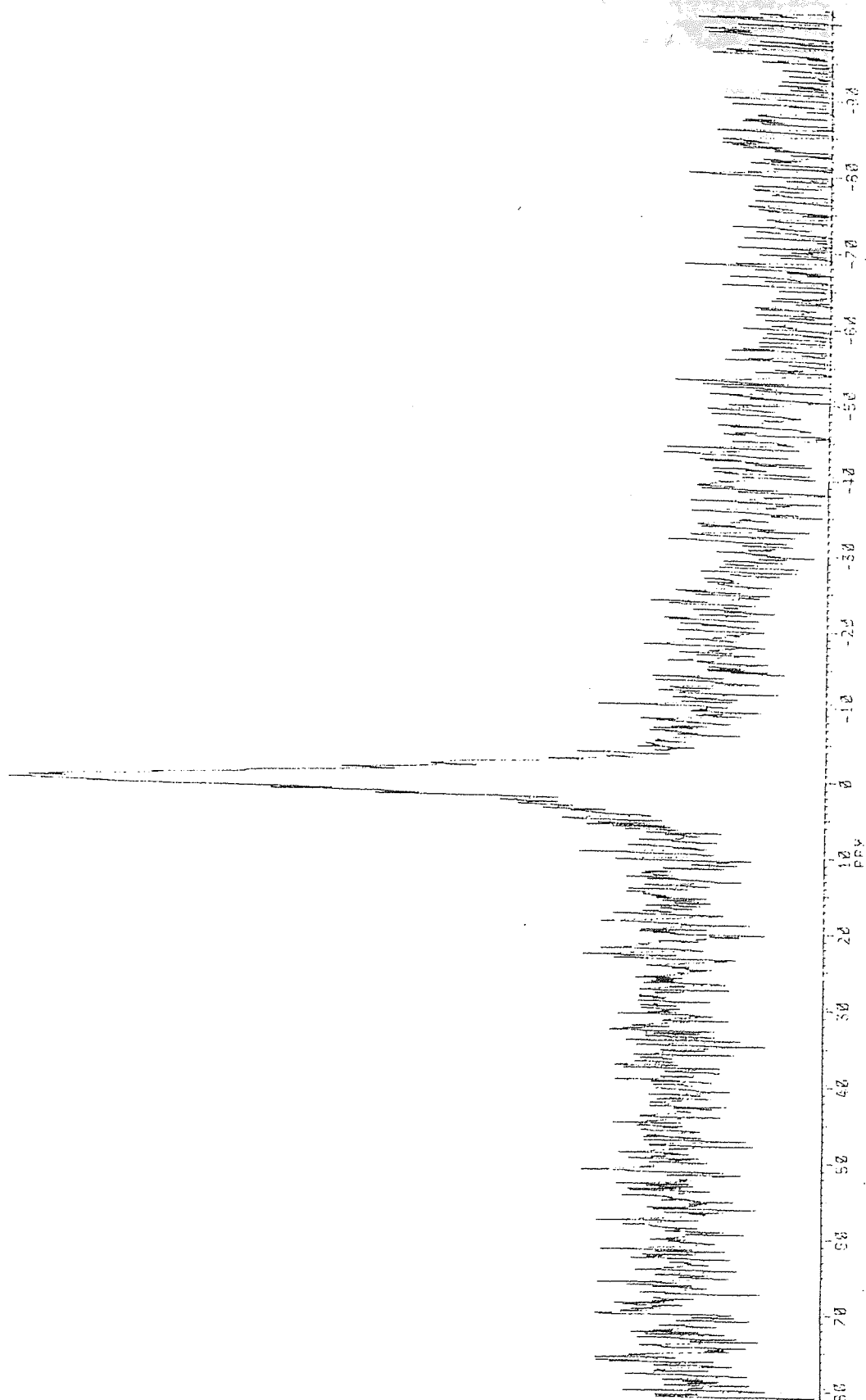


Fig 5.5 - A non proton decoupled ^6Li M.A.S.N.M.R. spectrum of 8-Lithoxoquinoline sesquihydrate showing a singlet of peak width 135Hz

compound / measurement condition	$\delta(\text{ppm})^a$	FWHM / Hz ^b
8-lithoxoquinoline sesquihydrate		
⁶ Li M.A.S. (dipolar decoupling, 1H)	1.397	128
⁶ Li M.A.S. (no dipolar decoupling)		135
⁶ Li 'off angle' spinning	-1.881	750
⁷ Li M.A.S. (no dipolar decoupling)	-0.437	926
⁷ Li static		5150
lithium (12-crown-4) bromide in D ₂ O		
⁶ Li solution (linewidth measurement made with high digital resolution)	0.504	0.39
⁷ Li solution (linewidth measurement made with high digital resolution)	-0.169	0.46

a - 'apparent' chemical shift, i.e. at experimental peak maximum

b - FWHM = full width at half maximum

Table 5.2 - Measurement of linewidths for ⁶Li and ⁷Li resonance lines under a variety of experimental conditions

Attempts were made to obtain spectra for lithium in a low symmetry environment but these were restricted to the examination of Li (12-Crown-4) Br due to solubility problems experienced with the other samples. The sharp lines observed suggest the presence of Li (D₂O)⁺_n species and hence any information gained from these spectra are not comparable to that obtained from the solid species. However, even in the liquid phase the ⁶Li lines are narrower than ⁷Li and the measurement of the linewidths of the example cited under conditions of high digital resolution, reveals an 18% narrowing of the aquated lithium line for ⁶Li over ⁷Li. Therefore under all experimental conditions considered, ⁶Li gave narrower lines. Since neither series of spectra gives the isotropic chemical shifts directly from the observed resonance maxima, the direct comparison of ⁶Li and ⁷Li chemical shifts is not possible. However, comparison of ⁶Li chemical shifts measured under identical conditions should yield chemical information.

Prior to the utilisation of ⁶Li for the above comparisons information was sought regarding the chemical shift range of the ⁶Li nucleus. Several compounds were examined by ⁶Li M.A.S. N.M.R. and the data obtained from these analyses is displayed in table 5.1. The chemical shift data in table 5.1 do imply that the lithium is most shielded when it is more covalent (ie LiI) and interestingly the most ionic of the compounds considered was Li(C₉H₆ON).1/2H₂O which must imply that the coordination of the nitrogen lone pair is, at best, extremely weak. However

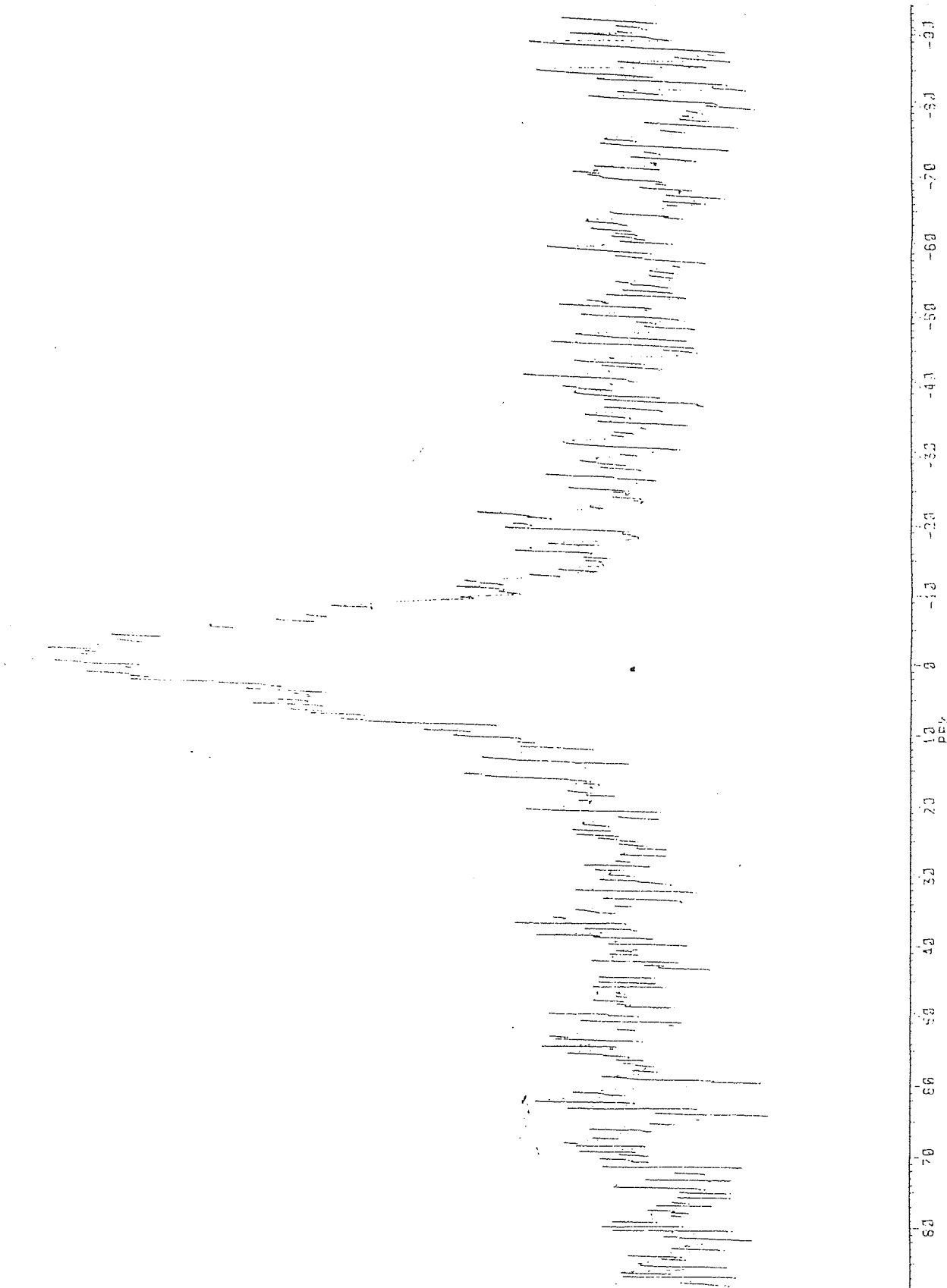


Fig 5.6 - ^6Li 'off angle' N.M.R. spectrum of 8-Lithoxoquinoline sesquihydrate showing a peak width of 750Hz

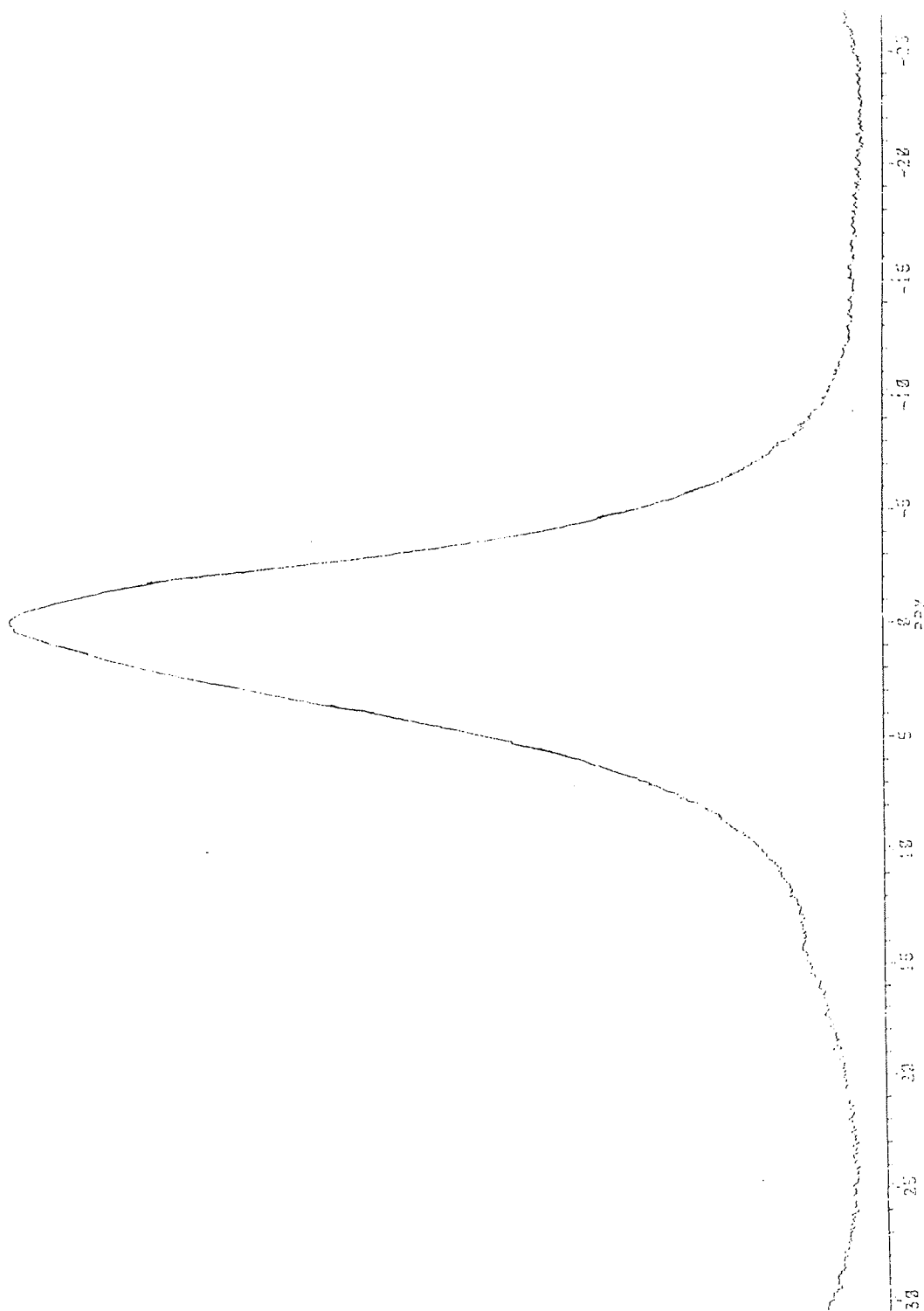


Fig 5.7 - A non decoupled ^7Li M.A.S.N.M.R. of
8-Lithoxoquinoline sesquihydrate

with the most shielded compound giving a δ of -2.3 ppm and the least shielded a value of +1.4 ppm the chemical shift range of ^6Li is somewhat narrow, and similar in magnitude to the range of ^7Li .

The spectrum of lithium bromide provided some interesting points during accumulation. During the initial stages of acquiring the spectrum a single resonance was observed suggesting the nucleus was shielded. However as the experiment proceeded a second, more deshielded resonance was seen. This second, weaker resonance was attributed to the resonance of LiBr(aq) and reflecting the hygroscopic nature of the salt. The more heavily shielded resonance arose from LiBr .

Laponite is a synthetic smectite clay (the closest natural counterpart is hectorite) and contains approximately 0.62% lithium in its normally sodium exchanged form ($\text{Na}_{0.67}(\text{Li}_{0.67}\text{Mg}_{5.33})\text{Si}_8\text{O}_{20}(\text{OH})_4$). Mandair et al⁷⁸ recently completed a combined N.M.R. (Na,Si) and X.R.D. study of the thermolysis of laponite and it was of interest to complement this study by analysing the thermolysis products by ^6Li M.A.S.N.M.R..

T / °C	d (ppm vs. satd. aq LiCl)	
	heated specimen	rehydrated
room temp	-0.735	-
200	-0.631	-0.81
400	-0.395	-0.52
600	-0.227	-0.12
800	-0.145	0.051
1300	-0.077	-

Table 5.3 - ^6Li M.A.S.N.M.R. data for thermally treated laponite and for Li^+ exchanged laponite

The samples examined were undoped laponite and despite this, the resultant spectra were of excellent quality with the FWHM of spectral lines being of the order of 62Hz and were obtained without excessive demands on instrumental time. The ^{29}Si M.A.S.N.M.R. data derived from the thermolysis study of laponite suggested that there was some loss of crystallinity of the samples heated up to 400°C. There is also a possibility of structural breakdown of the silicate network but these physical alterations appeared reversible when the samples were subjected to rehydration. The ^6Li study reflects these results well and the results obtained are displayed in table 5.3. In comparison to the untreated sample a deshielding of the Li nucleus is experienced upon heating to 200 and 400°C. A possible explanation is the dehydration of the interlamellar sodium ions since on rehydration the lithium becomes more shielded and the shift value returns to a value close to

that of the untreated sample. Mandair suggests in the earlier study that on heating to 600°C there is a migration of lithium from the octahedral to the edge sites and this was reiterated in the current study by the increase in deshielding exhibited by the ^6Li nucleus on rehydrating. These data are consistent with the formation of $\text{Li}^+(\text{aq})$ on the edge of interlamellar sites. On heating the sample to 800°C the silicate network suffers major structural breakdown and the formation of simple silicates is evident. Enstatite (MgSiO_3) is the dominant phase observed but it was also suggested that lithium silicate phases may have been formed. The ^6Li N.M.R. data are not inconsistent with this view but the X.R.D. traces are dominated by enstatite polymorphs and no distinctive lithium silicate lines were observed. This situation is also observed in the sample heated to 1300°C.

An attempt was made to distinguish between the structural and interlamellar lithiums after lithium counterions were exchanged into the clay in place of the sodium. The ion exchange was carried out using two methods, the classical and long Posner and Quirk method⁷⁹, and a new microwave method (see section 5.4). ^6Li M.A.S.N.M.R. analyses were carried out on the ion exchanged clays. The Posner and Quirk method produced a material giving a singlet of FWHM approximately 80Hz, centred on +0.232 ppm. The completely exchanged microwaved clay was examined by both ^6Li and ^7Li N.M.R.. Excellent spectra were obtained for both nuclei and ^7Li gave a singlet centred around -0.316 ppm. The corresponding ^6Li spectrum gave a clearly defined doublet. The same sample reanalysed after three months revealed a singlet. A fresh preparation of the microwaved sample again provided a doublet by ^6Li M.A.S.N.M.R. and both preparations had a 1 : 1 intensity ratio.

The arising of a doublet of this nature could be due to a single lithium site split by the quadrupolar nature of the nucleus but subsequent work has provided evidence that this is not the case and that the doublet is two distinct lines.

If the line observed is quadrupolar split then the quadrupolar shifts ν_Q in the first order would be given by :-

$$\nu_Q = (-3eq^2Q/4)(3\cos^2\theta-1)(M_I - 1/2) / I(2I - 1)$$

It can be seen that this term depends on θ , the angle that the nuclear vector makes with the magnetic field B_0 . If this angle is changed then the quadrupolar shift will change and the line splitting observed on the spectrum will change also.

The sample was spun 'off angle' by a small amount and the line splitting measured. The separation remained constant (within experimental error $\pm 0.5\text{Hz}$) for the two spectra at 11.3Hz

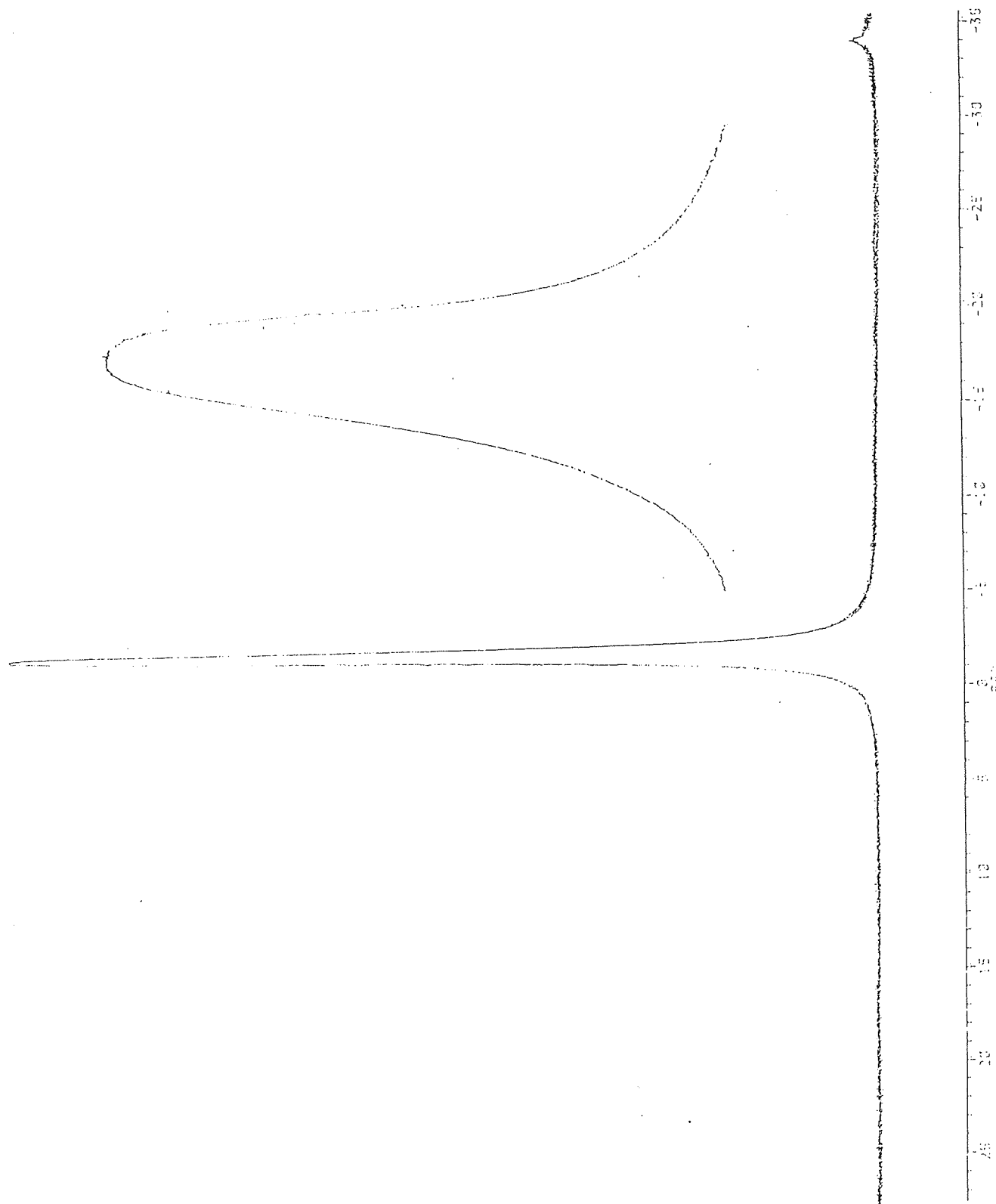


Fig 5.8 - ^6Li M.A.S.N.M.R. spectrum of a Lithium ion exchanged clay using the Posner and Quirk method

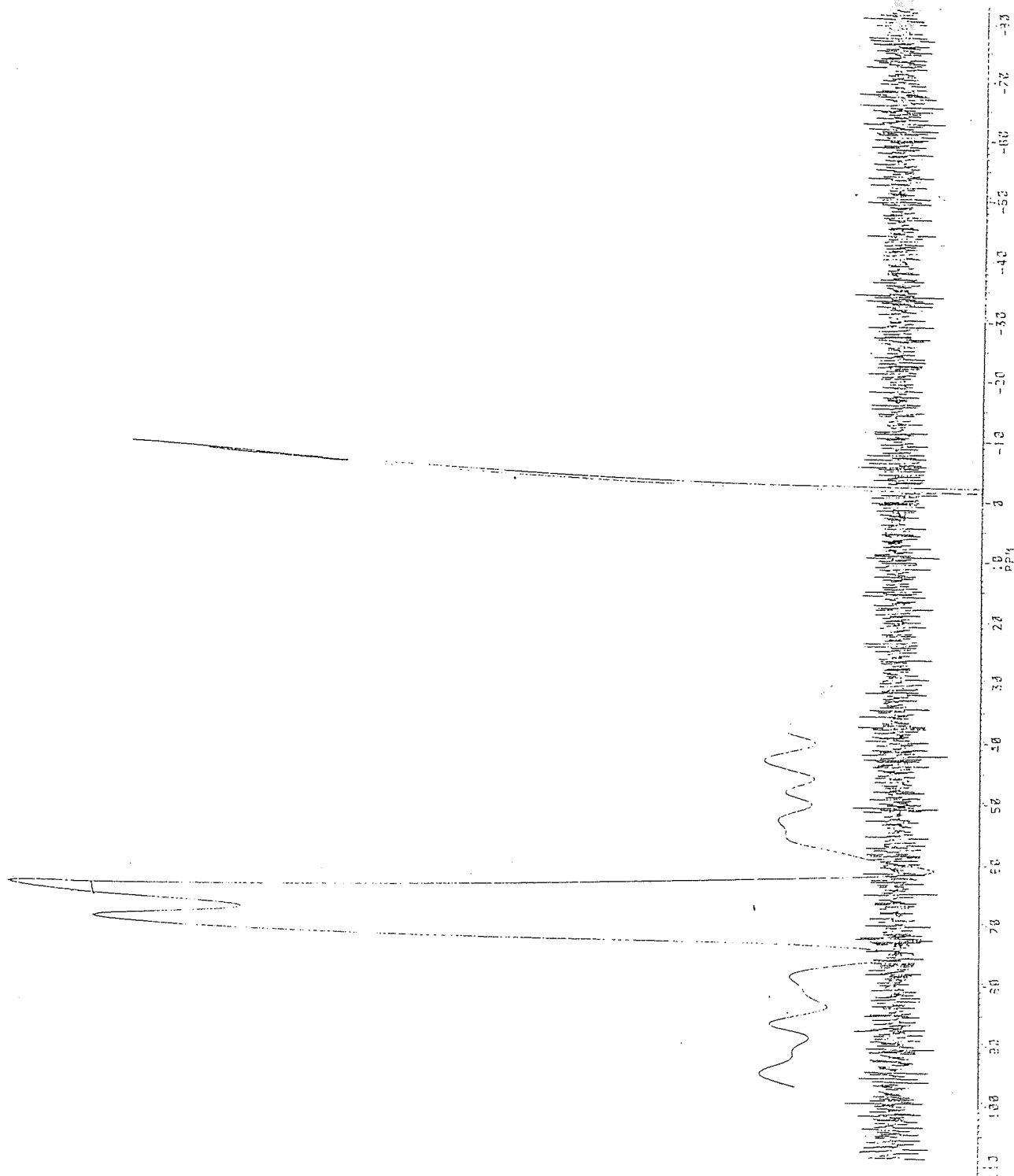


Fig 5.9 - ^6Li M.A.S.N.M.R. spectrum of a Lithium ion exchanged clay using the Microwave method

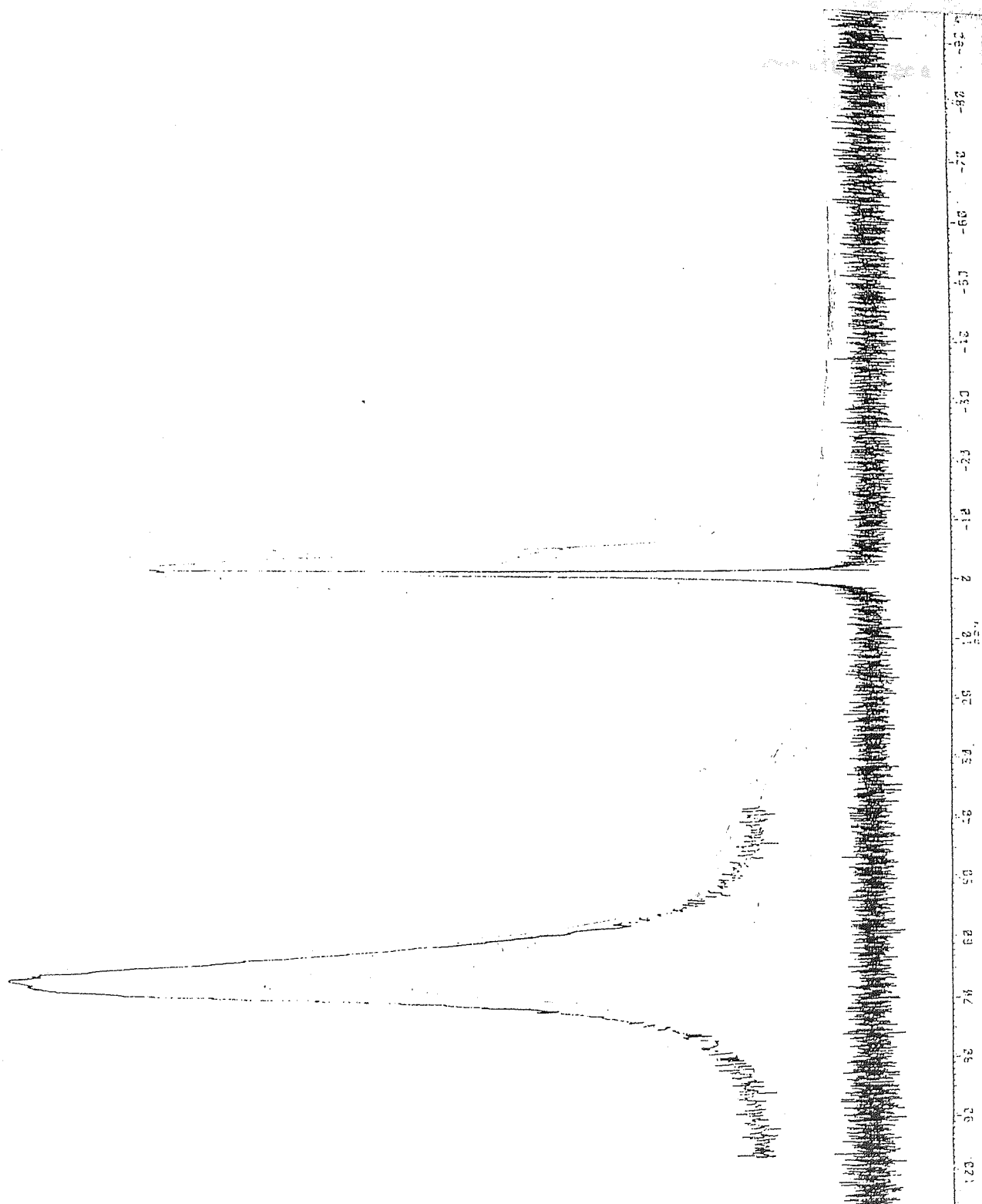


Fig 5.10 - ^6Li M.A.S.N.M.R spectrum of a Lithium ion
exchanged clay using the Microwave
method, three months after preparation

(M.A.S.) and 11.9Hz ('off angle'). It should be noted that if the sample is spun at too large a deviation from the magic angle then the dipolar broadening experienced caused the loss of resolution and the disappearance of the splitting. Secondly it can be suggested that if the lines were the result of quadrupolar interactions then there is no mechanism for the transformation into a singlet over the three month period. Therefore the evidence strongly suggests the presence of two distinct resonances that can be attributed to two lithium sites.

Material (experimental conditions)	$\delta^a(\text{ppm})$	FWHM ^b / Hz
^6Li M.A.S. (microwave method; fresh specimen)	-0.192 -0.438 $\Delta\nu = 11.3 \text{ Hz}$	25.0
^6Li 'off angle' ^c (microwave method; fresh specimen; small departure from magic angle)	$\Delta\nu = 11.9 \text{ Hz}$	37.1
^6Li 'off angle' (microwave method; fresh specimen; large departure from magic angle)	broad singlet	86.8
^6Li M.A.S. (microwave method; aged specimen, 3 months)	-0.179	37.7
^6Li M.A.S. (conventional method ⁷⁹)	0.232	
^7Li M.A.S. (microwave method) ^d	-0.316	86.5
^7Li 'off angle' (microwave method; ^d small departure from magic angle)	broad singlet	267

^a Chemical shift, i.e. position of resonance maximum; ^b FWHM = full width at half maximum; ^c the same small departure was used for both ^6Li and ^7Li spectra; ^d freshly prepared specimens.

Table 5.4 - Some ^6Li and ^7Li N.M.R. data on Li^+ -exchanged laponite

The 1 : 1 intensity ratio of the two peaks is consistent with expectation if the signals rise from the interlamellar and trioctahedral lithiums. The more deshielded resonance is assigned to the exchanged and hence aquated lithium and the -0.438 ppm is assigned to the trioctahedral structural lithium. The slight deshielding relative to the sodium laponite reflects the sensitivity of the lithium chemical shift to the identity of the interlamellar cations. It was of interest to note that the investigation of the aged specimen failed to reveal two sites. Also if the lithium was exchanged by conventional methods⁷⁹ (ie washing several times with 1 mol dm⁻³ LiCl, stirring for 36 hrs at pH4, followed by extensive washing and dialysis of the clay with deionised water, the whole procedure taking several weeks), a single resonance was noted (table 5.4). The data are consistent with the slow migration of lithium from the trioctahedral sites into a common environment; the acceleration of the ion exchange process in the microwave method enables the distinct lithium sites to be detected, but only if ^6Li M.A.S.N.M.R. spectroscopy is used, the ^7Li spectrum is a singlet.

5.6 Other N.M.R. Studies

In chapter 2 an account of the synthesis and subsequent analysis of various products from the pyrolysis of finely divided lithium metal and several ceramic materials is given. A lithium M.A.S.N.M.R. study of one particular product derived from the reaction of lithium and alumina produced a heavily deshielded resonance that was outside the normally accepted chemical shift range at 264 ppm (see figure 5.11). This peak was unique amongst the compounds studied and its appearance led to an investigation of Knight shifts. Knight shifts are named after W.D. Knight⁸² who first discovered that the resonance frequency in metals is higher than that for nuclei of the same isotope in an insulating material in the same magnetic field. The effect is caused by the local field produced by the conduction electrons as was first shown by Townes⁸³. An explanation of the spurious peak observed in figure 5.11 can thus be proffered. During the violent reactions where phases such as lithium meta and orthosilicates are synthesised, particles of lithium metal as small as a few atoms in size became entrapped within the synthesizing silicate matrix. Once entrapped they were protected from further reaction and it was these pockets of lithium metal that created the Knight shift pictured in figure 5.11.

A ^{27}Al and $^6,^7\text{Li}$ M.A.S.N.M.R. study of a commercial Li / Al alloy (8090) in powder form confirmed that Knight shifts could be produced for lithium and a metal shift was obtained for both aluminium and lithium and these are shown in figures 5.12 and 5.13. Studies into the Knight shifts observed in alloys and the effect of alloy composition have been carried out by Bloembergen⁸⁴ and Teeters⁸⁵. Several conclusions can be drawn from these studies:

(i) Strong quadrupole interactions usually obliterate the magnetic resonance and therefore nuclei of study should possess a spin 1/2 with cubic symmetry or possess a small quadrupole moment.

(ii) The metal shift observed for the solute in a dilute alloy is, in general, different from the value of the pure solute metal.

(iii) For dilute alloys upto several atomic percent solute concentration the metal shift differs relatively little from the value appropriate to the pure solvent metal ie the electronic conduction band of a dilute alloy seems to differ very little from that of the pure solvent metal.

The alloys analysed by both Bloembergen and Teeters contained a solute concentration range of 5 - 15 atomic % but commercial Li / Al alloys are primarily manufactured within a 1 - 10 atomic % lithium range. As these alloys are at the lower end of the range, of the previous study conclusion

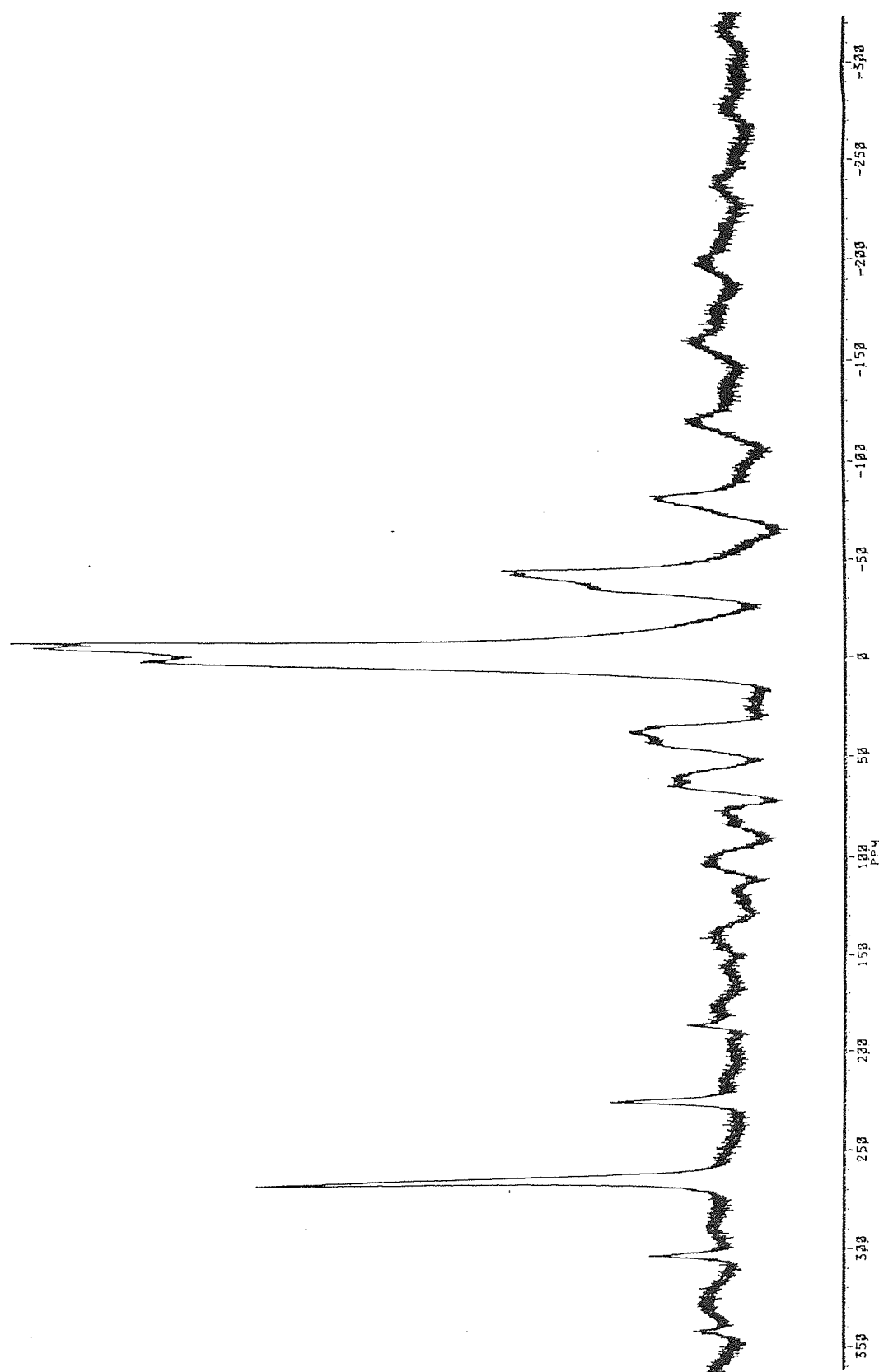


Fig 5.11 - ${}^7\text{Li}$ M.A.S.N.M.R. spectrum of the reaction products of a Lithium / alumina pyrolysis reaction

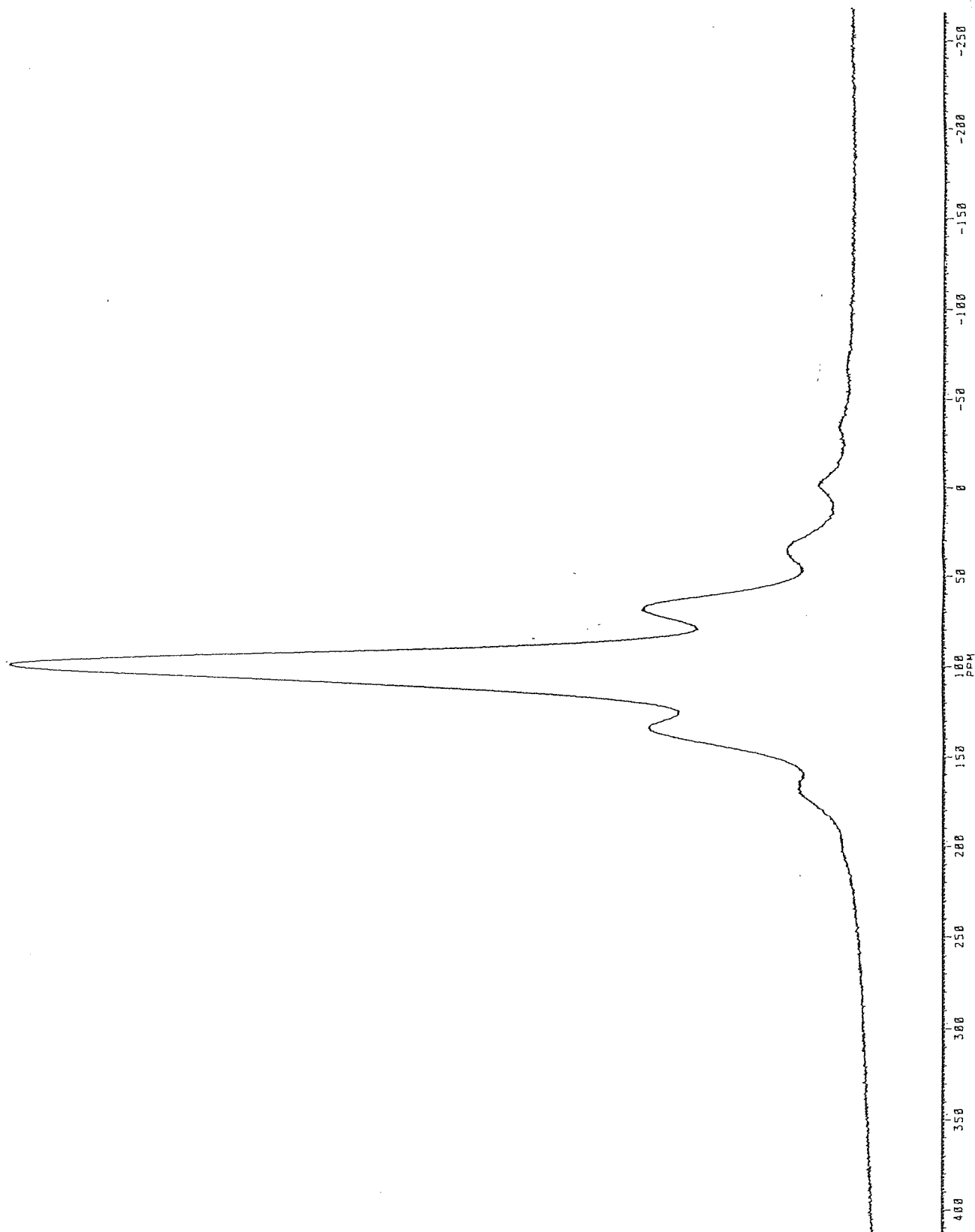


Fig 5.12 - ${}^7\text{Li}$ M.A.S.N.M.R spectrum of 8090 alloy showing the Knight shift at 103 ppm

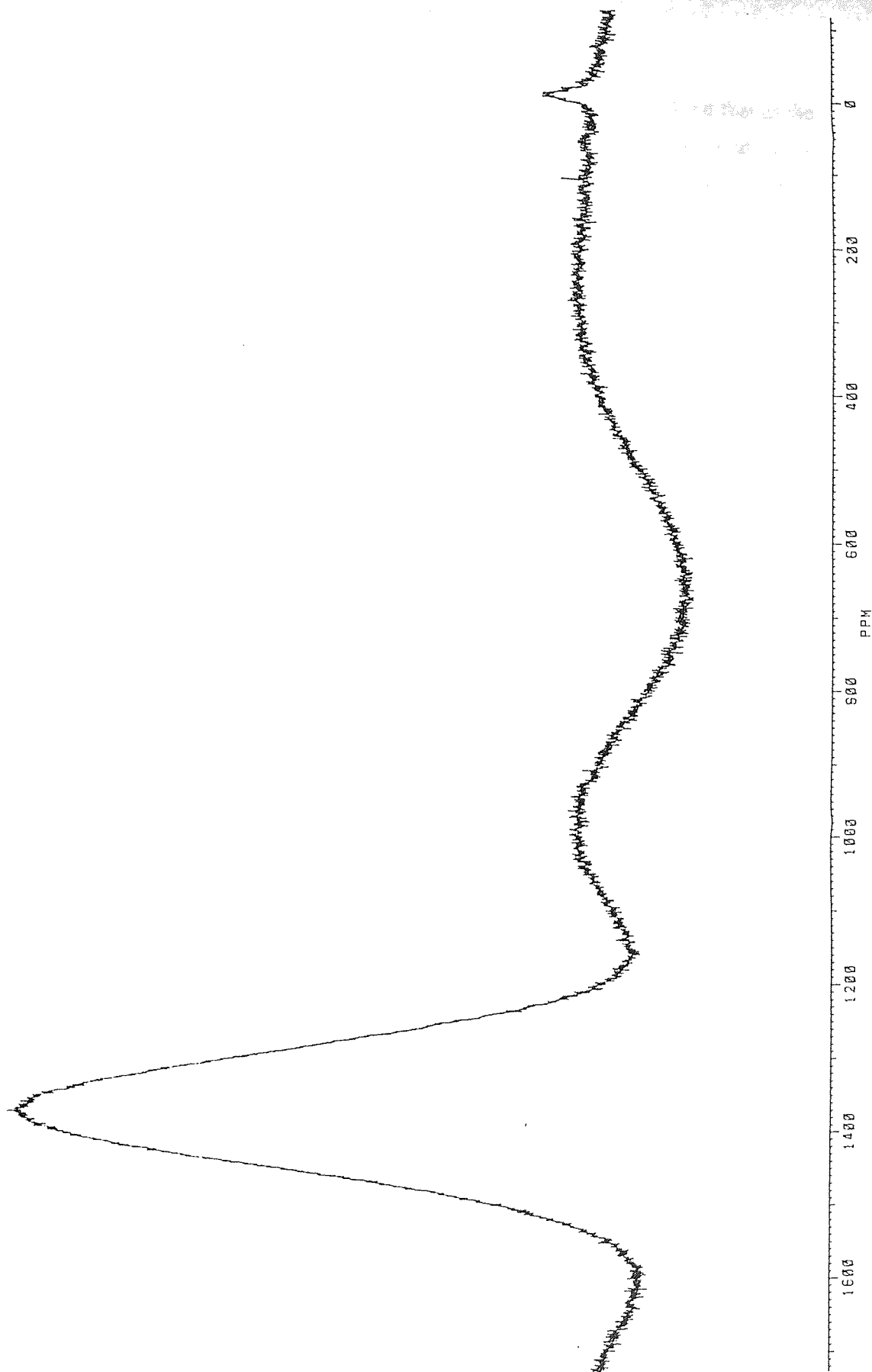


Fig 5.13 - ^{27}Al M.A.S.N.M.R. spectrum of 8090 alloy showing the broad Knight shift at 1369 ppm

three does not necessarily hold for this low alloy composition. It can be pointed out that as the electron concentration increases in the Cu / Al system it might be expected that the metal shift for both copper and aluminium to increase with aluminium concentration, but the data indicate that $\Delta H/H$ is relatively constant for the 5 - 15 atomic % composition range. For both Al and Cu there is a slight shift in the metal shift up to 5% and this shift maybe proportional to the solute concentration. This point, if true, could be exploited for the Li / Al system. Within the chemical and metallurgical industries it is well known that direct and simple analytical techniques are useless when the lithium concentration is required and a simple and effective technique is sought. To test the above hypothesis it was considered prudent to investigate as to whether the shift in the Knight shift was significant for this particular composition range.. The four alloys produced for the casting experiments were employed for this purpose and their production is described in section 4. M.A.S.N.M.R. studies were initiated but it was discovered that the production of particles of a size required for M.A.S. was difficult without specialist powder alloy manufacturing techniques. M.A.S. requires a powder with a particulate size of around 50μ and producing a sufficient quantity from a solid chill casting is impractical. Nevertheless, sufficient quantity of the 3% alloy was made and a M.A.S.N.M.R. spectrum was produced using ^7Li . Figures 5.14 and 5.12 show the spectrum for the binary alloy sample and also for a commercially produced powdered sample of an 8090 alloy. The resonance position for both the 8090 alloy and the laboratory produced binary alloy are essentially identical at 102.91ppm suggesting that the alloying elements other than lithium used in the commercial alloy have no effect on the conduction band for the lithium nucleus.

Due to the sample preparation difficulties advances in this study have had to rely upon the development of a novel technique of SINNMR (pronounced 'cinema') i.e. sonically induced narrowing of nuclear magnetic resonance spectroscopy. This technique is an alternative to M.A.S. as it creates a liquid like environment for solid particles by agitating them in an inert liquid medium using an ultrasound horn. The technique requires particles of mm size for densities of 2.5 gcm^{-3} typical of Al alloys and particles of such size are easy to produce. SINNMR is still in the experimental stage and much work is needed to be done to produce spectra equal to that of M.A.S., nevertheless early studies on the binary alloys in question suggest that there may be some dependence on alloy composition.

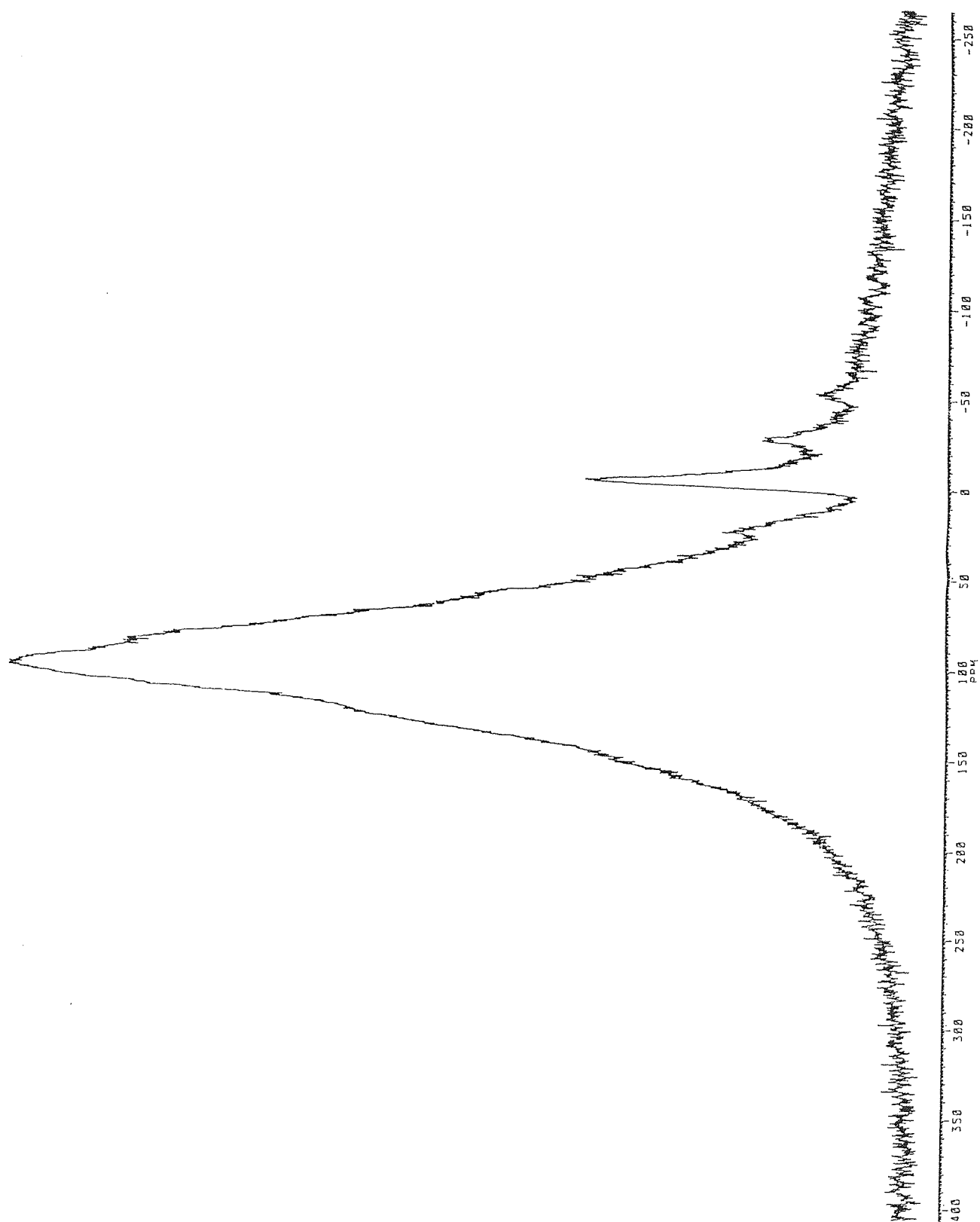


Fig 5.14 - ${}^7\text{Li}$ M.A.S.N.M.R. spectrum of a 3% lithium aluminum alloy produced under laboratory conditions showing the Knight shift of 102.91ppm

CONCLUSIONS

CONCLUSIONS

At the beginning of this thesis several objectives were outlined. The primary objective of the project was to prevent metal mould reaction from occurring between aluminium lithium alloys and the surface of conventional sand and investment moulds. A methodical approach was taken, and the mould constituents and the alloy were separated into their respective components. Each of the mould components were pyrolysed with lithium metal and the products analysed for composition. It can be concluded from this set of experiments that lithium does play a significant part in the metal mould reaction. The reactions also revealed that the lithium will, and probably does, react with all constituents of the mould to some degree. The analyses, via X-Ray diffraction and nuclear magnetic resonance spectroscopy, revealed the presence of several lithium aluminate and silicate species as a result of the pyrolysis of lithium with alumina and silica respectively. The N.M.R. results also showed that lithium metal was present within the lithium silicate structure, a phenomenon that parallels sodium chemistry where sodium vapour is known to be drawn into sodium silicate structures. This feature of the reaction was observed in the form of a Knight shift and further study into Knight shifts was undertaken as a separate research topic.

Visual analysis of the pyrolyses reactions revealed that the reactions between lithium and the organic binder material for sand moulds were the most vigorous and that they released a flammable gas as a product. The chemical composition of the binders suggests that hydrogen is the most probable gas to be released from such a reaction. This analysis compares well with the findings of Whitaker who suggested that hydrogen was the cause of metal mould porosity in the castings of aluminium magnesium alloys although she concluded that it was moisture within the mould that was attributable. It can be concluded from the research carried out within this project that not only does water in the mould cause metal mould reaction but the reaction between mould and alloy constituents contribute significantly to the final porosity.

Study into the curing nature of the binder products reveals that the phenolic hydroxide groups on the phenolic binder remain unreacted and it can be concluded that it is these hydroxide groups that are reacting with the lithium in the alloy to synthesize a lithoxo species and hydrogen gas.

Work was carried out to assess the effect of various hydroxide inhibiting groups on the castability of sand moulds. Several sand moulds were prepared in the appropriate manner and on completion a hydroxide inhibitor was applied to the surface of the mould and allowed to dry prior to casting. The resultant casting was sectioned laterally and mounted for visual and microscopic investigation. A preliminary conclusion can be drawn from the casting experiments. The casting procedure was carried out on a very small scale and it was important to ascertain that the metal

mould reaction was occurring. The desired porosity was observed readily in the untreated moulds and it was concluded that a significant amount of metal mould reaction was occurring. Several propriety inhibitors were tested and their affect monitored. After repeat trials of each compound trimethylchlorosilane (T.M.C.S.) was found to inhibit the reaction to the greatest degree. It reduced porosity within the body of a casting by an estimated 70-80%. No other agent was found to compare with this rate of inhibition.

Investment moulds are prepared differently to sand moulds. The bulk of the mould is ceramic silicate materials bound with colloidal silica. After firing there are no organic species present within an investment mould and hence the porosity problem has a different cause. Inorganic silicates are built up from 2 and 3 dimensional structures of silicon and oxygen but at the edge sites the structures are terminated by hydroxide groups. Therefore the metal mould problem is essentially identical to that caused by a sand mould. Using the same inhibitors the same conclusions can be drawn. Trimethylchlorosilane was the best inhibitor, reducing the visual porosity by 90+%. Some other inhibitors closely related to T.M.C.S., trimethylbromosilane and triphenylchlorosilane, were applied to some investment moulds with a similar outcome. It can be concluded that the mechanistic simplicity of the T.M.C.S., T.M.B.S. and T.P.C.S. provides the best coverage on both sand and investment moulds. Application methods do have an effect on the amount of coverage and using a theory proposed by Tolman a mechanism for trimethylsilyl addition was proposed. A coverage of approximately 50% can be achieved by the gassing method but the more intimate application procedure of spraying provides a coverage of 60-70%.

N.M.R. was a prominent analysis technique throughout the project and several experiments were carried out using ^6Li as the analysis nucleus. The use of this nucleus has not been widely reported in the literature for solid state N.M.R. but the results from the research carried out during the project revealed that ^6Li provided more structural information than ^7Li for the same system.

A Knight shift is a highly deshielded chemical shift caused by the local field produced by conduction electrons in a metal sample. Knight shifts were observed in lithium silicate samples formed through pyrolysis experiments using lithium and mould materials. Investigations into aluminium lithium alloys showed that a Knight shift can be produced for both lithium and aluminium. The observation of the Knight shift has provided evidence to suggest that the change in the Knight shift maybe proportional to the variation in the lithium concentration in an aluminium lithium alloy (for small lithium concentrations < 4 weight %). This could be used as a relatively quick analysis technique for ascertaining the lithium concentration of an unknown alloy. This technique would be useful to industry due to the present difficulties in detecting lithium using conventional techniques

APPENDIX

Lithium Orthosilicate

Li₄SiO₄ Monoclinic 2Li₂O . SiO₂

Measured 'd' Value	Theoretical 'd' Value	I / I ₀	hkl
5.32	5.29	30	100
5.17	5.15	20	001
4.01	4.00	100	110
3.94	3.93	80	011
3.69	3.68	45	101
3.17	3.16	55	111
2.65	2.65	100	200,120
2.57	2.57	55	002
2.38	2.35	30	121,201

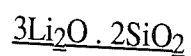
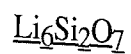
Lithium Metasilicate



Orthorhombic

Measured 'd' Value	Theoretical 'd' Value	I / I ₀	hkl
4.706	4.696	-	-
3.349	3.302	-	-
2.712	2.708	-	-
2.336	2.341	-	-
1.770	1.764	-	-
1.659	1.656	-	-
1.566	1.565	-	-

Lithium Disilicate



Measured 'd' Value	Theoretical 'd' Value	I / I ₀	hkl
3.645	3.63	-	-
3.403	3.45	-	-
2.851	2.81	-	-
2.458	2.43	-	-
---	2.18	-	-
1.982	1.989	-	-
1.962	1.957	-	-
1.916	1.925	-	-
1.819	1.818	-	-

alpha - Lithium Aluminate

α - LiAlO₂

Trigonal

Measured 'd' Value	Theoretical 'd' Value	I / I ₀	hkl
4.76	4.72	70	003
2.38	2.38	40	101
2.00	2.00	100	104
1.55	1.55	40	107
1.43	1.43	60	018
1.40	1.40	60	110
---	1.34	40	113

gamma - Lithium Aluminate

γ - LiAlO₂

Tetragonal

Measured 'd' Value	Theoretical 'd' Value	I / I ₀	hkl
3.99	3.98	100	101
3.66	3.65	40	110
3.16	3.15	50	111
2.68	2.67	90	102
2.58	2.58	90	200
2.17	2.17	30	211
1.86	1.86	50	212
1.82	1.82	30	220
1.81	1.81	30	113
---	1.63	30	310
1.60	1.58	30	311
1.56	1.565	40	004
1.51	1.508	80	302
---	1.340	50	204
1.30	1.303	70	322

REFERENCES

References

- (1) M. Van Lancker, "Metallurgy of Aluminium Alloys," Chapman and Hall, London, 1967.
- (2) F. King, "Aluminium and its Alloys," Ellis Horwood Ltd, Chichester, 1987, 17.
- (3) P.A. Cox, "The Elements," Oxford Science Publications, Oxford, 1989, 182 - 186
- (4) P. Berthier, "Analyse de L'Alumine Hydratée Des Baux," Ann. Mines., 1821, 6, 531 - 534.
- (5) J.W. Shaffer, "Bauxitic Raw Materials," in Industrial Minerals and Rocks, ed Lefond, S. J., 5th ed, Vol 1, Am. Inst. of Mining Eng., Port City Press, Baltimore, 1983, 503.
- (6) J.D. Edwards, "The Story of Aluminium," in The Aluminium Industry, eds J.D. Edwards, F.E. Frary, Z. Jefferies, McGraw Hill, New York, 1930, 1 - 15.
- (7) F. King, "Aluminium and its Alloys," Ellis Horwood Ltd, Chichester, 1987, 62
- (8) F. King, "Aluminium and its Alloys," Ellis Horwood Ltd, Chichester, 1987, 70
- (9) F. King, "Aluminium and its Alloys," Ellis Horwood Ltd, Chichester, 1987, 242
- (10) N.N. Greenwood, A. Earnshaw, "Chemistry of the Elements," Pergamon Press, Oxford, 1984.
- (11) Non Ferrous Metal Data, American Bureau of Metal Statistics inc., New York, 1989.
- (12) "Source Book on Selection and Fabrication of Aluminium Alloys," American Society for Metals, Ohio, 1978.
- (13) D.F. Othmer, R.E. Kirk, "Encyclopaedia of Chemical Technology," Vol 2, J. Wiley and Sons, New York, 1981.
- (14) M.E. Weeks, "Discovery of the Elements," 6th ed, Journal of Chemical Education, Easton, 1968.
- (15) L. Gmelin, "Handbook of Chemistry," Harrison and Son, London, 1849.
- (16) J. Czochralski, E. Rassow, " Binary Alloys of Lead and Lithium," Z. Metallkunde, 1927, 19, 111 - 112. C.A., 21, 1617.
- (17) P.E. Landolt, "Lithium," in Rare Metals Handbook, ed C.A. Hampel, Reinhold, New York, 1954.
- (18) G.E. Foltz, "Lithium and Lithium Compounds," Encyclopaedia of Chemical Process and Design, Vol 28, ed J.J. McKetta, Marcel Dekker inc., New York, 1988.
- (19) P.A. Cox, "The Elements", Oxford Science Publications, Oxford, 1989, 89.
- (20) Industrial Minerals and Rocks, 5th edition, ed S.J. Lefond Port City Press, Baltimore, 1983, 869 - 881.

- (21) A.N. Zelikman, O.E. Krein, G.V. Samsonov, "Metallurgy of Rare Metals," I.S.P.T. Ltd, Jerusalem, 1966
- (22) Encyclopaedia of Chemical Process and Design, Vol 28, ed J.J. McKetta, Marcel Dekker inc., New York, 1988
- (23) J.R. Nelli, T.E. Arthur, "Recovery of Lithium from Bitterns," U.S. Pat. 3,537,813 Nov 3, 1970, (to the Lithium Corporation of America)
- (24) R.D. Goodenough, "Recovery of Lithium," U.S. Pat. 2,964,381 Dec 13, 1960, (to the Dow Chemical Company)
- (25) I. Pelly, "Recovery of Lithium from Dead Sea Brines," J. Appl. Chem. Biotechnol., 1978, **28**, 469 - 474.
- (26) B.J. Wakefield, "The Chemistry of Organolithium Compounds," Pergamon Press, Oxford, 1974
- (27) O. Reuleaux, "Scleron Alloys," J. Inst. Met., 1925, **33**, 346.
- (28) I.M. LeBaron, "Aluminium - Copper - Lithium - Cadmium Alloys," U.S. Pat 2,381,219, Aug 7, 1945, (to the Aluminium Corporation of America)
- (29) H.K. Hardy, "Trace-Element Effects in Some Precipitation-Hardening Aluminium Alloys," J. Inst. Met., 1955 - 56, **84**, 429 - 439.
- (30) E.H. Spuhler, A.H. Knoll, J.G. Kaufman, "Lithium in Aluminium-X2020," Met. Prog., 1960, **79**, 80 - 82.
- (31) E.S. Balmuth, R. Schmidt, "Development of Aluminium-Lithium alloys," Proc. 1st Int. Aluminium-Lithium Conference, Stone Mountain, Georgia, May 1980, Met. Soc. AIME, 1981, 69 - 88.
- (32) C.J. Peel, B Evans, D.S. McDarmid, "Development of Aluminium - Lithium Alloys in the U.K.," Metals and Materials, Aug 1987, **3**, 449 - 455.
- (33) A.F. Smith, "Aluminium-Lithium Alloys for Helicopter Structures," Metals and Materials, Aug 1987, **3**, 438 - 444.
- (34) Binary Alloy Phase Diagrams, Ed in Chief T.B. Massalski, American Society for Metals, Metals Park, Ohio, 1986
- (35) J.M. Silcock, "The Structural Ageing Characteristics of Aluminium-Copper-Lithium Alloys," J. Inst. Met., 1959 - 60, **88**, 357 - 364.
- (36) B. Noble, G.E. Thompson, "Precipitation Characteristics of Aluminium-Lithium Alloys," Met. Sci. J., 1971, **5**, 114 - 120.
- (37) D.B. Williams, J.W. Edington, "The precipitation of δ' (Al_3Li) in Dilute Aluminium-Lithium Alloys," Met. Sci., 1975, **9**, 529 - 532.
- (38) A.F. Wells, "Structural Inorganic Chemistry," Oxford University Press, Oxford, 1984.
- (39) W.R.D. Jones, P.P. Das, "The Mechanical Properties of Aluminium-Lithium Alloys," J. Inst. Met., 1959 - 60, **88**, 435 - 443.

- (40) R. Nozato, G. Nakai, "Thermal Analysis of Precipitation in Al_3Li Alloys," Trans. J. I. M., 1977, **18**, 679 - 689.
- (41) T.V. Shchegoleva, O.F. Rybalko, "On the Question of the Ageing Mechanism of the Alloy Al-Li," Phys. Met. Metallog., 1976, **42**, 83 - 93.
- (42) D.B. Williams, "Microstructures of Al-Li Alloys," Proc. 1st Int. Aluminium-Lithium Conference, Stone Mountain, Georgia, May 1980, Met. Soc. AIME, 1981, 90 - 100.
- (43) A.P. Divecha, S.D. Karmarker, "Casting Problems Specific to Aluminium-Lithium Alloys," Proc. 1st Int. Aluminium-Lithium Conference, Stone Mountain, Georgia, May 1980, Met. Soc. AIME, 1981, 49 - 62.
- (44) C.M. Adam, "Overview of D.C. Casting," Proc. 1st Int. Aluminium-Lithium Conference, Stone Mountain, Georgia, May 1980, Met. Soc. AIME, 1981, 37 - 48.
- (45) Atlas of Defects in Casting, The Institute of British Foundrymen, 2nd revised edition, London, 1961.
- (46) Atlas of Defects in Casting, The Institute of British Foundrymen, 2nd revised edition, London, 1961, 53.
- (47) "Fundamentals of Foundry Technology," ed P.D. Webster, Portcullis Press, Redhill, 1980, 50.
- (48) P.R. Beeley, "Foundry Technology," Butterworth and Co, London, 1972.
- (49) "Fundamentals of Foundry Technology," ed P.D. Webster, Portcullis Press, Redhill, 1980.
- (50) W.B. Parkes, "Clay Bonded Foundry Sand," Applied Science Publishers Ltd, Barking, 1971.
- (51) M. Whitaker, "Mould Reaction in Aluminium Alloy Castings," Proc. Inst. Br. Foundrym., 1953, **46**, A236 - 246
- (52) R.W. Ruddle, "Mould Reaction," Proc. Inst. Br. Foundrym., 1953, **46**, B112 - 122
- (53) R. Millgate, Private Communication.
- (54) M. Magi, E. Lippmaa, A. Samoson, "Solid State High Resolution Silicon - 29 Chemical Shifts in Silicates," J. Phys. Chem., 1984, **88**, 1518 - 1522.
- (55) M. Marezio, "The Crystal Structure and Anomalous Dispersion of γ - LiAlO_2 ," Acta Cryst., 1965, **19**, 396 - 400.
- (56) M. Marezio, J.P. Remeika, "High Pressure Synthesis and Crystal Structure of α - LiAlO_2 ," J. Phys. Chem., 1966, **44**, 3143 - 3144.
- (57) M. Marezio, J.P. Remeika, "High Pressure Phase of LiGaO_2 ," J. Phys. Chem. Solids, 1965, **26**, 1277 - 1280.
- (58) R.W. Grimshaw, "The Chemistry and Physics of Clays and Allied Ceramic Materials," Benn, London, 1971
- (59) "Fundamentals of Foundry Technology," ed P.D. Webster, Portcullis Press, Redhill, 1980, 122.

- (60) R.O. Sauer, " Derivatives of Methyl Chlorosilanes. I Trimethyl Silanol and its Simple Ethers," J. Am. Chem. Soc., 1944, **66**, 1707 - 1710.
- (61) R.O. Sauer, R.H. Hasek, " Derivatives of Methyl Chlorosilanes. IV Amines," J. Am. Chem. Soc., 1946, **68**, 241 - 244.
- (62) H.A. Schuyten, J.W. Weaver, J.O. Reid, " Preparation of Substituted Acetoxy Silanes," J. Am. Chem. Soc., 1947, **69**, 2110 - 2112.
- (63) H.H. Anderson, " Monoethyl Germanium and Alkyl Silicon Esters. Dimethylgermanium diacetate," J. Am. Chem. Soc., 1952, **74**, 2371- 2372.
- (64) " Treating the Surface of a Water Insoluble Solid Material," Brit Pat 957, 389, May 6, 1964, (to the Dow Corning Corporation). C.A., 61, 2808.
- (65) E. Robbart, " Shrinkproofing Cellulose Fibres," Ger Pat 1,178,395, Sept 24, 1964. C.A., 62, 2873.
- (66) C.A. Tolman, "Steric Effects of Phosphorus Ligands in Organometallic Chemistry and Homogeneous Catalysis," Chem Rev, 1977, **77**, 315 - 348.
- (67) C.R.C. Handbook of Chemistry and Physics, ed in Chief D.R. Lide, C.R.C. Press, Boca Raton, Fla., 1990.
- (68) A.J. Gordon, R.A. Ford, "The Chemists Companion," J. Wiley and Sons, New York, 1972.
- (69) J.F. Klebe, H. Finkbinder, D.M. White, " Silylations with bis(trimethylsilyl)acetamide, a Highly Reactive Silyl Donor," J. Am. Chem. Soc., 1966, **88**, 3390 - 3395.
- (70) A.E. Pierce, Silylation of Organic Compounds, Pierce Chemical Co., Rockford, 1968, 16.
- (71) W.J.A. VandenHeuvel, " The Gas-Liquid Chromatography of Dimethylsilyl, Trimethylsilyl and Chloromethyldimethylsilyl ethers of Steroids - Mechanism of Silyl Ether Formation and Effect of Trimethylsilylation upon Detector Response," J. Chromatog., 1967, **27**, 85 - 95.
- (72) R.G. Griffen, " High Resolution N.M.R. in Solids," Anal Chem, 1977, **49**, 951A - 962A.
- (73) Multinuclear N.M.R., ed. J. Mason, Plenum Press, New York, 1987, 116.
- (74) S. Harder, J. Boersma, L. Brandsma, J.A. Kantas, W. Bauer, P. von R. Schleyer, " Crystal Structure of [2,6 bis (dimethylamino)phenyl] lithium: The First Trimeric Organolithium Compound," Organometallics, 1989, **8**, 1696 - 1700.
- (75) D.R. Armstrong, D. Barr, W. Clegg, S.M. Hodgson, R.E. Mulvey, D.E. Reed, R. Snaith, D.S. Wright, " Ladder Structures in Lithium Amide Chemistry: Syntheses and Solid State and Solution Structures of Donor Deficient Lithium Pyrrolidide Complexes, $\{[H_2C(CH_2)_3NLi]_3 \cdot PMDETA\}_2$ and $\{[H_2C(CH_2)_3NLi]_2 \cdot TMEDA\}_2$ and ab initio MO Calculations Probing Ring vs Ladder vs Stack Structural Preferences," J. Am. Chem. Soc., 1989, **111**, 4719 - 4727.
- (76) C. Brevard, P. Grainger, Handbook of High Resolution Multinuclear N.M.R., Wiley, New York, 1981.

- (77) J.H. Gilchrist, A.T. Harrison, D.J. Fuller, D.B. Collum, " ^6Li and ^{15}N N.M.R. Spectroscopic Studies of Lithiated Cyclohexanone Phenylimine Revisited. Aggrigation State Determination by Single Frequency ^{15}N Decoupling," J. Am. Chem. Soc., 1990, **112**, 4069 - 4070.
- (78) A-P.S. Mandair, P.J. Michael, W.R. McWhinnie, " ^{29}Si M.A.S.N.M.R. Investigations of the Thermochemistry of Laponite and Hectorite," Polyhedron, 1990, **9**, 517 - 525.
- (79) A.M. Posner, J.P. Quirk, " The Adsorption of Water from Concentrated Electrolyte Solutions by Montmorillonite and Illites," Proc. R. Soc. London, Ser. A, 1964, **278**, 35 - 56.
- (80) N. Poonia, " Co-ordination Chemistry of Sodium and Potassium Complexation with Macrocyclic Polyethers," J. Am. Chem. Soc., 1974, **96**, 1012 - 1019.
- (81) H. Eckert, Z. Zhang, J.H. Kennedy, " Structural Transformation of Non-Oxide Chalcogenide Glasses. The short range order of $\text{Li}_2\text{S}-\text{P}_2\text{S}_5$ Glasses studied by Quantitative ^{31}P and $^{6,7}\text{Li}$ High Resolution Solid State N.M.R.," Chem. Mater., 1990, **2**, 273 - 279.
- (82) W.D. Knight, " Electron Paramagnetism and Nuclear Magnetic Resonance in Metals," Solid State Phys., 1956, **2**, 93 - 136.
- (83) C.H. Townes, C. Herring, W.D. Knight, " Effect of Electronic Paramagnetism on Nuclear Magnetic Resonance Frequencies in Metals," Phys Rev, 1950, **77**, 852 - 3
- (84) N. Bloembergen, T.J. Rowland, " On the Nuclear Magnetic Resonance in Metals and Alloys," Acta Metallurgica, 1953, **1**, 731- 746.
- (85) D.R. Teeters, W.D. Knight, " Nuclear Magnetic Resonance in CuAl Alloys," Phys Rev, 1954, **96**, 861